Immunomodulatory Peptide Dendrimers Inspired from Glatiramer Acetate

Inaugural dissertation

of the Faculty of Science,

University of Bern

presented by

Dina Erzina

from Russia

Supervisor of the doctoral thesis:

Prof. Dr. Jean-Louis Reymond

Department of Chemistry, Biochemistry

and Pharmaceutical Sciences

University of Bern

Immunomodulatory Peptide Dendrimers Inspired from Glatiramer Acetate

Inaugural dissertation

of the Faculty of Science,

University of Bern

presented by

Dina Erzina

from Russia

Supervisor of the doctoral thesis:

Prof. Dr. Jean-Louis Reymond

Department of Chemistry, Biochemistry

and Pharmaceutical Sciences

University of Bern

Bern, 26.10.2021 The Dean

Prof. Dr. Zoltan Balogh

Table of Contents

Acknowledgements

I would also like to thank my mom **Marina** and dad **Rifat,** my aunt **Marusya**, my grandmothers **Sveta** and **Rita** for their support and unconditional love.

Abstract

Glatiramer Acetate (GA) is a popular first-line treatment drug for relapsing remitting multiple sclerosis (RRMS), a chronic autoimmune disease of central nervous system. GA is a mixture of random copolymers with the average size distribution between 4-9 kDA. Although, GA has been present on the market for more than 24 years, an active epitope or a sequence were not identified. One of the major difficulties preventing the discovery of the most active components of the mixture is due to the complexity of its synthesis.

With the aim of identifying a precisely defined alternative to GA, we designed a diverse library of peptide dendrimers, which differ in their molecular weight, charge, and amino acid ratio. The design was conducted using computational approach as well as manually to produce peptide dendrimers with different structural features. Having a diverse library of peptide dendrimers, we then challenged the dendrimers to trigger the release of the anti-inflammatory cytokine interleukin-1 receptor antagonist (IL-1Ra) from human primary monocytes. IL-1Ra is a natural inhibitor of IL-1β, a proinflammatory cytokine, which is one of the effects of GA on immune cells. Several of the largest dendrimers were as active as GA. In order to understand better the structure-activity relationship, we then created a library, consisting of the active dendrimers analogs. Activity of the active dendrimer was strongly influenced by variations in amino acid sequence and stereochemistry.

Having a defined active sequence, we performed a detailed biological evaluation of the cytokine secretion and regulation of the surface markers. In result, the differentiation of monocytes towards an M2 (anti-inflammatory) state was observed in response on the treatment. The confocal imaging with the fluorescent labelled analogs pointed out the distribution of the dendrimers mostly on the membrane of the monocytes but not the one of leukocytes. Since the active peptide dendrimer did not show measurable cellular toxicity, and its exact sequence is perfectly defined, this compound might serve as a starting point to develop a new class of immunomodulatory analogs of GA.

1. General Introduction

Treatment of autoimmune inflammation is a complicated task due to the complexity of its pathogenesis and the involvement of numerous processes. Here, we review the pathogenesis of multiple sclerosis (MS) development and accessible medication for its treatment. Glatiramer acetate (GA) is the one of the most popular drugs on the multiple sclerosis market, nevertheless it exposes many disadvantages and misunderstandings due to its structural complicity. We look at the most known medications for multiple sclerosis and at their history of the discovery, synthesis and manufacture processes of GA and explain why there are no close analogs reported. Subsequently we describe the mechanism of action of glatiramer and discuss its *in vitro* model of action. For better understanding of structure relationship and anti-inflammatory properties, we then discuss anti-inflammatory peptides and dendrimers.

1.1 Multiple sclerosis

MS is a chronic autoimmune disorder, characterized by damage of the central nervous system (CNS). MS is the one of the most frequent cause of disability in young adults affecting approximately 2 million patients worldwide. It is two to three times more prevalent in women than in men. The literal meaning of MS is "many scars", which describes the multiple lesions that accumulate in the brain and spinal cord during development of the disease. In healthy individuals, the myelin sheath is protecting nerve cells from damage and facilitates conduction of the nerve impulses. Damage to the myelin layer, nerve cells or both results in symptoms such as impaired vision, organ dysfunction, pain, spasms, numbness, muscle stiffness or cognitive dysfunction.[1]

There are two major forms of MS: Relapsing Remitting MS (RRMS) is the most frequent form (85% of patients) and about 15% of the cases of patients present with insidious disease onset and steady progression, termed Primary Progressive PPMS. RRMS is characterized by episodes of new or worsening signs or symptoms i.e. relapses, followed by periods of recovery (remission) (Figure 1.1.).
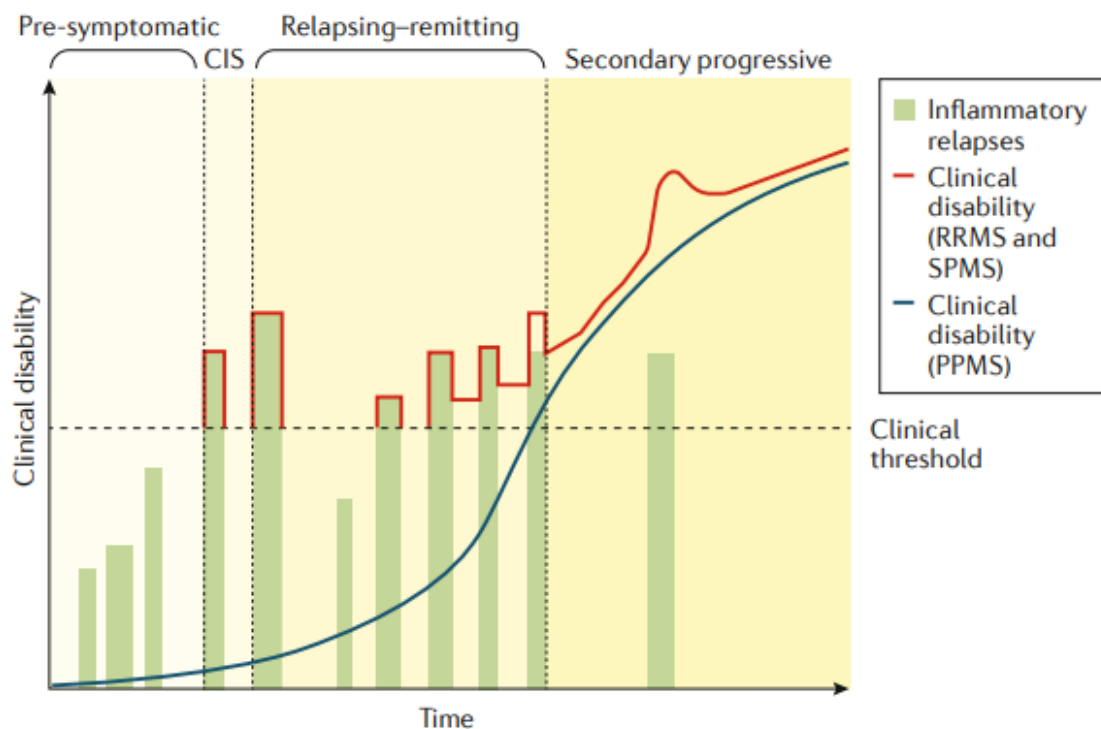
Figure 1.1. *The National Multiple Sclerosis Society Advisory Committee on Clinical Trials in multiple sclerosis (MS) defined four clinical courses of MS: relapsing–remitting MS, secondary progressive MS, primary progressive MS and progressive relapsing MS. Figure taken from Filippi et al.*[2]

Symptomatically, MS has been described since the 18th century, yet the mechanism of pathogenesis remains elusive. Different factors have been proposed to play a major role in the development of the disease, such as genetic predisposition, environmental factors, Epstein-Barr virus (EBV), ultraviolet radiation exposure and Vitamin D deficiency. [1,3] Genes in the HLA antigen locus are the strongest risk factor of MS development, however, they only explain only 20% to 30% heritability, suggesting the remainder of heritability is related to epigenetic factors and gene-gene or gene-environment interactions.[4] Environmental factors such as early life events, coupled with predisposing genotypes lead to faulty immune response, causing activation both adaptive and innate immune cells, which can penetrate the blood brain barrier (BBB). Numerous complex events take place to set off pathologic events which result in demyelination, axon and neuron damage, and gliosis. Continuous inflammation, oxidative damage, abnormal energy metabolism, activation of the innate immunity in the CNS and incomplete repair of the neuron tissue, forms the injury and exhaust the compensatory mechanisms. All mentioned processes result in progressive neuronal degeneration.[1,5]

Recent studies indicated that multiple genes are shared by other autoimmune disorders. However immunosuppressive therapies modify the disease course, as well a high risk of several autoimmune

diseases in MS patients.[6] Due to the lack of autoantibodies or antigens associated with the disease, MS is considered a primary organ-specific autoimmune disease.

1.2. Disease mechanism

The full mechanism of action of MS remains unresolved. Historically, MS was considered as a T-lymphocyte–mediated disease, however, later studies showed that both innate and adaptive immune cells are involved in the inflammatory process, and resident immune cells of the CNS are causing damage to the neural tissue. The overexpressed Major Histocompatibility Complex (MHC) I and II together with secreted cytokines lead to infiltration of the immune cells crossing the BBB and leading to CNS lesions. T (CD4 and CD8) cells, B cells, monocytes, macrophages and dendritic (DC)-like cells secrete pro-inflammatory cytokines, nitric oxide, and matrix metalloproteinases that contribute to the damage of the myelin sheath.[7,8]

Macrophages and microglia are the most common cells involved in the lesions, where they reactivate T cells and B cells and directly damage neural tissue (Figure 1.2.).
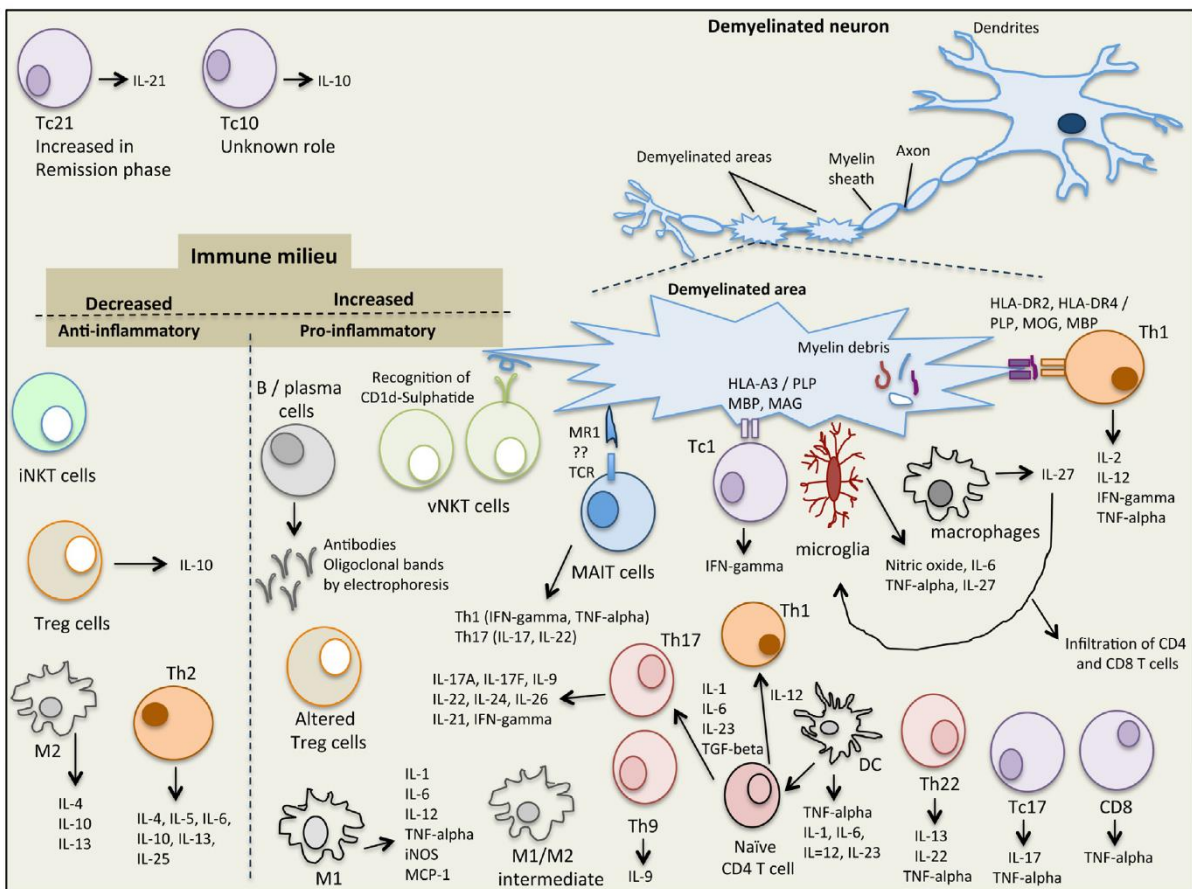
Figure 1.2. *Detailed mechanism of MS development. Figure is taken from Dargahi et al.[9]*

The innate immune system is the oldest protective mechanism, which was the earliest one developed in the living organisms. Monocytes, macrophages, and dendritic cells are part of innate immunity. They are the most reactive among white blood cells and the first protective line against microorganisms. However, if the immune system does not work properly, cells of the innate immunity facilitate in development of the autoimmune processes. Astrocytes, dendritic cells, mast cells, and natural killer cells are involved in the innate immune reactions in the nervous system, macrophages and microglia are the most important innate contributors to pathological changes in MS.[10]

Circulating monocytes and macrophages can be polarized into pro-inflammatory M1 or anti-inflammatory M2 cytokine secretion phenotype. [11] M1 phenotype is characterized by the expression of CD40+, CD86+, CD64+, CD32+ surface markers and induced by the presence of pro-inflammatory cytokines, toll-like receptors, LPS and chemokines. M1 polarized cells secrete IL-1β, TNF-α, IL-12, IL-6, nitric oxide (NO) and reactive oxygen species (ROS). The M2 polarized cells are characterized by the expression of CD163+, CD206+ and induced in the presence of IL-4, IL-10, IL-13. M2 cells secrete anti-inflammatory cytokines, such as IL-1Ra (receptor antagonist), IL-4, IL-10 and transforming growth factor (TGF)-β1.

Monocytes and macrophages play an important role in the pathogenesis of MS. Similar to macrophages, microglia cells belong to innate immunity and can be polarized towards M1 or M2 microglia cells. Proinflammatory M1 cells show inflammatory properties, if M2 are anti-inflammatory and expose CD206 and C-C motif chemokine 22(CCL22) as surface markers. M2 cells were shown not only to reduce inflammation, but are also important for remyelination.[12]

T cells include several cell types characterized by different functions. CD4 cells are T helper cells and can be differentiated into Th1, Th2, Th17 phenotypes. Th1 and Th 17 cells belong to pro-inflammatory phenotype and produce high levels of IL-2, IL-12, IL-17, TNF-α and IFN-γ. Th2 are an anti-inflammatory subset and produce IL-4, IL-5, IL-6, IL-10, IL-13, IL-25. During the development of MS Th1 and Th17, activated by the cells of the innate immunity, they infiltrate the CNS lesions and promote inflammation. Th1 recognize short 9–17 amino acid epitopes of the myelin basic protein (MBP) presented on the surface of antigen presenting cells (APC) in a complex with MHC class II (9-17 amino acids fragment). This leads to immune activation and induced autoimmunity against CNS.

CD8 cells are cytotoxic T cells or T killers and analogically recognize MHC class I which includes 7-9-mer peptide epitope presented on the surface of APC. MHC I is highly expressed within demyelinated scars of neurons, dendritic cell, macrophages, astrocytes, and oligodendrocytes. CD8 cells play a major

role in the inflammation development and are counted as 10:1 CD8:CD4 T cells for MS patients. CD8 cells secrete high levels of IL-17, IFN-γ, TNF-α.

Additionally, B cells play an important role in the development of the MS. Since the major role of B cells in the adaptive immunity is antibody production, for a long time it was believed to detect myelin basic protein binding antibodies, since B cells are widely present in the cerebrospinal fluid and brain parenchyma. More than 50 different antibodies were isolated from cerebrospinal fluid of MS patients. Interestingly, those antibodies did not react to MBP, however the activity of B cells within CNS of MS patients suggests that B cells contribute to the development of the disease.

1.3. Accessible treatment

Currently, MS is not curable. There is only disease-modifying treatment available, which targets different aspects of immuno-inflammatory processes. Approved treatments suppress the immune system, which increases the risks for infections and cancer.[13] Glatiramer acetate (GA), together with β-interferons (IFN-βs)[14], Dimethyl fumarate (DMF)[15] and sphingosine-1-phosphate receptor modulators are considered first-line treatment, and are administered subcutaneously or intramuscularly and orally respectively. They are considered the lowest risk medications but with modest effectiveness.[16] The second-line treatment show higher effciency, but also exhibit the higher toxicity and include natalizumab (Tysabri), fingolimod (Gilenya), alemtuzumab (Lemtrada), ocrelizumab (Ocrevus) and mitoxantrone (Novantrone). [17] The whole drug market volume of these medications is valued at US $22 billions in 2016, and GA and DMF making up the major part, followed by Fingolimod, a sphingosine 1-phosphate receptor modulator (S1P), and Natalizumab, the monoclonal antibody against the cell adhesion molecule α4-integrin (Figure 1.3.). The drugs can be classified by mechanism of action and be divided into S1P modulators, neurorestorative agents and immunomodulators.
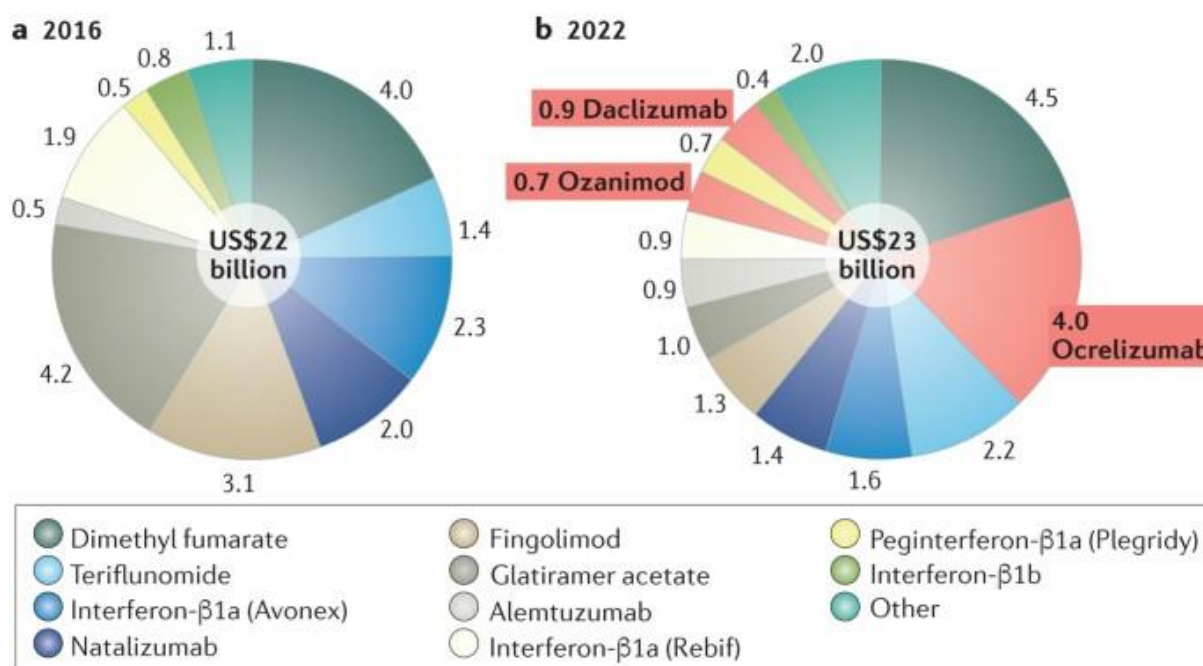
Figure 1.3. Worldwide sales (2016) and a consensus forecast (2022). New entrants are shown in red. Source: Evaluate Pharma. Picture taken from Westad et al.[18]

Immunomodulators, including GA, ocrelizumab and INF-β are meant to inhibit the immune response of MS. By preventing damage of myelin and inhibiting inflammation that produced as the consequence of the disease (Figure 1.4.).

The first immunomodulator for RRMS on the market was IFN-β.[19,20] Treatment with IFN-β results in balancing of expression of the inflammatory cytokines in the CNS, decreasing of the Th1 and Th17 reactive cells infiltrating through the BBB. This prevents further demyelination and promotes neuronal survival. IFN-β treatment decreases formation of the new lesions up to 50%, however it is associated with side effects such as liver damage. Due to its moderate effect and frequent side effects, the benefit of IFN is small.

Dimethyl fumarate (DMF) is another type of immunomodulators, was approved by the FDA in 2013. DMF prevents migration of inflammatory cells through the CNS as well as regulation of the oxidative stress by increasing glutathione levels. Comparatively low side effects and high effectiveness made DMF a widely used drug for MS treatment.

Teriflunomide is another example of small molecule drug being approved in 2012 by the FDA and used since for MS treatment. Teriflunomide has immunosuppressive properties and inhibits the

enzyme dihydroorotate dehydrogenase, and B and T cells proliferation. Side effects and limited efficientcy make the drug less common nowadays.

Fingolimod (S1P) is a sphingosine 1-phosphate (S1P) receptor modulator, which was approved by the FDA in 2010. By blocking the S1P receptor, it reduces the infiltration of the activated T cells into the CNS together with inhibition of proliferation of T cells.[21,22] Fingolimod accounts in 2016 for 3 billion USD in sales worldwide. However, subsequent studies showed an increase in bradycardia related to Fingolimod (SP1), which led to limited application of the drug.

Mitoxantrone is a strong immunosuppressor, used for cancer treatment. It disrupts DNA synthesis in cancer cells and rapidly dividing cells. By suppression of B and T cells, Mitoxantrone reduces disease progression by 84%.[23,24] The side effects for the treatment are severe due to high toxicity of the drug and limit its use as treatment for MS.

Several monoclonal antibodies are used for the treatment, such as Natalizumab - cellular adhesion molecule α4- integrin inhibitor, Ofatumumab - IgG1 kappa (IgG1κ) monoclonal antibody, Alemtuzumab - monoclonal antibody against CD52, Daclizumab - monoclonal antibody against CD25.
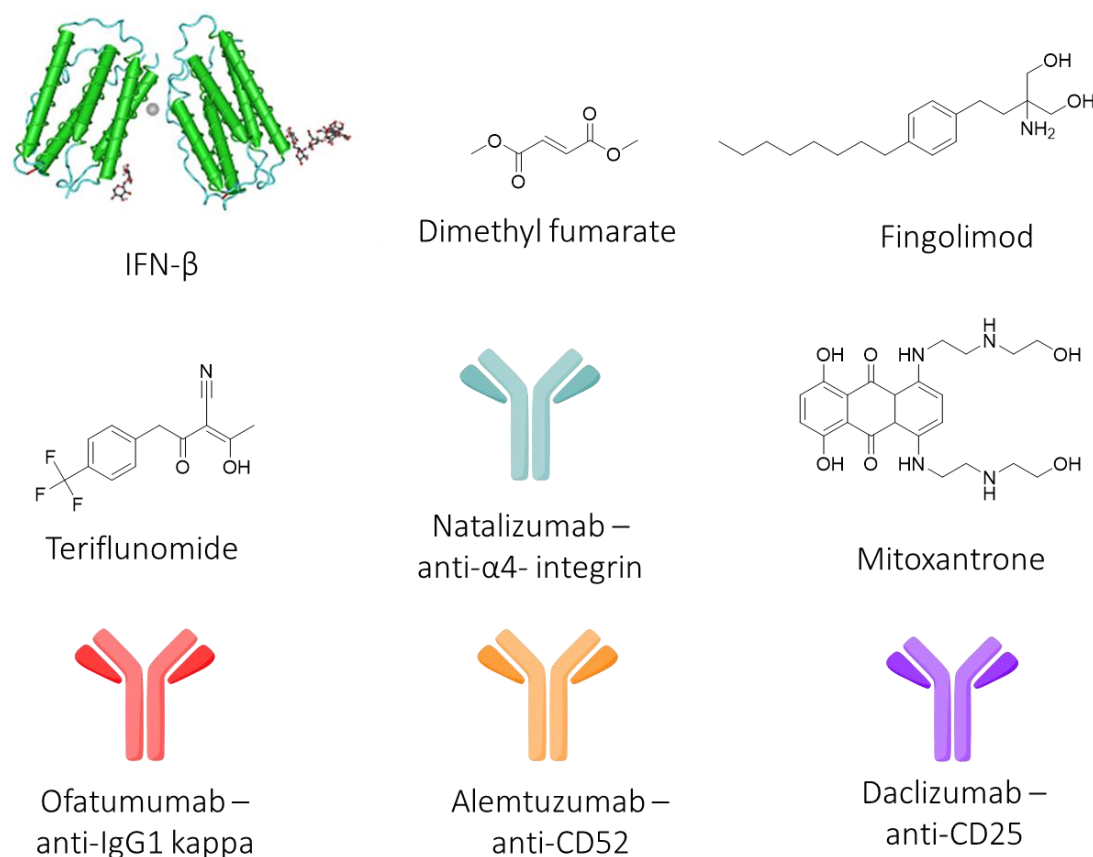
Figure 1.4. *Chemical structures of selected drugs for MS treatment.*

1.4. Discovery of GA

GA was approved in 1996 in the US and 2001 in Europe, being the dominant force on the market for treatment of MS for more than 20 years. The chemical composition makes GA a unique case among all existing medications, and it has no analogs on the market nor second generation compounds in clinical trials.

GA was initially synthetized in 1971 as an attempt to mimic myelin basic protein to induce experimental autoimmune encephalomyelitis (EAE) in mice, the most common animal model for MS. [25,26] Contrary to expectations, the synthesized polypeptides were not encephalitogenic, but actually exhibited a protective effect, perventing the development of the EAE in different species. [27]

The initial synthetic polypeptide Copolymer-1 was developed by the Weizmann Institute, Rehovot, Israel and was composed of only 4 amino acids. Glutamic acid, lysine, alanine and tyrosine, which led to the name GLAT, are composing the polymers with the ratio 1.9:4.7:6.0:1.0 respectively and has a molecular weight between 22-24 kDa. There were several copolymers synthesized, which are called glatiramoids. Having the same or similar amino acid composition, they differ a lot by their MW distribution. For market use, the copolymer is called GA and optimized to be in a range 5-9 kDa with amino acid ratio 1.4:3.4:4.2:1.0, which has better characteristics in terms of safety and effectiveness. Classical synthetic approaches (solid phase or synthesis in solution) do not allow to achieve the required size, so the following synthetic method was described.

The polymers were obtained from *N*-carboxyanhydrides of tyrosine, alanine, γ-benzyl glutamate and *N*-trifluoroacetyllysine (Figure 1.5.). The bifunctional amino acids are protected (the ε-NH_2 of lysine is protected by a trifluoroacetyl group and the γ-COOH of glutamic acid and -OH group of tyrosine are protected by a benzyl group). The polymerization occurs through the growth of linear chains from monomers at room temperature in anhydrous dioxane with diethylamine as initiator. For the polymerization reaction, the most important role plays the homopolymerisation constants of each activated amino acids, which differ due to steric factors, the nature of the substituent and the reaction conditions – temperature and concentration. After initialization of the polymerization by dimethylamine, the depolymerization and deprotection of the initially formed protected polypeptide mixture takes place. The final deprotection of the intermediate results in a large number of different polypeptides. The size distribution depends on the acetolytic conditions of the GA mixture. Purification and size exclusion followed by the ion exchange provide a desirable substance. [28,28,29]
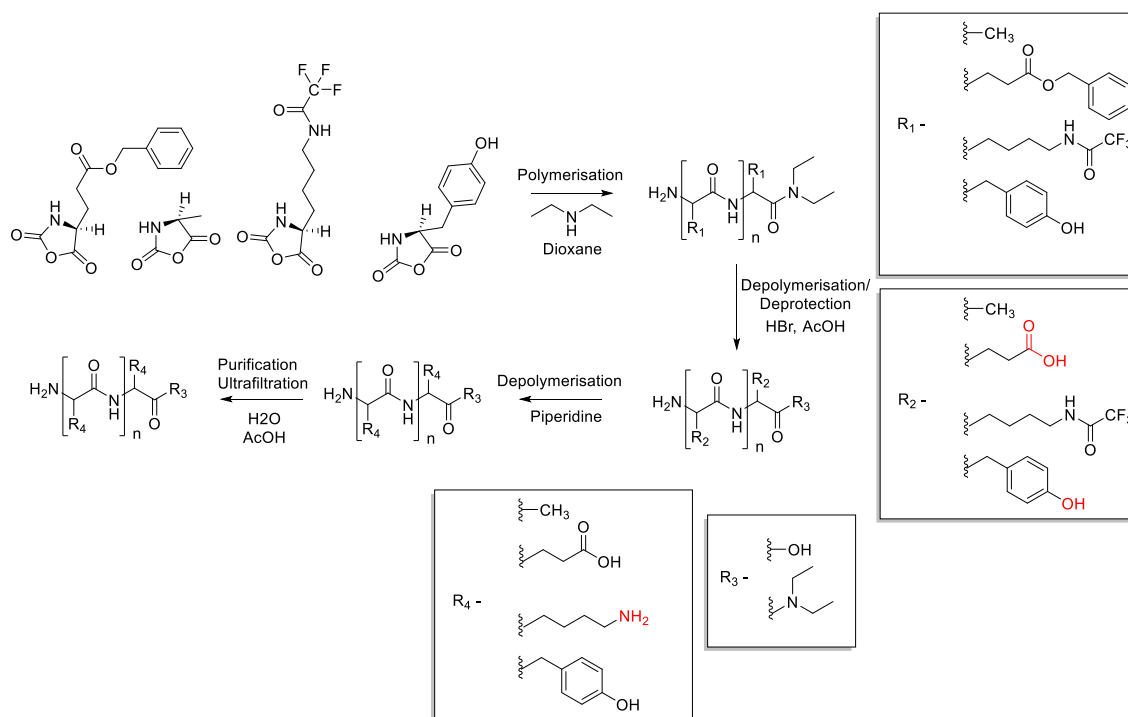
Figure 1.5. *General scheme of Glatiramer acetate synthesis and manifacture precesses.*

That unexpected discovery opened a new field for MS therapy. Placebo controlled trials successfully confirmed the activity and lack of significant side effects of GA, which led to its approvement as a drug.[30]

The consistency of polypeptide sequences within GA depends on a well-controlled proprietary manufacturing process. Copolymers can be distinguished by the molecular mass distribution profile, polypeptide mapping by capillary electrophoresis profile, certain non-random and reproducible patterns in amino acid sequences, secondary and tertiary structures, specific hydrophobic interactions due to unique charge dispersion, characteristic ratio between molecules with *C*-terminal carboxylates, *C*-terminal diethylamides, and proteolytic enzymatic profile.

Molecular mass distribution profile is a first method applied to the polypeptide mixture, which allows to determine the size distribution of the mixture using well characterized peptide markers. The polypeptide mapping by capillary electrophoresis allows to analyze the difference between copolymers. Following by the proteolytic hydrolysis by carboxypeptidase P (hydrolyses the peptide bond between glutamic acid and tyrosine) and separation on RP-HPLC of the fragments. Then the digested fragments are mapped via capillary electrophoresis. Additionally, classical spectroscopic techniques (Fourier-transform infrared, ultraviolet, proton and ^{13}C NMR spectroscopies) are used to characterize the primary structure of the polymers combined with Edman degradation method to characterize the amino acid composition.

Despite being available on the market for more than 20 years, the mechanism of action of GA remains elusive for both animal and *in vitro* models. The enormous number of potentially active epitopes 10^{36}, makes it impossible to identify or isolate the active sequences.[29]

1.5. General mechanism of action of GA

The general effect of GA is described as immunomodulation and neuroprotection. The effect of GA relies upon several mechanism of action as follows: GA is hydrolyzed at the site of injection, where it interacts with APC. Due to hydrophilic nature of GA and its metabolites it is very unlikely that these polypeptides would cross the BBB, suggesting that the effect must occur in the periphery.[31] In animal model, labelled GA was detected in the stomach and thyroid gland, while the lowest concentration was in the CNS.

The first hypothesis was based on the affinity of GA binds to purified MCH class II.[32,33] That fact was considered as an evidence of a direct interaction of the drug with antigen presenting cells (APC). However, this theory was abandoned since D-version of copolymer had similar affinity for MHC class II but had no activity towards Experimental Autoimmune Encephalomyelitis (EAE). Not only the stereochemistry plays role, but also has been shown that Lysine is essential for the activity, hence a copolymer composed of only glutamic acid, alanine and tyrosine was inactive. Additionally, the substitution of the other amino acids, for instance alanine with valine and isoleucine, tyrosine with phenylalanine and tryptophane and does not lead to a similar loss of activity.

The innate immune system is considered as one of the main targets of GA. It was shown that GA induces the differentiation of immune cells towards an anti-inflammatory M2 rather than a pro-inflammatory M1 state, an effect which can be tracked by monitoring various cell surface markers and cytokines.[28,34–38] GA treated monocytes and macrophages secrete increased amounts of IL-10, TGF-β, IL-1Ra, and decreased amounts of IL-1β, IL-12, Tumor Necrosis Factor alpha (TNF-α). Importantly, not only monocytes from healthy donors, but also circulating monocytes of the MS patients exhibited phenotypical shift towards M2.
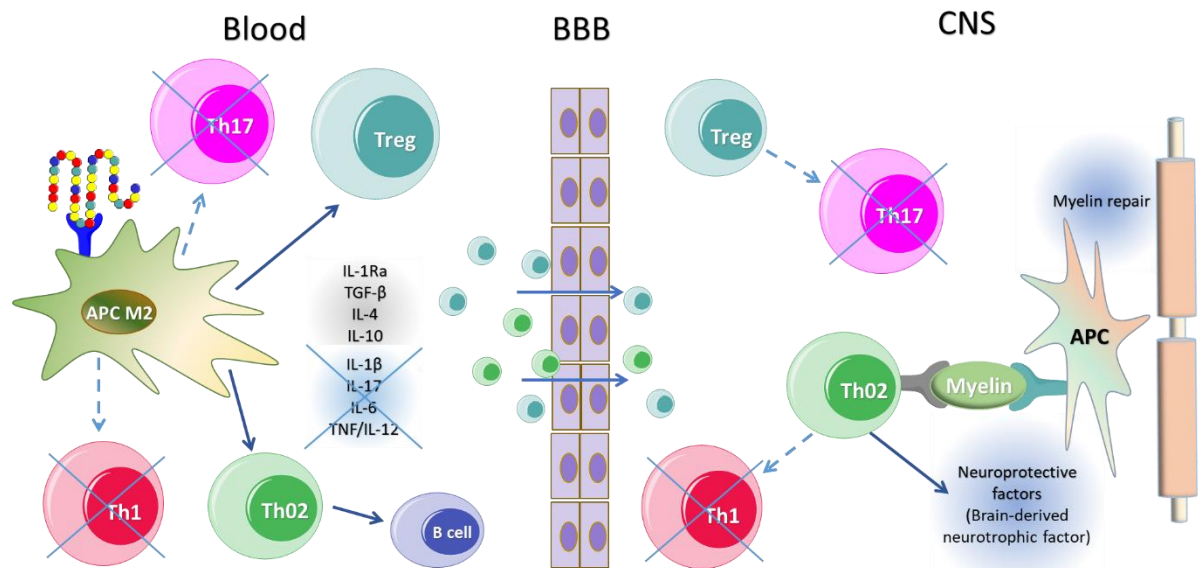
Figure 1.6. *Mechanism of action GA. GA binds to a receptor on APC, initiating the anti-inflammatory differentiation. APC stimulate T-cell differentiation towards T helpers 2 and T regulatory cells and downregulate T helpers 1 and T helpers 17. Reactive Th2/Treg cells cross the BBB, modulating B cell activation and down-regulate secretion of the proinflammatory cytokines in both in periphery and in CNS reducing the myelin degradation.*

Molecular mechanism for M2 shift for the APC is not clear, but the main hypothesis claims that GA interacts with a receptor on the surface of APC, leading to activation of second messengers resulting in M2 differentiation. It has been shown that PI3K/Act plays a role in the M2 polarisation. Also, treatment with GA inhibits signal transducers and activators of transcriptor (STAT)1. GA inhibits the reactivity of the monocytes in case of activation of its Toll-like receptors (TLR). [37]

APCs being shifted towards anti-inflammatory state promote T cell differentiation towards Th2 and Treg (Figure 1.6.). As discussed previously, T cells play a central role in the development of MS, therefore the polarized Th2 and Treg can cross the BBB and reduce inflammation in the CNS.

GA also showed an effect on B cells, similar to the cells of myeloid system: GA inhibits secretion of the inflammatory cytokines, such as IL-6, IL-12 and TNF-α and increase of IL-10 secretion.[39] Despite this, B cells play an important role in disease modulation. The effect of GA is indirect for B cells and is observed *in vivo*. However, it is still not clear if the response is achieved due to interaction with APC or via T cell regulation. GA effects B-cell phenotype downregulating the activation markers CD25, CD69 and CD95 *in vivo* together with up regulation of MHC class II.[39]

1.6. GA generics and analogs

The complexity of the polypeptide mixture represents a major challenge when it comes to industrial production of a generic version of GA. Only in 2015 the FDA approved the generic version of GA, Glatopa by Sandoz. The fact that the most widely used drug, which was sold for more than USD 4.2 billion worldwide did not have generics equivalents on the market for 19 years can be explained by the difficulties to reproduce the ratio and molecular weight of the polymers. Depolymerisation and purification also is present itself a complicated task which requires a detailed control and even then, the control of the polymers is extremely challenging. A number of glatiramoids was observed being active against EAE, some of them even exhibited cell toxicity.[29,40]

1.6.1 Glatopa

Glatiramer acetate is a chemically synthesized drug, hence for its generics there is a list of requirements for FDA approval. Active ingredients must be shown to be the same with the same dosage form, concentration, and bioequivalence as that of the approved drug. If the generics are therapeutically equivalent to the approved drug, then the need for the clinical trials can be avoided through an abbreviated new drug application (ANDA). Generic drug applications are named "abbreviated" because they are generally not required to include preclinical and clinical data to establish safety and effectiveness. Instead, generic applicants must scientifically demonstrate that their products are equivalent chemically and perform in the same manner as the innovator drug.*[28]*

GA is described as a complex mixture of amino acid copolymers, however it was eligible for approval via the abbreviated new drug application (ANDA) pathway. In 2015, the FDA approved the first generic version of glatiramer acetate, Glatopa, as an aqueous solution of the Copaxone in 20 mg/mL dosage form. It is a challenge to provide a definitive characterization of GA, but in combination with analytical quantitative analysis methods and a well-controlled, robust manufacturing process allowed to demonstrate the equivalence between Glatopa and Copaxone.

Four criteria had to be met to establish the equivalence of Glatopa and Copaxone:

1. Using the same starting materials and basic chemical steps (i.e., polymerization; depolymerization and deprotection; purification).

2. Structural signatures for each step during the synthesis, control of the amino acid ratio during polymerization, depolymerization and purification.

3. Analysis of the physicochemical properties includes amino acid composition, molecular weight distribution and spectroscopic fingerprints.

4. Biological and immunological properties are evaluated by a number of assays including antigen-presenting cell function, T-cell proliferation, B-cell biology, antibody response.

Additionally, to those mentioned criteria, other biological evaluation such as genes expression profiles and cytokine secretion were equal for Copaxone and Glatopa. However, 20-mg/mL version of Glatopa has been approved, 40-mg/mL dosage is still only available by Copaxone. Most likely it will change in the nearest future together with more generics coming to the market.

1.6.2. Star-shaped GA (sGA)

The only one known attempt to improve the performance of GA was demonstrated just recently.[41] Authors took a challenge to improve its fast degradation and clearance. The rapid hydrolysis occurring at the place of injection into amino acids and oligopeptides at the injection site within 1 h after injection. To solve that problem, it was proposed to change the structure.
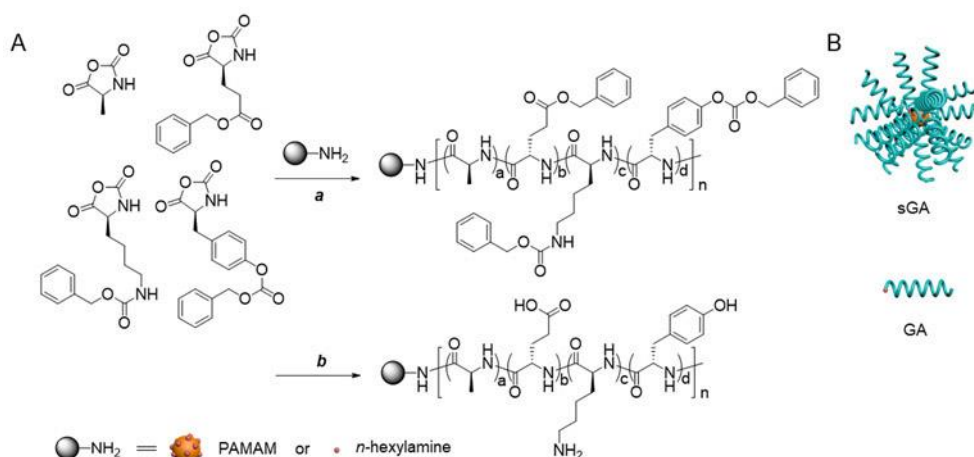
Figure 1.7. *Synthesis of sGA and GA. (A) Synthetic routes to sGA and GA. a DCM or DMF, room temperature, 2 h or overnight. b HBr, TFA, 0 °C, 1 h. (B) Schematic illustration of spherical, star-shaped sGA and linear GA. Picture is taken from Song et al.* [41]

The synthesis was similar to GA where *N*-carboxyanhydride (NCA) monomers were used. In case of the star-shaped GA the polymerization was conducted with poly(amidoamine) (PAMAM) 3rd generation as the initiator. Each PAMAM initiator contains 32 primary amine groups, which allows to generate a three-dimensional space, to form a star-shaped GA (Figure 1.7.). Even though the structure was different from linear GA, the secondary structure remains similar to GA (Figure 1.8.-a). Dynamic light scattering (DLS) analysis showed the size for both GA and sGA. sGA (98.4 nm) was much larger in size than GA (10.7 nm) (Figure 1.8.-b).
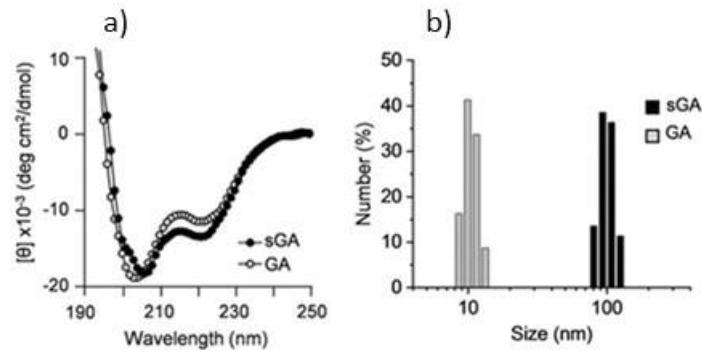
Figure 1.8. *Characterization of sGA and GA. (A) Normalized GPC-light scattering trace of polypeptide precursors of sGA and GA. (B) CD spectra of sGA and GA in an aqueous solution. Picture taken from Song et al.* [41]

This modification using PAMAM as an initiator allowed to obtain a GA derivative with a higher-ordered architecture. The modification resulted in increased density of its functional groups together with increased size of the final structure. Summarily, this is an improvement of its effect on immune cells by boosting its ability to bind cell surface molecules and cause greater internalization capacity.

Accordingly, the authors report in the article that sGA exhibits higher performance than linear GA in treatment of EAE. One injection of sGA at 2 days post-immunization at 10 mg/kg almost completely suppressed EAE symptoms (Figure 1.8. a). Addititonally, two injections of GA 10 mg/kg at 2- and 5-day post-immunization did not show significant suppression of EAE symptoms (Figure 1.9.)
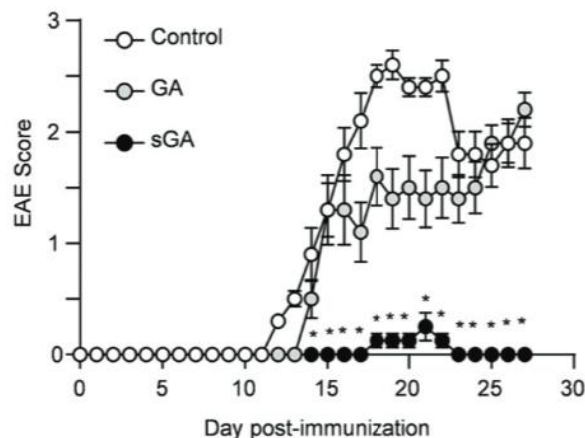
Figure 1.9. *In vivo therapeutic efficacy of sGA and GA treatment in EAE mice. (A) 6–8-week-old C57BL/6 mice were induced with EAE and treated with either sGA at 2 dpi (single injection, n= 4) or GA at 2 and 5 dpi (two injections=5) at 10 mg kg−1. The EAE behavioral score was monitored daily from 0 to 27 dpi for neurologic signs. *p< 0.05, two-tailed unpaired Student's t-test from 13 to 27 dpi. Picture taken from Song et al.* [41]

Overall, this precedent demonstrates significant improvements in effectiveness in treating EAE together with its improved stability toward degradation. At the same time, the problem of having a mixture of different structures remains unsolved and even becomes more complicated compared to linear GA. Those difficulties do not help either to solve mechanistic problems, or to simplify the synthesis.

1.7. In vitro model for GA

The classical way for drug discovery is to start from *in vitro* models using immortalized cell lines. Since the action of GA was discovered on the EAE model, most of the research use that model for the discovery of properties of the investigational drug. Another popular approach is using blood of MS patient's *ex vivo* which allows to observe the difference with the treatment and in its absence.

MS is a complex disease including many pathological processes running in parallel and interacting with each other. Hence, there is no standard *in vitro* assay for activity against MS, as it exists for cancer research or many others similar diseases. In case of MS, every drug has a particular mechanism of action, and it is important to investigate every mechanism and find an *in vitro* model specifically. For instance, the working *in vitro* model for GA would not work for DMF treatment or vice versa. Since GA is primarily affecting APC, measuring levels of different cytokines is a common method to assess the activity.

1.7.1. IL-1Ra secretion on primary human monocytes in response on GA treatment

One of the *in vitro* models for GA activity was proposed by checking the secretion of the IL-1Ra (receptor antagonist) for both monocytes of the healthy donors and MS patients. IL-1Ra is a natural inhibitor of IL-1β, the pro-inflammatory cytokine, which plays a major role in the development of inflammation. IL-1β can be secreted due to bacterial infection or via T cell activation and plays a significant role in the EAE pathogenesis. IL-1Ra binds to the same receptor as IL-1β, but without triggering a signal and is considered an important regulator of the overall immune response mediated by IL-1 family (Figure 1.20.).
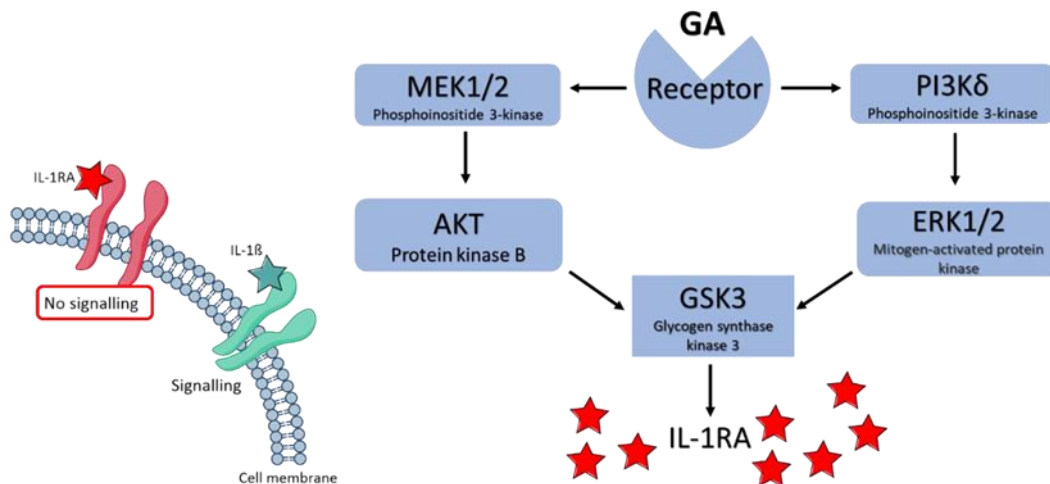
Figure 1.20. *Model of how GA activates PI3Kδ/Akt and MEK/ERK pathways to induce sIL-1Ra production. GA is recognized by a receptor (cell surface) or a sensor (inside the cell) that transduces signal via activation of both the PI3Kδ/Akt and MEK/ERK pathways. The two pathways then converge to phosphorylate/inactivate GSK3, resulting in the induction of sIL-1Ra production in monocytes.*

Previous studies showed, that GA signals through two parallel pathways, PI3Kδ/Akt and MEK/ERK cascades, which results in phosphorylation of GSK3α/β and induction of IL-1Ra production.[42]

GA affects both IL-1b and IL-1Ra on monocytes in chronic/sterile (via T cell activation) and acute/infectious (via LPS stimulation) inflammatory conditions (Figure 1.21.). The secretion of IL-1Ra was significantly increased in response on GA treatment, in presence of both stimuli – LPS and isolated T cell membrane and in neutral conditions. At the same time, expression of IL-1b was decreased in case of T cell activation, however in presence of LPS it remained high.
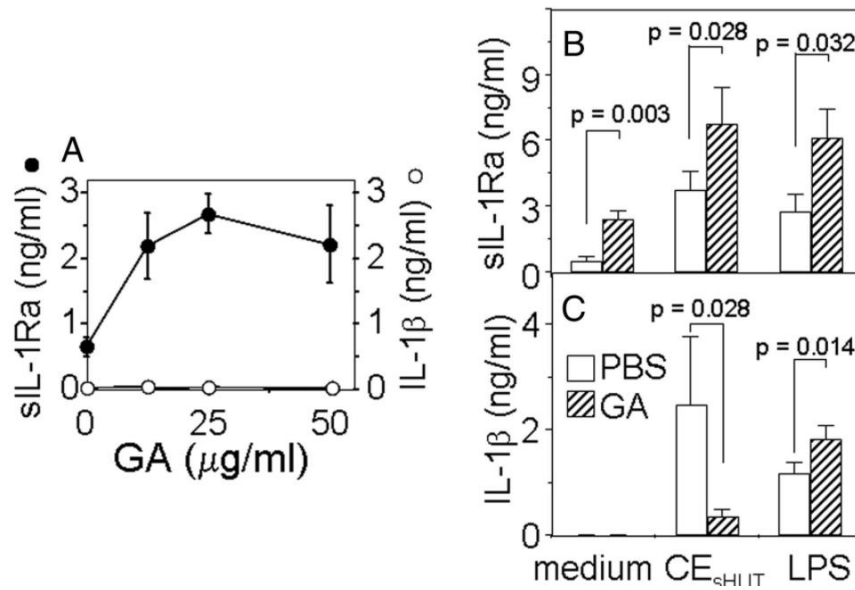
Figure1.21. *Regulation of IL-1β and sIL-1Ra in human monocytes by GA treatment. (A) Monocytes were activated with the indicated dose of GA. After 48 h, supernatants were harvested and the production of IL-1β (open circles) and sIL-1Ra (filled circles) were measured in triplicate wells and represented as mean ± SD. Results are representative of 3 different experiments. (B) Monocytes were preincubated for 1 h with or without 25 µg/mL GA and then cultured for 48 h in the presence or absence of CEsHUT (1 µg/mL) or LPS (100 ng/mL). (C) Monocytes were preincubated for 1 h with or without 25 µg/mL GA and then cultured for 48 h in the presence or absence of CEsHUT (6 µg/mL) or LPS (100 ng/mL). Figure taken from Burger et al.* [43]

To prove that IL-1Ra is affected in EAE model, mice were threated either with GA or PBS as a control. At the peak of disease development, mouse sera were analyzed for presence of IL-1Ra. Inthreated mice IL-1Ra was significantly higher compared to controls (Figure 1.22.).
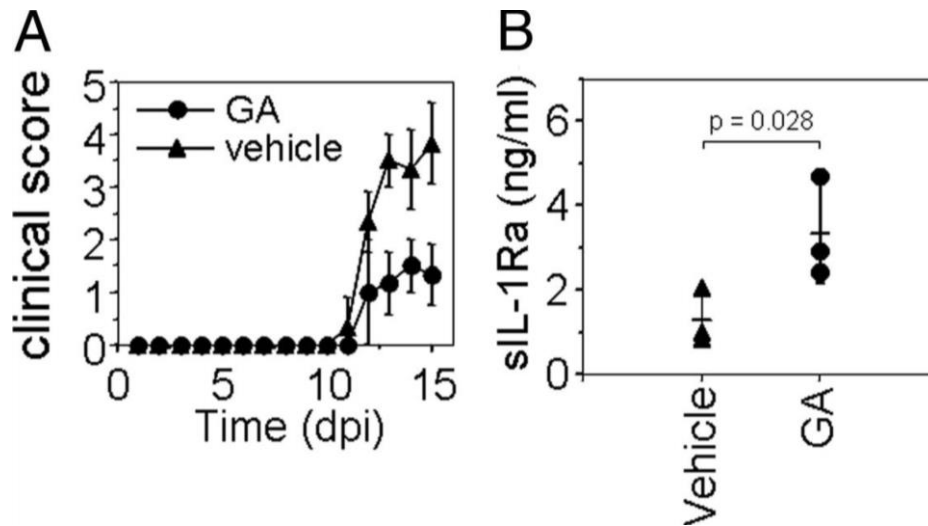
Figure 1.22. *sIL-1Ra levels are elevated in sera of EAE mice treated with GA. (A) GA ameliorates EAE. C57BL/6 mice were injected s.c. daily with GA (150 µg) or vehicle (PBS solution) 7 d before immunization with 10 µg myelin oligodendrocyte glycoprotein 35–55 peptide day post-immunization (dpi). (B) EAE mice treated (GA) or not (vehicle) were sacrificed at disease peak and their serum analyzed for IL-1β and sIL-1Ra content. Figure taken from Burger et al.[43]*

IL-1Ra is a potent regulator of the IL-1 family and considering its ability to penetrate the BBB, can reduce inflammation in both systemic and CNS compartments. Finally, discovery of two parallel pathways which result in the induction of IL-1Ra suggests the existence of a specific receptor for GA in monocytes.

1.7.2. Other cytokines modulation

Glatiramer is known to affect all types of APC cells and switch their activation towards M2 anti-inflammatory phenotype. Dendritic cells are the most potent APC and play a key role in the activation of Th cells either towards Th1 inflammatory or Th2 anti-inflammatory subsets. GA influences cytokine regulation on DCs. It has shown that for both DC of the healthy donors and MS patients the levels of secreted IL-10 are enhanced (Figure 1.23.). At the same time, levels of IL-12 were reduced. IL-10 is an anti-inflammatory immunoregulatory cytokine which downregulates development of the Th1 cells and inhibits synthesis of pro-inflammatory cytokines such as TNF-a, IFN-γ, IL-2 and IL-3. Upregulation of IL-10 serves as evidence of anti-inflammatory phenotype. Conversely, IL-12 induces inflammation and promotes Th1 differentiation. Similar properties of GA to induce IL-10 on DC and macrophages were observed in rats (Figure 1.23.).[35]
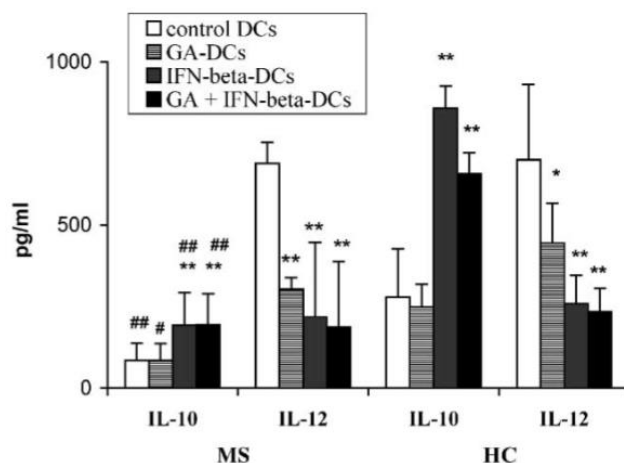
Figure 1.23. *Effects of INF-β and GA on cytokine production on dendritic cells of MS patients and heathy donors after 7 days of incubation. Results are shown as the mean ± S.E.M. Figure taken from Weber et al.*[36]

Not only the expression of anti-inflammatory cytokines plays an important role, but also inhibition of the secretion of the pro-inflammatory cytokines. It was shown that GA inhibits expression of the TNF-α in response to different concentrations of LPS (Figure 1.24.). This finding suggests that APCs may be the primary target for GA- mediated immune modulation. Monocytes have been observed to react less towards LPS stimulation and induce less signalling lymphocyte activation molecule (SLAM) presentation such as CD25 and CD69.
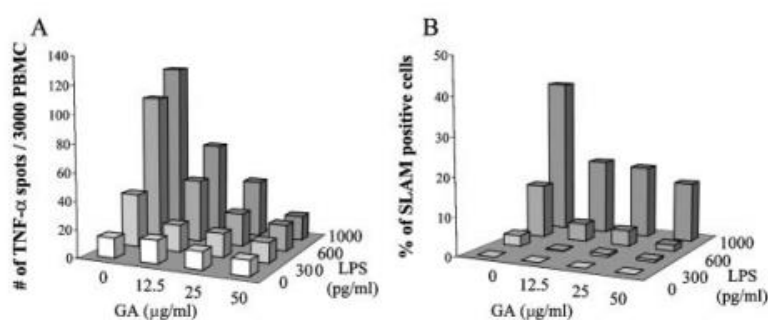
Figure 1.24. *GA-mediated inhibition of LPS stimulated monocyte responses in vitro. (A) Monocyte's reactivity was measured as LPS-induced TNF-α production by Elispot assay. (B) Monocyte's reactivity was measured as LPS-induced SLAM.). Picture is taken from Weber et al.* [36]

Similar effect to LPS stimulation has been observed for several of different TLR-2 (LTA – lipoteichoic acid and PNG - peptidoglycan), TLR-4 (LPS), TLR-5 (flagellin) ligands and inflammatory cytokines (GM-CSF – granulocyte-monocyte colony-stimulating factor, IFN-γ). GA consistently reduced the release of TNF-α for both TLR-stimulated (87% inhibition) and GM-CSF and IFN-γ -stimulated (47% inhibition) monocytes. (Figure 1.25).
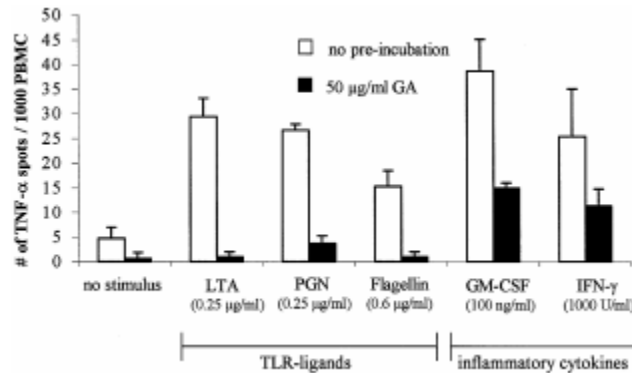
Figure 1.25. GA-mediated inhibition of monocyte responses simulated with different TLR ligands (LTA, PGN and flagellin) or inflammatory cytokines (GM-CSF, IFN-γ). Monocyte activity was measured as TNF-α by Elispot assay. Figure from Weber et al.[36]

1.7.3. Surface markers expression and M1/M2 differentiation

Not only the secreted cytokines, but also up- and downregulation of some specific surface markers can indicate the activation state of the APC and its phenotypical shift. Monocytes express a variety of different receptors, such as CD14, CD11b, CCR2, CD16, CD68, CD206. Depending on the environment, such as different cytokines or stimuli, cells have tendency to regulate the markers accordingly.

CD14 is the most expressed glycoprotein, which serves as an indirect receptor for complexes of LPS. Being highly present on monocytes, it often serves as a marker for monocytes/macrophages. CD14 plays a protective role against bacterial infections, the upregulation of the receptor can be caused by inflammatory activation. At the same time, treatment with anti-inflammatory cytokines leads to downregulation. It has been shown, that IL-4, as an anti-inflammatory cytokine not only inhibits secretion of IL-1 and TNF-a, but also downregulates CD14 secretion.[44]

Another highly expressed receptor CD16 is a low affinity IgG receptor, which is also crucially involved in phagocytosis.[45] Phagocytosis is an important step in the destruction of pathogens. It also promotes an inflammatory response in myeloid cells and induces cytokine expression or inflammasome activation. Downregulation of CD16 has beenobserved previously in response to treatment of monocytes with acetyl salicylic acid and *n*-butyrate.[46,47]

Recruitment of monocytes at inflammation sites is regulated by chemokines. Monocyte chemoattractant proteins (MCPs) activate inflammation of monocytes through activation of their cognate receptor, CC chemokine receptor 2 (CCR2). Recent studies have demonstrated, that expression of CCR2 is affected by inflammatory stimuli and is sufficiently upregulated by proinflammatory cytokines, growth factors such as granulocyte-macrophage colony-stimulating factor, macrophage colony-stimulating factor, and MCP-1 itself.[48]

Human leukocyte antigen-DR (HLA-DR) is involved in antigen presentation of antigens to adaptive immune system cells, particularly T cells. Monocytes that have lower levels of HLA-DR expression, are considered important mediators of immunosuppression. It was shown, that those monocytes which downregulate HLA-DR expression, convert from an inflammatory to an anti-inflammatory phenotype.[49] Interestingly, even though GA has high affinity to MHC II, on mature dendritic cells of MS patients, GA shows decreased HLA-DR expression.[50,51]

CD206, a mannose receptor, is mostly expressed on the surface of macrophages and dendritic cells. CD206 is widely recognized as a representative M2 marker.[52,53] This finding supports the previous report that CD206 was significantly increased on M2-polarized monocytes. Opposite, CD206 was reduced if these cells had M1 phenotype.[54]

CD68 is well known as a surface marker, specific for myeloid cells, especially highly expressed in macrophages. CD68 is a glycosylated transmembrane glycoprotein. The function of CD68 is not well understood. It is known, that its preferential location within late endosomes suggests about its role in peptide transport/antigen processing.[55,56] CD68 belongs to the receptors which are expressed due to activation of the monocytes and macrophages, however it has been shown to be downregulated in response to treatment with infliximab. Infliximab is a chimeric monoclonal antibody against tumour necrosis factor and induces M2 immunosuppressive macrophages. Infliximab is used for treatment of autoimmune inflammatory diseases, such as Crohn's disease (CD) and ulcerative colitis (UC).[57]

1.8. Anti-inflammatory peptides and dendrimers

There are no analogs which with action patterns to GA. Several examples of peptides and peptide dendrimers exhibiting anti-inflammatory properties bringing a potential to cure autoimmune based diseases have been reported.

1.8.1. Anti-inflammatory peptides

Many peptides are known to exhibit anti-inflammatory properties, modulate EAE and in MS treatment, induce neuroprotective properties. The polarization, which occurs in response to treatment is triggered by different mechanisms, at the same time there are no known analogs of GA sharing the structure features and similar mechanism. A variety of different peptides is known to have cyclic structure, mimic myelin proteins or were achieved by computational docking to have specific protein–protein interactions (Table 1.1.). Several peptides have been discovered as anti-microbial peptides, having at the same time anti-inflammatory properties, hence it is a popular combination.[58–60] To expose anti-microbial properties peptides are often positively charged, to increase interaction with the negatively charged bacterial surfaces. Alternatively, they have a higher ability to penetrate cell membrane better or expose

higher affinity to a cell membrane. Intracellular uptake can be achieved by coupling to a carrier system – liposomes or protein transduction domain.

Table 1.1. *Sequences of the anti-inflammatory peptides and their mechanism of action.*

Name	Sequence	Activity
Suppressor of Cytokine Signaling proteins (SOCS)	DTHFRTFRSHSDYRRI	Inhibition of Janus kinase, active towards Autoimmune encephalitis
Chromofungin	RILSILRHQNLLKELQDLAL	Upregulation of M2 macrophages, inhibits TLR 4 and NF-κB signaling
[K6T]P8 peptide	KVTAMTCFLL	Inhibitor of IL-15 receptor, active towards Rheumatoid Arthritis
Cyclotide	GLPVCGETCVGGTCNTPGCTCSWPVCTRN	Inhibits T cells proliferation

Suppressor of cytokine signaling proteins (SOCS) are known to prevent LPS activation and on APC together with inhibition of NO, interleukins, and TNF-α. The mechanism of action is related to regulation of the Janus kinase (JAK)/signal transducer of activation (STAT) pathway by reducing the phosphorylation of JAKs and STATs.[61]

Chromofurgin is a shorter fragment of Chromogranin-A, is a natural protein, secreted by neuroendocrine cells to regulate intestinal inflammation and immune dysregulation. Cromofurgin exhibited activity towards Crohn's disease and ulcerative colitis, which is caused by abnormal immune response within the intestinal wall is directed against luminal bacterial antigens inducing intestinal tissue damage. [62] Cromofurgin suppresses the pro-inflammatory macrophages by inhibition of Toll-like receptor 4/nuclear factor kappa-light-chain-enhancer of activated B cells (NF-κB) signaling, which results in reduced levels of IL-8 and leads to expression of IL-10 and TGFβ1, causing the repair of tight junction (TJ) and the recovery of the IECs (intestinal epithelial cells) homeostasis.[63]

Peptides can be structurally modified to fulfil certain properties such as inhibition of inflammatory cytokines. IL-15 is an inflammatory cytokine which is prevalent in the development of autoimmune disorders as MS and rheumatoid arthritis (RA). An antagonist of IL-15, [K6T]P8 peptide has been discovered by screening of IL-15 fragments. The short sequence [36]KVTAMKCFLL[45] was binding the IL-15 receptor but did not trigger a signal.[64]

Cyclotides are a group of peptides which can be produced ribosomal and characterized by cyclic topology. This structure leads to an unique biological activity and significantly increased stability.

Cyclotide [T20K] kalata B1 expresses an activity towards T cell regulation and inhibiting IL-2 biology, causing proliferation inhibiting and reducing IFN-γ and TNF-α production.[65,66]

1.8.2. Dendrimers

Dendrimers are highly ordered and repetitively branched molecules, composed of a group of branched monomers. Dendrimers consist of different layers, which are termed generations and branching points. Generally, the core is termed as generation 0, and while increasing the number of branching points the number of generations grows accordingly.[67,68]

Dendrimers can be synthetized in two different approaches: convergent and divergent. The convergent way was proposed in 1989 by Hawker and Frechet. [69] The dendritic fragments are obtained by starting from the periphery and finishing on the core (Figure 1.26.). The advantage of the convergent approach is in the control over the nature of the core.

In the divergent approach the growth is initiated at the core and progresses towards periphery (Figure 1.26.). [70] A characteristic of the divergent growth approach is that the number of terminal functional groups follows a strict geometrical progression and was described by Tomalia in 1894.[71,72]
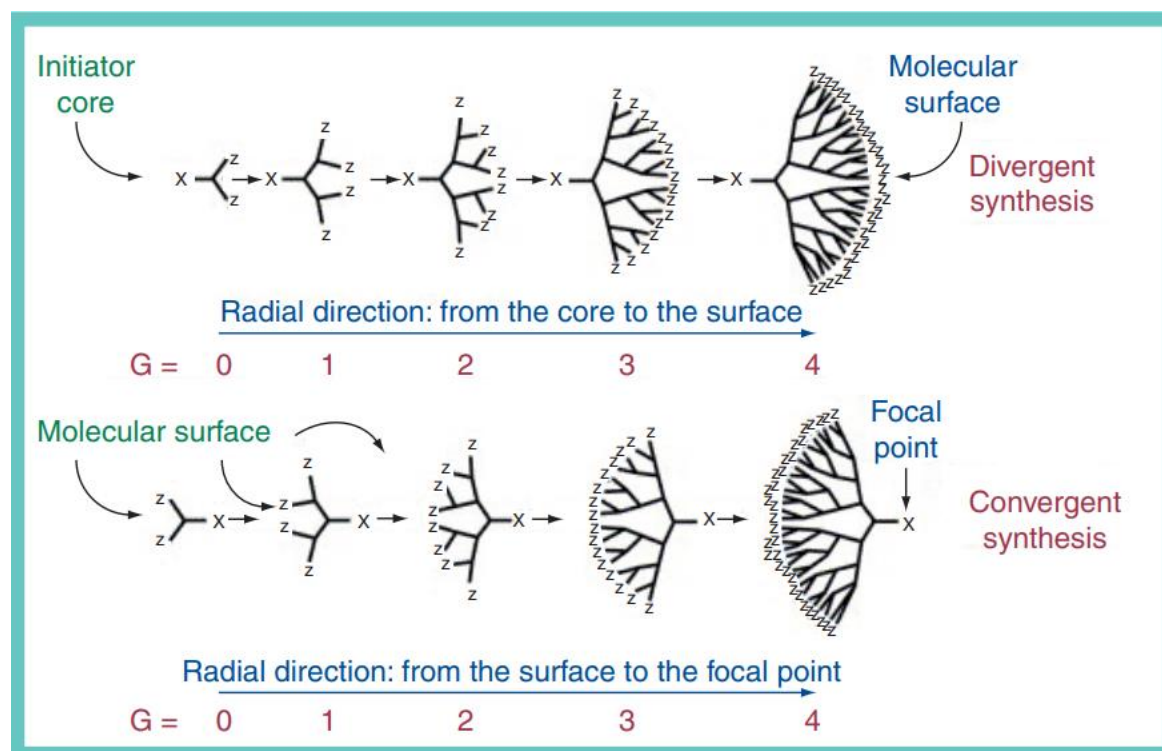
Figure 1.26. *Convergent and divergent ways for synthesis of dendrimers. Figure taken from Pearson et al.*[73]

1.8.3. Anti-inflammatory dendrimers

PAMAM dendrimers are known to exhibit inti-inflammatory properties towards inhibition of LPS-induced nitric oxide (NO) and cyclo-oxygenase 2 (COX-2) activity (Figure 1.27.).[74–76]
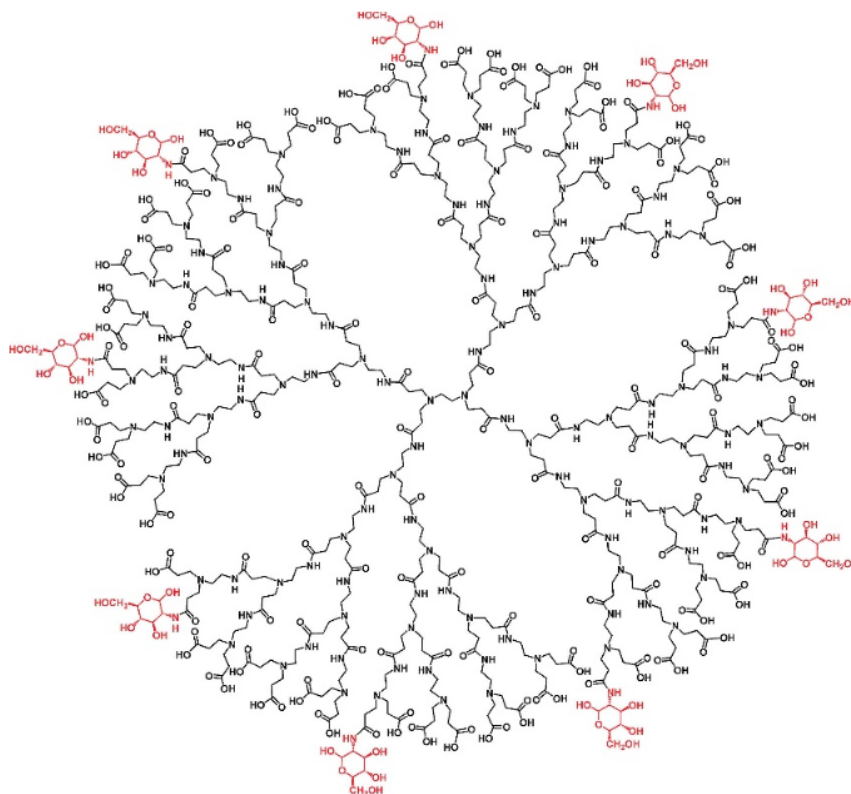
Figure 1.27. *Representative structure of protonated, generation 3.5 PAMAM dendrimer glucosamine. Picture taken from Park et al.[77]*

PAMAM dendrimers are highly symmetrical macromolecules exhibiting very systematic nanoscale diameter enhancements as a function of generation (1-10; ∼1-12 nm). PAMAM dendrimers are often used as delivery agents for poorly soluble drugs and opens the possibilities for genes delivery. High surface functionality allows to design the carrier depending on each requirement being useful for both passive and receptor mediated targeting.[78–80]

Anti-inflammatory activity of PAMAM dendrimers was a serendipitous discovery, while the dendrimer was used to increase solubility of the indomethacin by utilizing known PAMAM dendrimer encapsulation and complexation properties for sustained release/targeting of indomethacin. Later it was noticed that PAMAM on its own was exhibiting higher activity than the poorly soluble indomethacin.

Another example of anti-inflammatory modulators is azabisphosphonate (ABP) dendrimers (Figure 1.29.). Compared to PAMAM dendrimers, ABP present a group of anionic dendrimers, however,

are also used in drug encapsulation. Human monocytes have been shown to be activated by phosphonic-capped dendrimers, which has been confirmed by morphological and phenotypical changes (Figure 1.28.).[81,82]
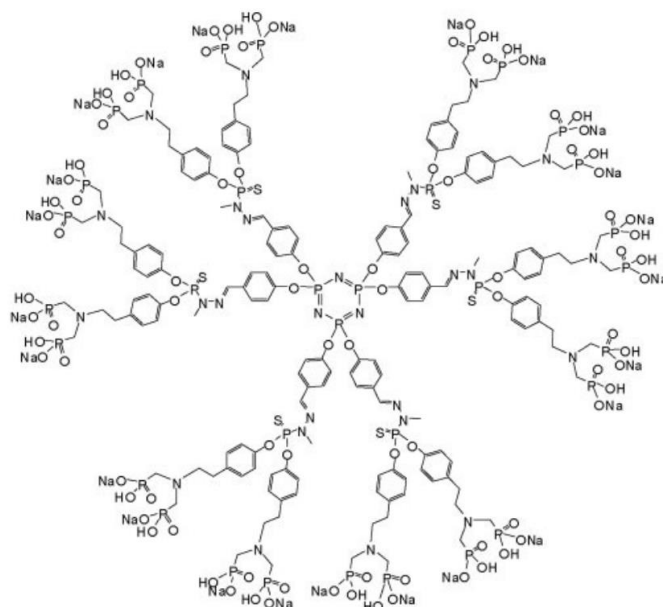
Figure 1.28. Representative structure of acid azabisphosphonic-capped, phosphorus-containing dendrimer. Picture taken from Degboé et al., 2014 [83]

Anti-inflammatory phenotypical shift on primary human monocytes has been confirmed by qRT-PCR where expression of proinflammatory cytokines was diminished, and the cytokines of an alternative activation were upregulated compared to untreated control (Figure 1.27.).[68]
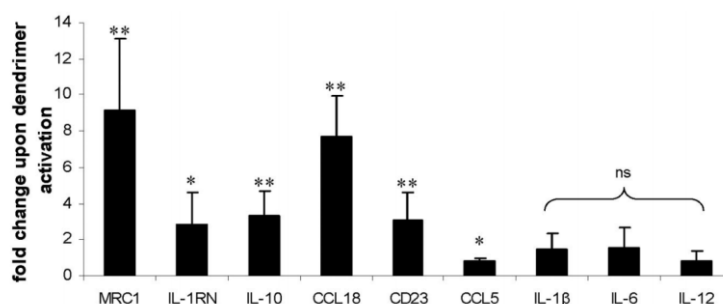
Figure 1.29. Representative qRT-PCR quantification of mRNA expression for nine selected genes on human monocytes in response on treatment with acid azabisphosphonic-capped, phosphorus-containing dendrimer (structure is shown above). Expression was normalised to the GAPDH mRNA. Data are expressed as mean ± SD from six independent experiments. Figure from Fruchon et al. [84]

While both dendrimers expose strong evidence of M2 phenotype shift of the immune cells, the mechanism of activation towards anti-inflammatory response is not clear for both cationic and anionic dendrimers.

1.9. Conclusion

In the current review we discussed the pathogenesis of the MS, the pathway of the development of the disease. Here we observed the current issues of the MS treatment and its main drugs, which are available at the market. Giving an historical review on the GA discovery, we describe how the Glatiramer was discovered and explain why there is a difficulty identifying an *in vitro* model for the activity testing not only for GA, but also in general for the MS.

Next, we discuss the current manufacture process of the GA and its difficulties, leading to the lack of the generics at the market. After looking into the mechanism of action of the GA, we observe the available *in vitro* models for the GA and its properties in the modulation of the inflammation on primary blood cells. We discuss the difference in the response of the different donors on the treatment with GA, which we have observed later while conducting our experiments.

Then, we bring into the discussion several anti-inflammatory peptides and peptide dendrimers, showing the findings of the other groups about their properties and their biological action.

Considering the complicity of the given task to prepare a well-define molecule with the size range of GA and the similar amino acid composition in the next chapter we discuss in the details all the methodological findings we had to perform to be able to achieve our goals in the post efficient way.

Overview of the thesis

The aim of the thesis is to find peptide dendrimers with anti-inflammatory properties similar to Glatiramer acetate, the blockbuster drug for MS treatment. Here we discuss the pathogenesis of MS, its mechanism of action and the most popular drugs for its treatment and investigate their action. Since there are only a few analogs have been published, we look in details on the complex manufacture process of GA synthesis and *in vitro* model. Here we also report peptide and peptide dendrimers with anti-inflammatory characteristics, which can serve as a reference point in building our peptide dendrimers.

To access the library of peptide dendrimers and their fluorescently labelled analogs, we describe our optimisation findings in the methods. Nevertheless, the Solid Phase Peptide Synthesis (SPPS) is well optimised, the size limitations of the required more optimisation of the synthesis and careful design of the experiments. To evaluate the activity of the dendrimers we focused on the *in vitro* model requiring primary blood cells of healthy donors, specifically monocytes. Here we explain in detail how the selection of the extraction conditions worked. Then, we describe in detail the blood separation techniques and discuss which are the best suited to fulfil the limitations of the experiments. Then we explain how the libraries of peptide dendrimers were generated and the visualisation using TMAR was achieved.

In this thesis we report 89 peptides and peptide dendrimers tested for anti-inflammatory activity. Initially, we discovered two active dendrimers **32** and **34** exhibiting the anti-inflammatory properties. In order to investigate the Structure Activity Relationship (SAR), we created a library of analogs of the active dendrimers and their fluorophore conjugates.

To investigate better the biological action, the performed a detailed biological evaluation of our dendrimers on the cells of adaptive and innate immunity. Here we describe the affinity of the fluorescently labelled dendrimers within a cell and to the different types of white blood cells. We observed the donor specificity in response on treatment with both GA and our dendrimers. Finally, the multicolor flow cytometry and immunostaining experiments indicated the difference in the action of our dendrimers and GA.

2. Methods

To assess and confirm the immunomodulatory properties of GA on primary blood cells but with chemically define peptide dendrimers, we demonstrate a range of different synthetic and biological experiments, which are explained below with detailed procedures present in the experimental part.

2.1. Solid phase synthesis of peptide dendrimers

The Fmoc-SPPS strategy for peptide synthesis is the most reliable and efficient technique, which allows to achieve reliably any type of peptides avoiding multiple purifications. In our research group, we employed SPPS not only for the linear peptide synthesis, but also to obtain peptide dendrimers (Scheme 2.1). Having lysine as a branching point and expanding symmetrical branches, a broad range of different structural properties can be achieved.
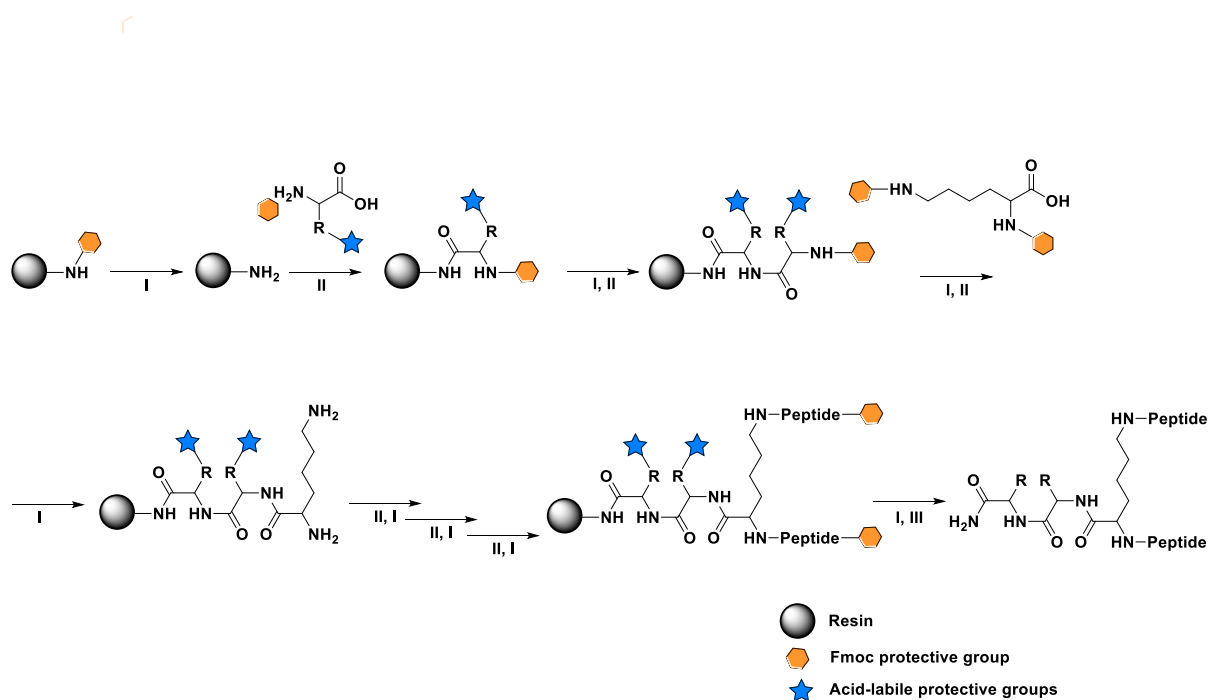
Scheme 2.1. General scheme of solid-phase synthesis of peptide dendrimers. I Fmoc-Deprotection: piperidine/DMF (1:4, v/v). II Coupling: 5eq/coupling-site Fmoc-amino acid, 5eq/coupling-site Oxyma, and 5eq/coupling-site DIC in DMF. III Cleavage: TFA (94%), TIS (1%), H2O (2.5%), EDT (2.5%). After peptide dendrimers were lyophilized and purified by preparative RP-HPLC. In all cases, yields are calculated for the corresponding TFA salts.

Peptide dendrimers showed activity as antimicrobial agents, siRNA and DNA transfection reagents and are interesting molecules to explore anti-inflammatory properties. Synthesis starts with attaching to the resin bead an indicial amino acid at the C-terminus using standard coupling conditions. Depending on the resin choice C-terminus can variate between acid (Wang resin) and amide (TentaGel,

Rink amide resin) groups. Another parameter, which is important to consider while planning synthesis, is the size of the beads and the loading. The size usually variates in the range of 75-150 µm (100-200 mesh) and 37-75 µm (200-400 mesh). The beads size does not affect synthesis, and normally variates depending on the need for further usage (sequencing and so on). The most relevant factor for the synthesis is the loading of the resin, normally for the short sequences (up to 10 residues) can be used resin with the loading 1.00 mmol/g, however if the targeted peptides are longer or have branches as in case of peptide dendrimers, the preference for the resin loading should shift to 0.2-0.35 mmol/g.

The amino acids are attached using the standard peptide coupling procedure and the Fmoc-protecting groups were removed under mild basic conditions without affecting orthogonal protective groups of the side chains.

Following the straightforward strategy, alternating the deprotection and coupling conditions the longer sequences can be reached. After switching to higher generations by branching the dendrimers, the numbers of couplings and deprotection rounds must be increased accordingly: two for G1, three for G2 and from three and four to five for G3 depending on the length and the sequence. Once the desired sequence is achieved, the cleavage mixture is applied to remove the acid-labile protective groups of the side chains and the peptide from the resin. After the cleavage, peptide dendrimers are precipitated in cold ether via centrifugation to remove the excess of TFA, and purified by preparative RP-HPLC and characterized by analytical LCMS and MS.

2.2. Coupling of peptide dendrimers in solution

2.2.1 Fluorophore labelled peptide dendrimers

There is a variety of methods to attach a fluorophore group on a peptide dendrimer: using alloc-protected groups of the side chains of lysine. That method is a convenient way to attach a fluorophore without changing the structure, since alloc-group can be selectively deprotected. Another widely used method is introducing a cysteine residue to attach a fluorophore. The thiol group is a strong nucleophile, which allows to proceed with attachment in the solution with unprotected peptide in an extremely selective manner in presence of a week base. (Scheme 2.2).
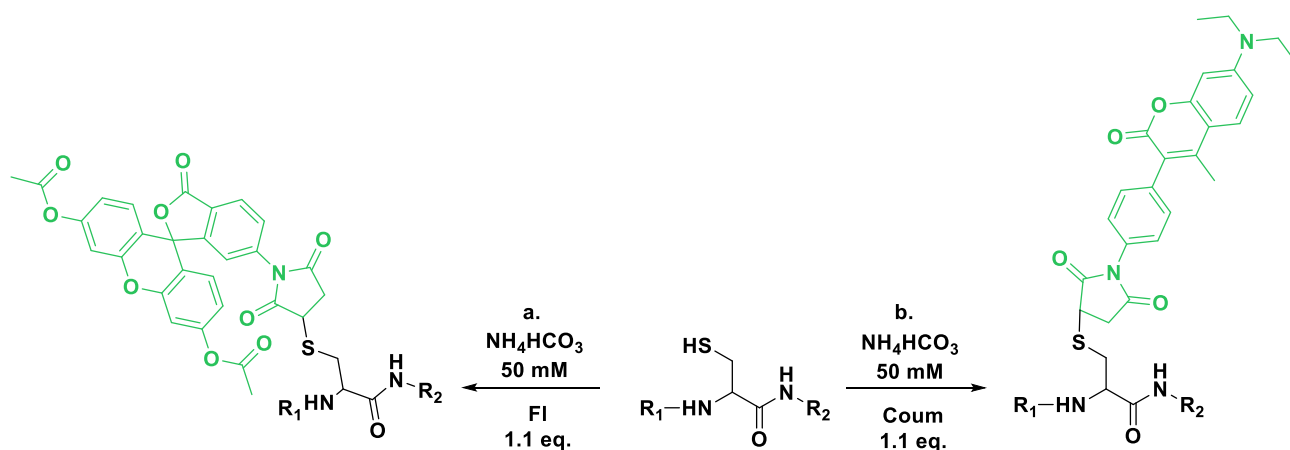
Scheme 2.2. *Synthesis of fluorophore containing peptide dendrimers. 1eq of a peptide dendrimer in H₂O, NH₄HCO₃ pH 8, 1.1eq of fluorescein diacetate 5-maleimide (Fl) (a) or 7-Diethylamino-3-(4-maleimidophenyl)-4-methylcoumarin (Coum) (b) were dissolved in acetonitrile and added to the dendrimer solution. Reaction stirred at RT for 2 h, lyophilized and purified by preparative HPLC. Yields are given for the coupling step. In all cases, yields are calculated for the corresponding TFA salts.*

The advantage of the method is that using already purified peptide dendrimers, which allows to obtain a desired labeled dendrimer via fast analytical RP-HPLC. To avoid the formation of dimers via disulfide bond formation is preferred to conduct that reaction under inert atmosphere.

2.2.2 Dimerization of peptide dendrimers

Disulfide bridges are commonly present in the nature and play an important role stabilizing the secondary structure of the proteins. Here we used disulfide bond formation as an easy method to connect two peptide dendrimers in order to achieve higher molecular weight. This reaction occurs in presence of oxygen of air in slightly basic conditions, connecting the thiol groups of cysteines. Depending on the structural properties the formation of the bond can take from 12 to 36 h under reflux at room temperature (Scheme 2.3).
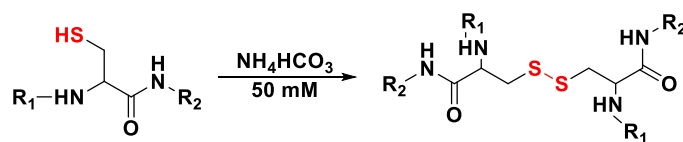
Scheme 2.3. *Synthesis of disulphide containing peptide dendrimers. Peptide dendrimer (2 eq., 10-20 mg) was solubilized NH₄HCO₃ (50 mM) solution. Then, reaction stirred for 24 h.*

2.3. Primary cells extraction

2.3.1 PBMC extraction via density gradient centrifugation

Anticoagulant-treated blood was obtained from Interregional Blood Transfusion SCR Ltd. Bern in blood bags 45 mL each. In accordance with the ethical committee of the Interregionale Blutspende SRK AG the blood was obtained from the healthy donors, who are thus informed that part of their blood will be used for research purposes. In order to have the most reliable results, the blood samples were distributed before the tasting on presence of pathogens and had to be treated in biosafety level 2 lab. Since the blood could be contagious, the samples had to be treated in another hood and incubated in an empty incubator to avoid contamination of immortalised cell cultures. After the experiments, the environment had to be properly cleaned and all the materials had to be discarded accordingly. Blood was diluted twice with HBSS and carefully overlayed on 20 mL of the Ficoll-Paque PLUS medium (1.077 g/ml). After centrifugation (400×g, 30 min, 20 °C) buffy coat at the interface was collected, washed with 40 mL of RPMA-1640 supplemented with 10% heat-inactivated FBS, 50 g/mL streptomycin, 50 U/mL penicillin, 2 mM glutamine, (RPMI supplemented). After centrifugation (200×g, 7 min, 20 °C) sedimented cells were diluted with RPMI-1640 supplemented and overlayed for second time over 20 mL of the Ficoll-Paque PLUS medium and centrifuged at the same conditions. PBMC collected from the interface were washed 3 times with supplemented RPMI (Figure 2.1).
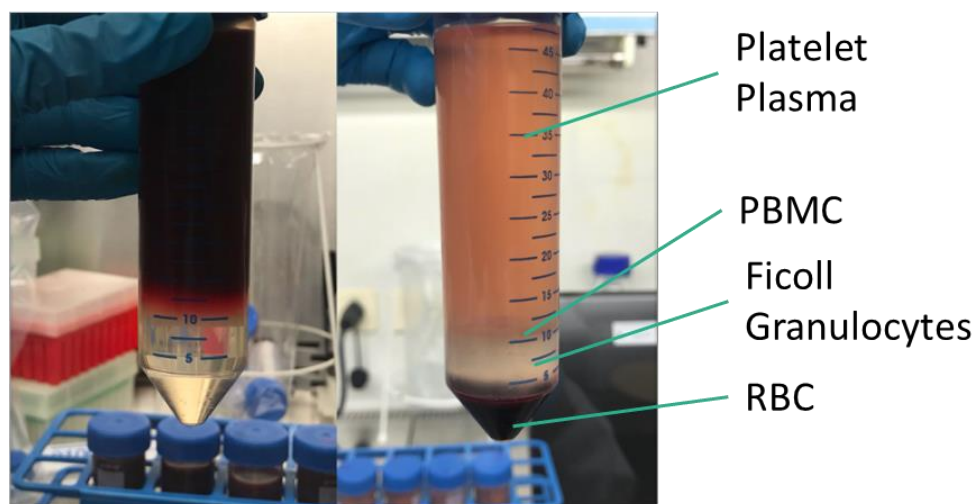
Figure 2.1 *Ficoll gradient before (on the left) and after (on the right) centrifugation.*

To avoid he activation of the PBMCs, only heat inactivated serum was used and the long storage of the cells at room temperature should be avoided, it is preferred to keep cells on ice.

Depending on the donor, after the set of centrifugations pellets can still remain among isolated PBMC. For that reason, after isolation, cells have to be carefully analyzed and counted by light microscope. Platelets (thrombocytes) normally do not interfere with an immune response, but the further

purification (especially via magnetic labelling) cannot be achieved successfully and the noise level for some assays can be increased. To eliminate the excess of the platelets, extra centrifugations (150-200×g, 7 min, 20 °C) can be conducted, which would cause a loss of some desired cells, but give the cleaner response.

PBMCs are the mixed population and includes myeloid and lymphoid cells. The myeloid cells include monocytes, dendritic cells and macrophages. Lymphoid cells include B, T cells and NK Cells. The myeloid cells are responsible for innate immunity and the first defence line of the organism and the most reactive once to trigger the immune response via cell-cell interactions or secreted cytokines. Those signals trigger the further cascade of the responses of the adaptive immunity.

Depending on the purposes and the required purity two methods of extraction of monocytes has been used. For the initial screening with ELISA for secreted IL-1Ra only pure monocytes were used to obtain the cleanest results. For that reason, the magnetic labeling (negative selection) is the best solution which provides the untouched and not activated monocytes. The disadvantage of that method is that the number of the monocytes which could be archived is limited and the purification itself is time and cost demanding.

In case of an experiment demands a big number of cells (such as qRT-PCR) the magnetic labelling cannot satisfy with its outcome, however Percoll centrifugation can provide a higher amounts of monocyte enriched fraction.

2.3.2. Monocytes purification using magnetic beads and labelling Isolation KITII

Monocytes were purified from whole PBMC by negative selection, all procedures were carried out according to manufacturer protocols. Briefly, the non-monocytes were labeled with a cocktail of biotin-conjugated monoclonal antibodies as a primary labeling reagent (Figure 2.2.). Then as a secondary labeling reagent were used anti-biotin microbeads. The mixture was run through the MACS column (MACS, Miltenyi Biotech) in the magnetic field of a MACS Separator (MACS, Miltenyi Biotech). In this case, non-monocytes are retained in the column and the unlabeled monocytes pass through the column. The purity of the monocytes was checked by fluorescent microscopy counterstaining with CD14-FITC. In the same way, the presence of the non-monocytes can be verified by staining with fluorochrome-conjugated anti-biotin antibody (Anti-Biotin-PE, AntiBiotin-APC).
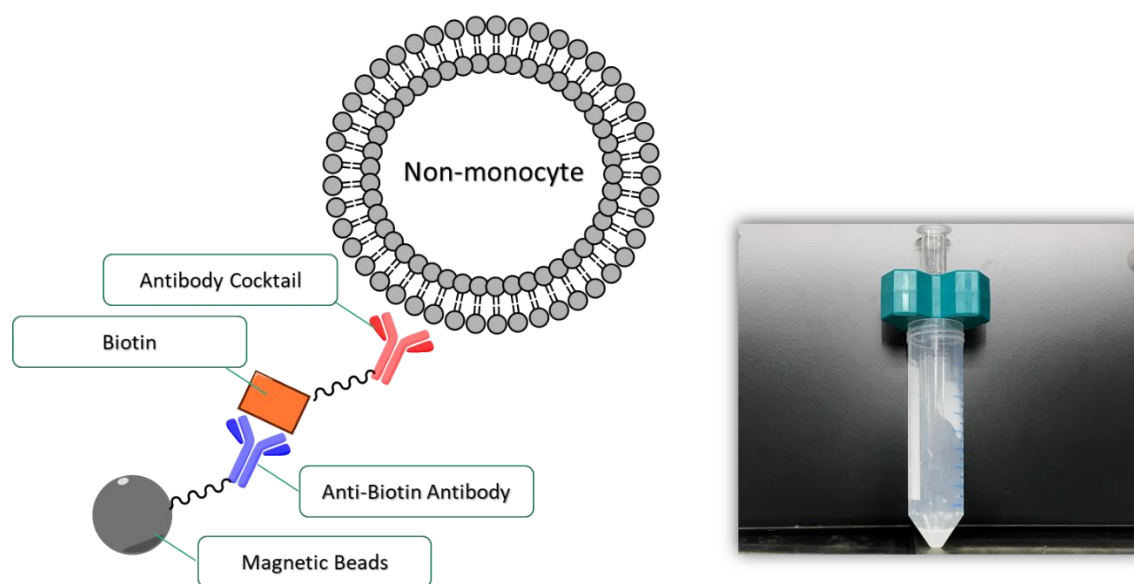
Figure 2.2 *General scheme of the negative selection with magnetically labelled antibodies (left). Extraction of untouched monocytes via filtration through magnetic field (right).*

2.3.3. Monocyte's enrichment using Percoll gradient centrifugation

Monocytes enriched fraction was obtained from PBMC by hyper-osmotic Percoll solution[85]. Briefly, for 100 mL of solution, 48.5 mL of Percoll, 41.5 mL of water and 10.0 mL of 1.6 M NaCl were mixed. $150\text{-}200\times10^6$ cells were overlayed over 10 mL of density medium and centrifuged at 580 g for 15 min. Cells at the interface were collected and washed 2 times with RPMI supplemented.

2.3.4. Accessing cells survival by AlamarBlue

To quantitatively measure the survival of the PBMCs in response on the treatment resazurin-based solution was used. Resazurin is a blue dye which is not toxic to the cells. After the penetration of the living organisms, it reacts with $NADH/H^+$ and giving NAD^+/H_2O is reduced to resorufin, which is fluorescent and can be measured. That method is commonly used for measuring cell viability, however since PBMC do not divide in the chosen conditions, that assay still can be applied due to normal metabolic activity. Since cells do not multiply, the number of cells per experiment and the time of incubation have to be chosen correctly. PBMCs include different types of cells which in the most cases to not attach to the bottom of the plate, washing steps were avoided and AlamarBlue was added directly.

2.4. Peptide libraries generation

A linear peptide library, a second-generation dendrimers library, and a third-generation dendrimers library of 50,000 sequences were generated as follows. Three different "sequence-templates" were used: (i) "XXXXXXXXXX" for the linear peptides, (ii) "XXXXXBXXXXXBXXXXX" for the second-generation dendrimers, and (iii) "XXXXXBXXXXXBXXXXXBXXXXX" for the third-

generation dendrimers, where X was a Lys, Ala, Tyr, or a Glu position, B was a branching lysine position, and the latter marked a doubling of the peptide chain. In all cases, the four amino acids had an equal probability of being picked in their respective positions. To allow sequences of different lengths, X positions were also allowed to be empty with a probability of 50%. Then, to assess the difference in composition of a peptide from Glatiramer, we counted the number of Tyr (Y), Glu (E), Ala (A), and the non-branching Lys (K). Then we considered the number of Tyr as unit, and we calculated the ratio relative to Tyr of the other three amino acids. Next, for each amino acid, we calculated the absolute value of the difference between its relative ratio and the relative ratio of the same amino acid in Glatiramer. Finally, we summed the four values, and we obtain the difference in composition (DC, Equation 1) from Glatiramer of the peptide.

$$P_{yr} = [\frac{A}{Y}, \frac{K}{Y}, \frac{E}{Y}, \frac{Y}{Y}]$$

$$G_{yr} = [4.2, 3.4, 1.4, 1.0]$$

$$DC = \sum_{i} |G_{yri} - P_{yri}| \qquad \text{(Equation 1)}$$

The three libraries were filtered based on their calculated composition, and only sequences with a DC from Glatiramer lower than ten were kept. For each of the three libraries, the filtered sequences were clustered in 500 k-means clusters using Scikit-learn,1 and the head of the cluster was picked. The procedure resulted in 500 linear 10-mer peptides, 500 second-generation dendrimers of linear sequence length spanning from 13 to 17, and 500 third-generation dendrimers of linear length spanning from 17 to 24. 3 linear peptides, 19 second-generation dendrimers, and 1 third-generation dendrimers were manually picked for synthesis.

3. Design of the initial library and the screening for biological activity

3.1 Introduction

Glatiramer acetate (GA) is a random polypeptide of approximately 5 – 9 kDa composed of L-alanine, L-lysine, L-glutamic acid and L-tyrosine in a 4.2/3.4/1.4/1.0 ratio approximating the composition of myelin basic protein.[25,86,87,28,88] GA has been on the market since 1996 as one of the most successful first-line treatments for multiple sclerosis (MS), a chronic autoimmune neurodegenerative disease.[10,89–91] Notwithstanding the subsequent introduction of new modalities for targeting MS,[92,93] GA remains a blockbuster drug.[18] There are currently no second-generation GA drugs and only a few generics of the original GA have been very recently introduced, probably due to the difficulty of replicating a polymeric preparation.[28,88]

Although its mechanism of action is still debated, one of the main effects of GA is to induce the differentiation of immune cells towards an anti-inflammatory rather than a pro-inflammatory state, an effect which can be tracked by monitoring various cell surface markers and cytokines.[17,37,43] In view of the many successful applications of dendrimers[94–97] including immunomodulation,[98–103] here we asked the question whether a peptide dendrimer[104] with a size and composition similar to GA might exhibit GA-like effects and provide a new starting point for immunomodulation. Similar to immunomodulatory synthetic peptides[105,106] and peptide dendrimers,[107] we envisioned a peptide dendrimer with a precise amino acid sequence prepared by solid-phase peptide synthesis.[108–110] As detailed below, these investigations led us to discover the immunomodulatory peptide dendrimer **32** (Figure 3.1).
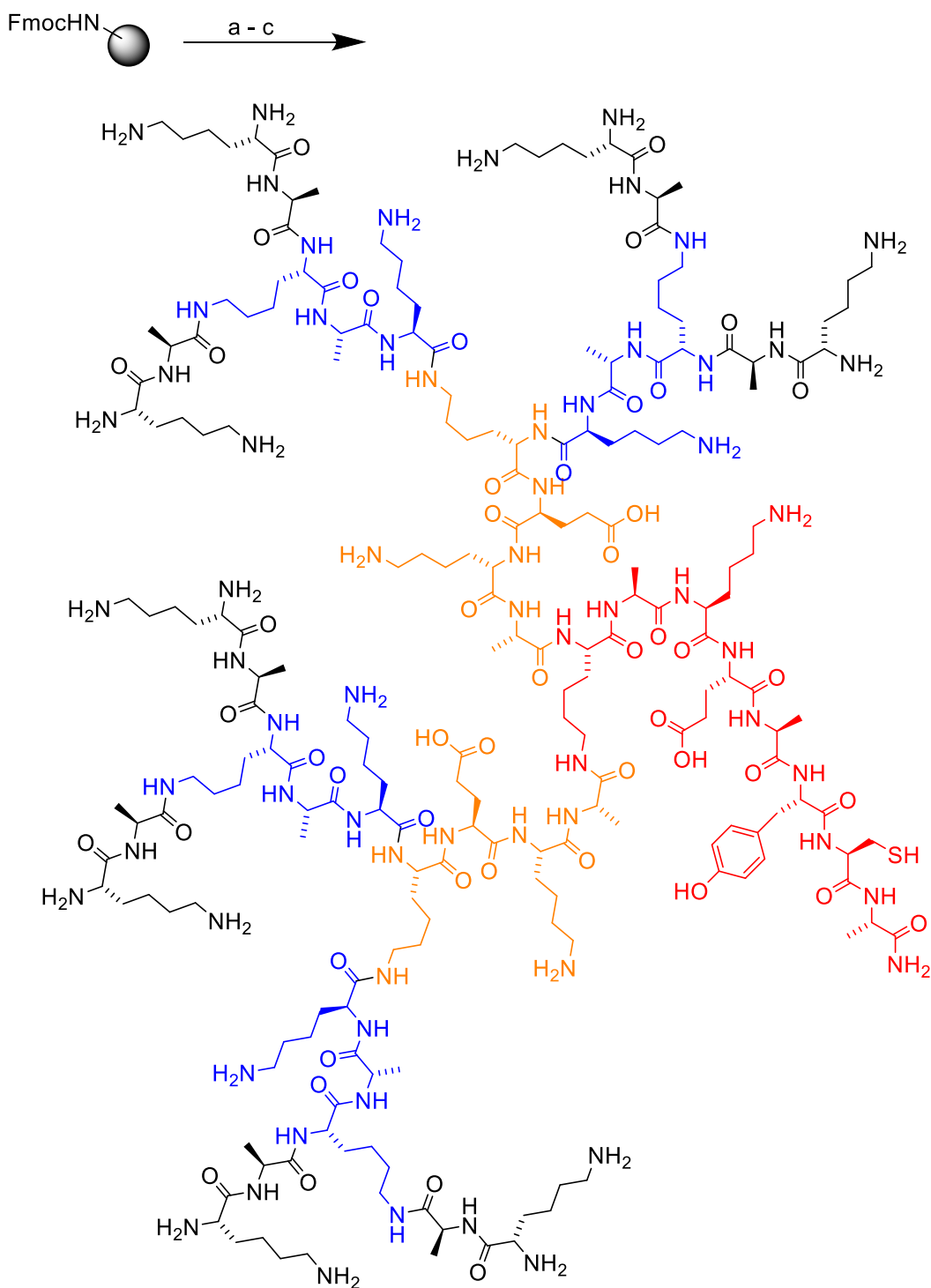
32: (KA)₈(*K*AK)₄(*K*EKA)₂*KAKEAYCA*

Figure 3.1. *Synthesis and structural formula of peptide dendrimer **32**. SPPS conditions: (a) 20% v/v piperidine in DMF, 5 min, 50 °C twice; (b) Fmoc-amino acid (5 eq./coupling site), Oxyma (7.5 equiv), DIC (10 eq.) in DMF, 15 min, 50 °C; (c) TFA/i-Pr3SiH/DODT/H2O (94:2.5:2.5:1), 4 h at room temperature.*

As an activity screen we focused on interleukin-1 receptor antagonist (IL-1Ra), a cytokine released by circulating antigen presenting cells (APC) in response to GA.[42,43] IL-1Ra crosses the blood-brain barrier (BBB) and is therefore a possible mediator of GA action in the CNS since GA itself does not cross the BBB.[111] To test our dendrimers, we quantified by immunoassay the release of IL-1Ra from human primary monocytes of healthy donors, an easily accessible type of APC, stimulated or not by addition of lipopolysaccharide (LPS) , which in our hands provided a reliable read-out.[43] In the initial screen the levels of secreted IL-1Ra remained below 1 ng/mL for all the smaller test compounds as well as with the linear peptide analogs of GA. However, two of the largest G3 dendrimers, **32** and **34**, induced IL-1Ra release to level comparable or higher than GA.

3.2 Results and discussion

3.2.1 1st library generation: Machine learning and manual design

To initiate our search, we selected 26 sequences from a virtual library of linear peptides and peptide dendrimers designed to have an amino acid composition similar to GA. Briefly, linear peptide library, a second-generation dendrimers library, and a third-generation dendrimers library of 50,000 sequences were generated. For each of the three libraries, the closest sequences to GA were chosen and filtered. Those sequences were clustered in 500 k-means clusters using Scikit-learn, and the head of the cluster was picked. Out of final 500 10-mer linear peptides, 500 second-generation dendrimers, 500 third-generation dendrimers. Out of three libraries 3 linear peptides (**1-3**), 19 second-generation dendrimers (**7-23**), and 1 third-generation peptide dendrimer (**33**) were manually picked for synthesis (Table 3.1., Figure 3.2.). Mainly the focus was on shorter second-generation sequences due to its good compromise between molecular weight and synthetic accessibility, however the size of G2 is significantly smaller than GA.
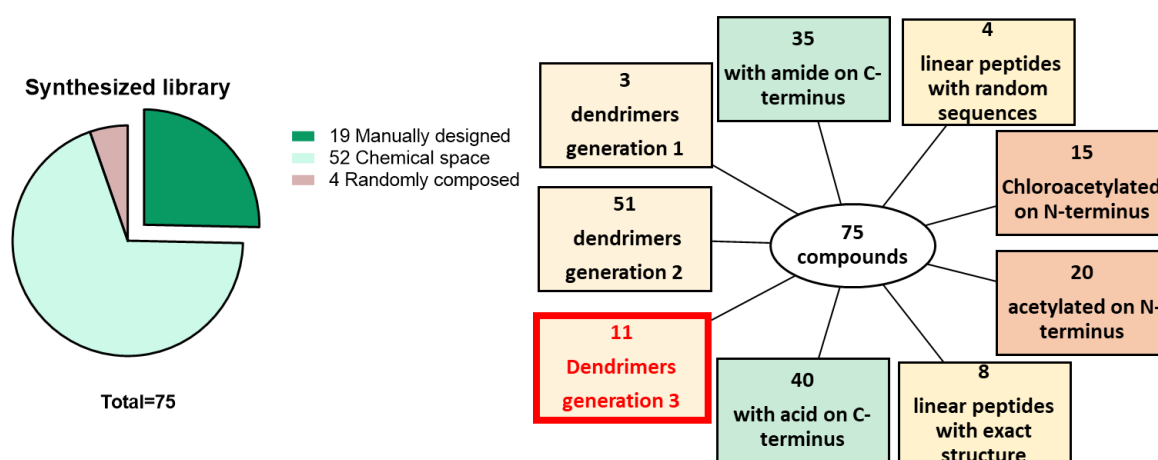
Figure 3.2. *1th library including both manually designed library and the library from the chemical space.*

To achieve the greatest diversity in term of the structure, total charge, amino acid ratio and molecular weight, for the manual design we did not strictly follow the GA ratio. We designed 3 first-generation peptide dendrimers (**4-6**), where two of them negatively charged. Considering that the previously described peptides were not reaching the lower MW end of GA, we designed additional dendrimers with longer sequences. 7 second-generation peptide dendrimers (**24-31**), 5 third-generation peptide dendrimers (**32-36**). The third-generation dendrimers are the largest in the library and the molecular weight corresponds with the lower molecular weight of the GA. The 3th generation was designed especially to expose the most of the positive charges of lysines. It was reported that the lysine is essential for the activity of these polymers. Some of the dendrimers were designed to additionally contain a cysteine at the core in order to allow for further modifications with fluorophore groups or for dimerization.

We also prepared a 30-mer and a 40-mer linear random peptide with GA-like composition. For that we used a mixture of the amino acid in the desired ratio. All the couplings were performed at 70 ºC to minimalize the influence of the reaction rate constant for each amino acid.

In selected cases we masked *N*-termini by acetylation, or turned them into cysteine reactive groups by chloroacetylation or by acylation with monoethyl fumarate to mimic the MS drug dimethyl fumarate.[112,113] This provided in total 73 test compounds (Table 3.1.).

Table 3.1. *Synthesis, structural properties, and activity of initial library.*

ID	Sequence[a]	Yield, mg (%)[b]	MS calc./obs.[c]	Tot. ch.[d]	A.A. ratio, E/K/A/Y[e]	Act.[f]
1	AAKEYAAEKK-OH	30.5 (54)	1107.5924/1107.5907	0	2/3/4/1	-
Ac**1**	AcAAKEYAAEKK-OH	23.6 (44)	1149.6030/1149.6007	0	2/3/4/1	-
ClAc**1**	ClAcAAKEYAAEKK-OH	25.2 (46)	1183.5640/1183.5634	0	2/3/4/1	-
2	EYAAKKEKAA-OH	61.6 (55)	1107.5924/1107.5929	0	2/3/4/1	-
Ac**2**	AcEYAAKKEKAA-OH	50.6 (51)	1149.6030/1149.6019	0	2/3/4/1	-
ClAc**2**	ClAcEYAAKKEKAA-OH	27.5 (50)	1183.5640/1183.5634	0	2/3/4/1	-
3	YAEKEKAKAA-OH	56.0 (54)	1107.5924/1107.5916	0	2/3/4/1	-
ClAc**3**	ClAcYAEKEKAKAA-OH	41.1 (56)	1183.5640/1183.5634	0	2/3/4/1	-
4	(A)₂*K*YKACA-NH₂	74.0 (40.2)	823.4474/823.4375	1	0/1/4/1	-
5	(AE)₂*K*AEYCA-NH₂	59.5 (58.9)	1082.4703/1082.4696	-3	3/0/4/1	-
6	(AEE)₂*K*AEYCA-NH₂	69.6 (50)	1340.5554/1340.5552	-5	5/0/4/1	-
7	(KA)₄(*K*AYE)₂*K*K-OH	77.2 (35)	2053.2048/2053.2054	2	1/2.5/3/1	-
Ac**7**	(AcKA)₄(*K*AYE)₂*K*K-OH	26.6 (18)	2221.2471/2221.2492	2	1/2.5/3/1	-
ClAc**7**	(ClAcKA)₄(*K*AYE)₂*K*K-OH	106.0 (40)	2357.0912/2358.0922	2	1/2.5/3/1	-
8	(KA)₄(*K*EYA)₂*K*KAK-OH	24.8 (20)	2252.3369/2252.3399	3	1/3/3.5/1	-
Ac**8**	(AcKA)₄(*K*EYA)₂*K*KAK-OH	10.8 (10)	2420.3791/2420.3812	3	1/3/3.5/1	-
ClAc**8**	(ClAcKA)₄(*K*EYA)₂*K*KAK-OH	9.3 (8)	2556.2232/2556.2283	3	1/3/3.5/1	-

9	(AK)$_4$(*K*KYE)$_2$*K*AAA-OH	12.2 (10)	2252.3369/2252.3332	3	1/3/3.5/1	-
Ac**9**	(AcAK)$_4$(*K*KYE)$_2$*K*AAA-OH	10.4 (9)	2420.3791/2420.3770	3	1/3/3.5/1	-
10	(AYK)$_4$(*K*E)$_2$*K*KAA-OH	34.8 (28.4)	2379.3315/2379.3345	2	0.5/1.25/1.5/1	-
Ac**10**	(AcAYK)$_4$(*K*E)$_2$*K*KAA-OH	50.2 (28.4)	2547.3315/2547.3775	2	0.5/1.25/1.5/1	-
11	(AKA)$_4$(*K*KEY)$_2$*K*E-OH	24.3 (17.6)	2452.4166/2452.4192	2	1.5/3/4/1	-
Ac**11**	(AcAKA)$_4$(*K*KEY)$_2$*K*E-OH	49.3 (31.1)	2620.4588/2620.4612	2	1.5/3/4/1	-
ClAc**11**	(ClAcAKA)$_4$(*K*KEY)$_2$*K*E-OH	43.4 (32.3)	2756.3029/2756.3066	2	1.5/3/4/1	-
12	(AKA)$_4$(*K*EK)$_2$*K*YEY-OH	34.2 (26)	2452.4166/2452.4208	2	1.5/3/4/1	-
Ac**12**	(AcAKA)$_4$(*K*EK)$_2$*K*YEY-OH	25.0 (21)	2620.4588/2620.4626	2	1.5/3/4/1	-
ClAc**12**	(ClAcAKA)$_4$(*K*EK)$_2$*K*YEY-OH	10.2 (8)	2756.3029/2756.3050	2	1.5/3/4/1	-
13	(KAA)$_4$(*K*EKA)$_2$*K*EKA-NH$_2$	169.5 (49.3)	2650.5646/2650.5679	4	3/7/11/0	-
14	(ClAcK)$_4$(*K*AYE)$_2$*K*AKYAEA-NH$_2$)	159.6 (46.1)	2575.2079/2579.1768	4	1/1.7/1.7/1	-
15	(KYA)$_4$(*K*EA)$_2$*K*KKA-OH	87.6 (39)	2578.4635/2578.4656	3	0.5/1.5/1.75/1	-
Ac**15**	(AcKYA)$_4$(*K*EA)$_2$*K*KKA-OH	88.0 (43)	2746.5058/2746.5094	3	0.5/1.5/1.75/1	-
ClAc**15**	(ClAcKYA)$_4$(*K*EA)$_2$*K*KKA-OH	65.3 (31)	2882.3499/2882.3549	3	0.5/1.5/1.75/1	-
Ac**16**	(AcAKA)$_4$(*K*EY)$_2$*K*YKK-NH$_2$	31.7 (49)	2653.4956/2653.4904	4	0.7/2/2.7/1	-
Fum**16**	(FumAKA)$_4$(*K*EY)$_2$*K*YKK-NH$_2$	15.0 (23.6)	2485.4533/2485.4561	4	0.7/2/2.7/1	-
17	(AKE)$_4$(*K*AYA)$_2$*K*KKK-NH$_2$	13.5 (11)	2708.5701/2708.5633	3	2/3.5/4/1	-
Ac**17**	(AcAKE)$_4$(*K*AYA)$_2$*K*KKK-NH$_2$	13.8 (13)	2876.6124/2876.6340	3	2/3.5/4/1	-
Fum**17**	(FumAKE)$_4$(*K*AYA)$_2$*K*KKK-NH$_2$	13.5 (11)	3212.6969/3212.7355	3	2/3.5/4/1	-
18	(K)$_4$(*K*AYAEY)$_2$*K*AKAEYA-NH$_2$	108.2 (43.5)	2741.4905/2741.4934	2	0.6/1/1.4/1	-
19	(KAE)$_4$(*K*AEK)$_2$*K*YYA-OH	49.3 (30.0)	2768.5072/2768.5122	-1	3/3/3.5/1	-
Ac**19**	(AcKAE)$_4$(*K*AEK)$_2$*K*YYA-OH	74.1 (34.1)	2936.5495/2936.5543	-1	3/3/3.5/1	-
ClAc**19**	(ClAcKAE)$_4$(*K*AEK)$_2$*K*YYA-OH	91.6 (33.8)	3072.3936/3072.3961	-1	3/3/3.5/1	-
Ac**20**	(AcKAA)$_4$(*K*YYE)$_2$*K*AY-NH$_2$	31.7 (30)	2794.4694/2794.4734	2	0.4/0.8/1.8/1	-
AcCl**20**	(ClAcKAA)$_4$(*K*YYE)$_2$*K*AY-NH$_2$	29.4 (26)	2930.3135/2930.3170	2	0.4/0.8/1.8/1	-
Ac**21**	(AcKAK)$_4$(*K*AEY)$_2$*K*AEA-OH	3.0 (2)	2876.6488/2876.6463	4	1.5/4/4/1	-
22	(AKK)$_4$(*K*YEK)$_2$*K*KEA-NH$_2$	168.3 (49.3)	2650.5646/2650.5662	8	1.5/5.5/2.5/1	-
23	(AKE)$_4$(*K*KAY)$_2$*K*YKY-NH$_2$	25.4 (18.6)	2892.6225/2892.6243	3	1/1.75/1.5/1	-
Ac**23**	(AcAKE)$_4$(*K*KAY)$_2$*K*YKY-NH$_2$	35,6 (27.9)	3060.6648/3060.6693	3	1/1.75/1.5/1	-
ClAc**23**	(ClAcAKE)$_4$(*K*KAY)$_2$*K*YKY-NH$_2$	8.9 (7)	3196.5059/3196.5148	3	1/1.75/1.5/1	-
24	(KYA)$_4$(*K*AE)$_2$*K*AEYKCA-NH$_2$	127.1 (29.5)	2913.5687/2915.5439	2	0.6/1/1.6/1	-
25	(KAA)$_4$(*K*EY)$_2$*K*AKEYEYA-NH$_2$	180 (41.1)	2920.5811/2920.5847	1	1/1.25/2.5/1	-
ClAc**26**	(ClAcK)$_4$(*K*EAKAKEY)$_2$*K*AKEYEY-OH	159.9 (22.8)	3640.7309/3640.7417	2	1.5/2.3/1.3/1	-
27	(AK)$_4$(*K*AEAKAKE)$_2$*K*KEYEYCA-NH$_2$	138 (39.1)	3865.0924/3865.1068	3	3/4.5/5.5/1	-
27Coum	(AK)$_4$(*K*AEAKAKE)$_2$*K*KEYEYC(Coum)A-NH$_2$	6.1 (55.3)	4267.2504/4267.2627	8	3/4.5/5.5/1	-
Ac**28**	(AcKEAKY)$_4$(*K*KYEA)$_2$*K*EKAYKA-NH$_2$	76.6 (34.3)	4719.5316/4719.5442	5	1/1.7/1.1/1	-
ClAc**28**	(ClAcKEAKY)$_4$(*K*KYEA)$_2$*K*EKAYKA-NH$_2$	56.7 (24.8)	4855.3757/4857.3959	5	1/1.7/1.1/1	-
29	(YAKAKE)$_4$(*K*AYKAKA)$_2$*K*AYKKA-NH$_2$	169.6 (23.4)	4988.8484/4988.8659	10	0.6/2/2.3/1	-
30	(KAEKAYA)$_4$(*K*EKYAKA)$_2$*K*EKYKA-NH$_2$	221 (25.6)	5447.0133/5447.0332	7	1/1/2.4/1	-
31	(YKAKAKY)$_4$(*K*EAKAKY)$_2$*K*AKEYEY-OH	154(12.3)	5976.3226/5976.3381	12	0.3/1.4/1.1/1	-
32	(KA)$_8$(*K*AK)$_4$(*K*EKA)$_2$*K*AKEAYCA-NH$_2$	61.9 (7.7)	4695.9470/4695.9625	12	3/15/17/1	+
Ac**32**	(AcKA)$_8$(*K*AK)$_4$(*K*EKA)$_2$*K*AKEAYCA-NH$_2$	53.9 (22.8)	5032.0315/5032.0448	12	3/15/17/1	-
Fum**32**	(FumKA)$_8$(*K*AK)$_4$(*K*EKA)$_2$*K*AKEAYCA-NH$_2$	47.6 (22.9)	5704.2005/5704.2057	12	3/15/17/1	-
33	(AKA)$_8$(*K*YEK)$_4$(*K*EKA)$_2$*K*AKY-OH	23.7 (9)	5775.3771/5775.3854	8	1.2/3/3.8/1	-

Ac33	(AcAKA)$_8$(*K*YEK)$_4$(*K*EKA)$_2$*K*AKY-OH	20.3 (9)	6111.4616/6111.4644	8	1.2/3/3.8/1	-
ClAc33	(ClAcAKA)$_8$(*K*YEK)$_4$(*K*EKA)$_2$*K*AKY-OH	20.9 (9)	6383.1499/6384.1461	8	1.2/3/3.8/1	-
34	(KA)$_8$(KKAKE)$_4$(KYKAKA)$_2$KAYKKA-OH	127 (9.0)	6016.7929/6016.7881	17	1.3/7.3/6/1	+
Ac34	(AcKA)$_8$(*K*KAKE)$_4$(KYKAKA)$_2$*K*AYKKA-OH	52.8 (19.9)	6352.8774/6352.8813	17	1.3/7.3/6/1	-
Fum34	(FumKA)$_8$(*K*KAKE)$_4$(KYKAKA)$_2$*K*AYKKA-OH	51.8 (18.1)	7025.0465/7025.0531	17	1.3/7.3/6/1	-
35	(KAA)$_8$(KKAKAK)$_4$(KAAKKY)$_2$KEKAKCA-OH	17.0 (2.6)	6934.4362/6934.4379	24	0.5/13/15/1	-
36	(AK)$_8$(*K*AKAKY)$_4$(*K*AKEYEY)$_2$*K*AKEYEY-NH$_2$	51.3 (5.8)	6916.1419/6916.1596	13	0.6/1.9/1.9/1	-
37	(X)$_{30}$-NH$_2$	46,3		3		-
ClAc37	ClAc(X)$_{30}$-NH$_2$	67,2		3		-
38	(X)$_{40}$-NH$_2$	34		4		-
Ac38	Ac(X)$_{40}$-NH$_2$	62,4		4		-

[a] One-letter code amino acids are used, *K* is the branched lysine residue, Ac is acetyl group at the *N*-terminus, ClAc is Chloroacetyl group at the *N*-terminus, Fum is monoethylfumarate at the *N*-terminus, OH is the carboxyl *C*-terminus, NH$_2$ is carboxamide *C*-terminus, Coum is 7-Diethylamino-3-(4'-succinylphenyl)-4-methylcoumarin. [b] Isolated yields as trifluoroacetate salt after preparative RP-HPLC purification. [c] ESI-MS data. [d] Charge of a dendrimer at neutral pH. [e] Amino acid ratio without counting branching Lys. [f] Ability to induce IL-1Ra on primary monocytes after 48 h of incubation.

3.2.3. The initial screening for the biological activity

To access the biological activity of the first library we tested if they stimulate secretion of IL-1Ra on human primary monocytes similarly to GA in the presence or the absence of LPS (100 ng/mL). All dendrimers were tested in the range of concentrations which were previously used for GA (50 and 25 µg/mL). LPS, as a strong inflammatory stimulus was used to determine behaviour of the monocytes in acute inflammatory conditions. The levels of IL-1Ra were measured with an ELISA assay. The assay supernatants were collected after a round of centrifugations to avoid the cells material for the further analysis and stored in -80 ºC prior to use.
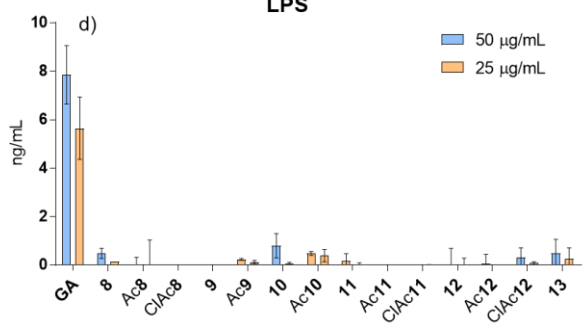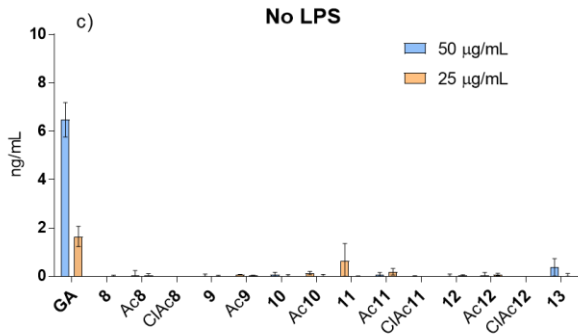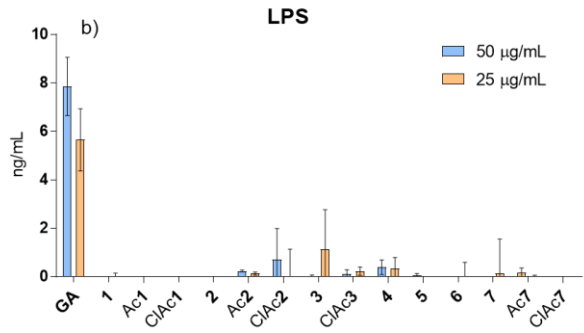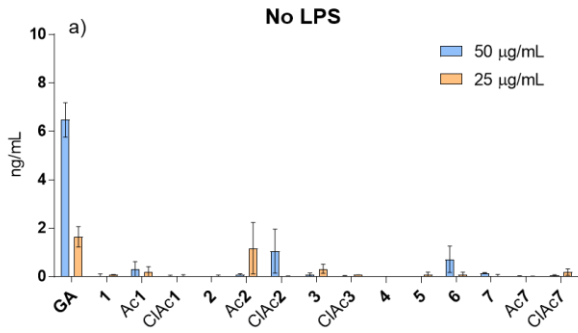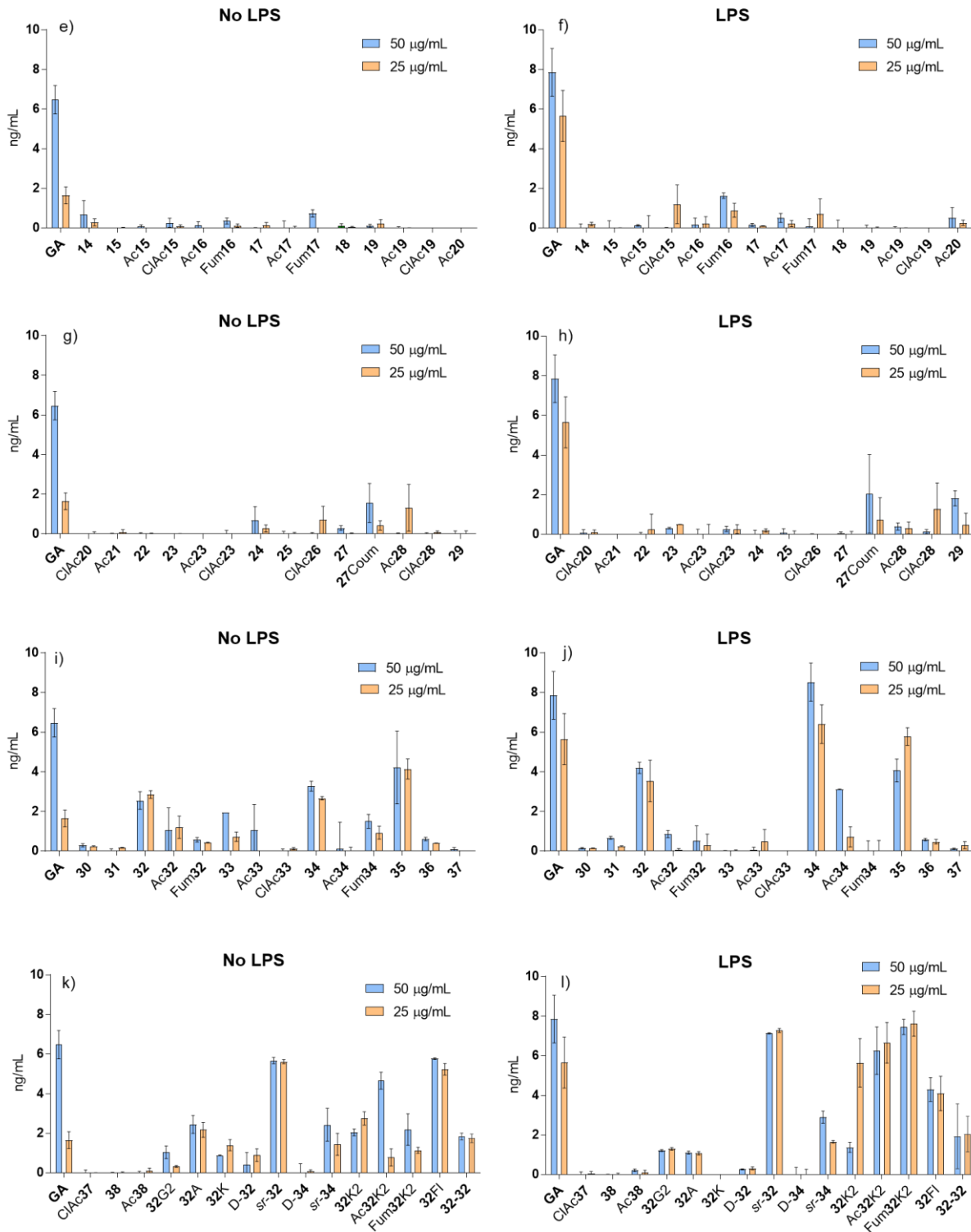
Figure 3.3*. Total screening for the first library and the library of the analogs: Cytokine level of IL-1Ra in supernatants of monocytes for active dendrimers and analogues evaluated by ELISA assay on primary human monocytes of healthy donors. 5×10^4 cells/200 µL in 96 well plates, were incubated with dendrimers or GA as a control for 48 h in the presence or the absence of LPS (100 ng/mL), in a range of concentrations (50-25 µg/mL) (mean ± SD, n = 2 different experiments). The results are presented as*

the difference between each sample and the non treated sample to consider the difference between baselines for each donor.

Initial screening showed the levels of secreted IL-1Ra remained below 1 ng/mL for all the smaller test compounds as well as with the linear peptide analogs of GA (Figure 3.3.). However, two of the largest G3 dendrimers, **32** and **34**, induced IL-1Ra release to level comparable or higher than GA.

3.2.4. Optimisation of the IL-1Ra secretion time

Recent reports describe supernatants collected and analysed after 48 h of incubation,[43] however there is no data published indicating earlier time points for IL-1Ra secretion. To check wherever the incubation is relevant for the experiment and the treatment induces secretion but not release of the cytokine, cells were incubated with different time intervals (15 min, 30 min, 1 h, 4 h, 8 h, 12 h, 24 h, 48 h). Analysis of the supernatant indicated that there is no significant amount of the cytokine detected within first 12 h, and only traces after 24 h (below 1 ng/mL) of the cytokine observed (Figure 3.4.). 48 h of incubation showed the most reliable readout with the highest response, which is also compatible with what is known about the biosynthesis process.
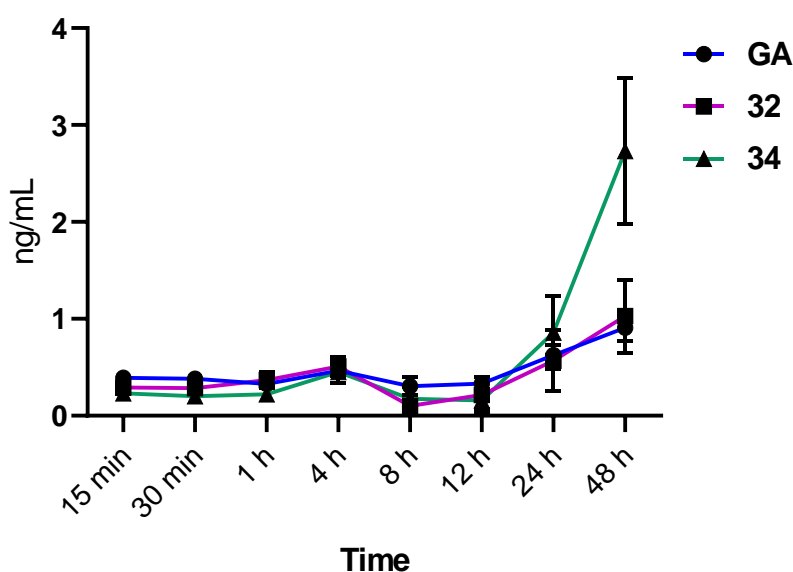
***Figure 3.4**. Cytokine level of IL-1Ra in supernatants of monocytes for active dendrimers and analogues evaluated by ELISA assay on primary human monocytes of healthy donors. 5×10^4 cells/200 µL in 96 well plates, were incubated with dendrimers or GA (50µg/mL) as a control for15 min, 30 min, 1 h, 4 h, 8 h, 12 h, 24 h, 48 h in the presence of LPS (100 ng/mL) (mean ± SD, n = 3 different experiments).*

3.2.5. Structure–activity relationship

The screening indicated structural features of the dendrimers, which are relevant for the activity. As was expected, MW played a significant role, however not all large dendrimers with MW in the range of GA were active. Carboxyl *C*-terminus or carboxamide *C*-terminus did not interfere with activity since both active compounds had a diverse option at the *C*-terminus.

Table 3.2. *Synthesis, structural properties, and activity of analogs of **32** and **34**.*

ID	Sequence[a]	Yield, mg (%)[b]	MS calc./obs.[c]	Tot. ch.[d]	A.A. ratio, E/K/A/Y[e]	Act.[f]
32G2	(KAK)$_4$(*K*EKA)$_2$*K*AKEAYCA-NH$_2$	21.9 (14.1)	3102.8903/3102.8874	20	3/11/9/1	-
32A	(AK)$_8$(*K*AK)$_4$(*K*EKA)$_2$*K*AKEAYCA-NH$_2$	23.2 (23.2)	4695.9470/4695.9469	12	3/15/17/1	+
32K	(KK)$_8$(*K*AK)$_4$(*K*EKA)$_2$*K*AKEAYCA-NH$_2$	18.9 (18.9)	5152.4098/5152.4134	12	3/23/9/1	+
D-**32**	(ka)$_8$(*k*ak)$_4$(*k*eka)$_2$*k*akeayca-NH$_2$	56.8 (18.3)	4695.9470/4695.9606	12	3/15/17/1	-
sr-**32**	(KA)$_8$(*K*AK)$_4$(*K*EKA)$_2$*K*AKEAYCA-NH$_2$	32.9 (7.6)	4624.9098/4624.9212	12	3/15/17/1	+
D-**34**	(ka)$_8$(*k*kake)$_4$(*k*ykaka)$_2$*k*aykka-OH	67.1 (16.7)	6015.8089/6015.8149	8	1.3/7.3/6/1	-
sr-**34**	(KA)$_8$(*K*KAKE)$_4$(*K*YKAKA)$_2$*K*AYKKA-OH	89.6 (15.6)	6016.7929/6016.8081	8	1.3/7.3/6/1	+
32K2	(KA)$_8$(*K*KKAK)$_4$(*K*EKA)$_2$*K*AKEAYCA-NH$_2$	28.0 (8.6)	5720.7067/5720.7093	20	3/23/17/1	+
Ac**32**K2	(AcKA)$_8$(*K*KKAK)$_4$(*K*EKA)$_2$*K*AKEAYCA-NH$_2$	28.6 (9.4)	6056.7912/6056.7988	20	3/23/17/1	+
Fum**32**K2	(FumKA)$_8$(*K*KKAK)$_4$(*K*EKA)$_2$*K*AKEAYCA-NH$_2$	27.5 (8.3)	6728.9602/6728.9614	20	3/23/17/1	+
32-**32**	(KA)$_8$(*K*AK)$_4$(*K*EKA)$_2$*K*AKEAYCA-NH$_2$)$_2$	7.9 (43.6)	9247.8040/9247.8422	12	3/15/17/1	+
32Fl	(KA)$_8$(*K*AK)$_4$(*K*EKA)$_2$*K*AKEAYC(Fl)A-NH$_2$	6.5 (40.6)	5207.0373/5207.0391	3	3/15/17/1	+

[a] One-letter code amino acids are used, *K* is the branched lysine residue, Ac is acetyl group at the *N*-terminus, Fum is monoethylfumarate at the *N*-terminus, OH is the carboxyl *C*-terminus, NH$_2$ is carboxamide *C*-terminus, Fl is fluorescein diacetate 5-succinimide. [b] Isolated yields as trifluoroacetate salt after preparative RP-HPLC purification. [c] ESI-MS data. [d] Charge of a dendrimer at neutral pH. [e] Amino acid ratio without counting branching Lys. [f] Ability to induce IL-1Ra on primary monocytes after 48 h of incubation.

To assess the activity requirement for **32** and **34**, we performed a structure–activity relationship (SAR) study on the level of induced IL-1Ra release measured by immunoassay, which we verified in selected cases at the mRNA level by RT-qPCR. During this study we tested a selection of active and inactive dendrimers on PBMCs and found that they did not measurably affect viability, suggesting that any modulation of IL-1Ra release indicated a specific effect and an apparent absence of toxicity (Figure 3.5.).
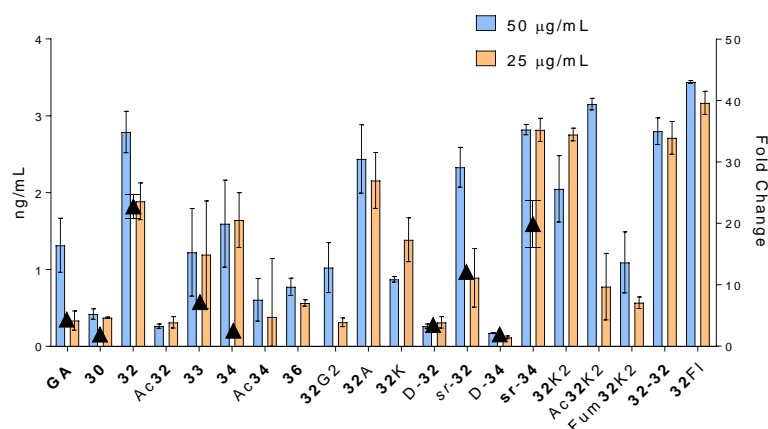
Figure 3.5. *Cytokine level of IL-1Ra in supernatants of primary human monocytes of healthy donors treated with peptide dendrimers, evaluated by ELISA assay (bars, left vertical axis) and mRNA levels (▲, right vertical axis). For ELISA $5x10^4$ cells/200µL in 96 well plates were incubated with 25-50 µg/mL dendrimer or GA for 48 h (mean ± SD, n = 2 different experiments). For mRNA levels evaluation $2x10^6$ cells/3 mL in 6 well plates were incubated with 50 µg/mL dendrimer or GA for 18 h.*

Activity was abolished by *N*-terminal modification of **32** and **34** for Ac**32**, Fum**32**, Ac**34**, Fum**34** as well as in dendrimer **32**G2 (Table 3.1, 3.2.), a smaller G2 analog of the most active dendrimer **32**. On the other hand, activity was preserved in close analogs of **32** featuring an additional lysine residue in the G2 branch and the *N*-termini free (**32**K2) or acylated (Ac**32**K2, Fum**32**K2), or with modified G3 branches either in reversed order (**32**A) or containing only lysine (**32**K). The disulphide bridged dimer **32-32** was also active (Table 3.1.-3.2., Figure 3.4.-3.5.). The importance of the lysine residues was shown previously on GLATiramer (glutamic acid, lysine, alanine, tyrosine) similar copolymers, where copolymers (GAT) which did not contain lysine were unable to inhibit EAE.[29] Taking into account that the presence of lysine is essential for the activity, we synthetized dendrimers having similar composition to GA and also some dendrimers containing extra lysine residues.

In terms of stereochemistry, activity was also lost with D-enantiomers D-**32** and D-**34**, similar to the inactivity reported for D-enantiomeric GA.[86] Furthermore, stereo randomised peptides were synthetized using on each coupling step a 1/1 L/D solution of a required amino acid. In this case we always have an approximately equal possibility of attachment either L or D amino acid. In the end we have a complex mixture of sterically different isomers but whose sequence is defined. Activity was preserved in stereo randomized analogs *sr*-**32** and *sr*-**34**, synthesized using racemic building blocks,[114] suggesting secondary structures were not required for activity (Figure 3.5.).

3.2.6. 2nd library designed using different amino acids from GA

Lysine is considered an essential amino acid required for the activity, howeverpeptides with valine or isoleucine instead of alanine and phenylalanine and tryptophane instead of tyrosine were reported as retaining some activity.[25] We decided to see if changing the amino acid composition will change the activity in case of peptide dendrimers.

AA	Ratio 1 Teva	Ratio 2 analog	Ratio 3 analog	Ratio 4 D-AA		
Glu	1,4	1,7	1,8	2,2		
Lys	3,4	3,8	4,0	4,0		
Ala	4,2	4,9	6,1	5,6	Val	Ile
Tyr	1,0	1,0	1,0	1,0	Phe	Trp
Size kDa	7	6	8,5	29		
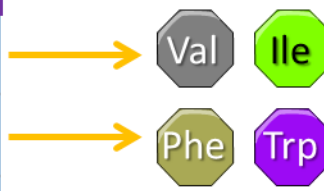
Figure 3.5. Table of amino acid ratio for some described glatiramoids.

Using as a starting point the active dendrimer **34**, we designed a library consisting of the analogs composed of amino acids, which are not present in GA. For example, alanine was substituted with glycine, proline, isoleucine, valine. Tyrosine was substituted with serine and phenylalanine. Glutamic acid was substituted on glutamine and asparagine. Lysine was substituted with arginine on the core and for the 3th generation for half of the sequences ornithine was used. All the dendrimers were at the same size range and had similar total charge. Two dendrimers *sr*-**41** and *sr*-**45** are composed of D and L amino acid in equal ratio to see if the activity will be preserved in case of stereorandomization.

Table 3.3. *Synthesis, structural properties, and activity of analogs of* *34*.

ID	Sequence[a]	Yield, mg (%)[b]	MS calc./obs.[c]	Tot. ch.[d]	Act.[f]
39	(KA)$_8$(KKGKE)$_4$(KYKAKA)$_2$KIFKSK-NH$_2$	61.7 (15.4)	6001.7932/6001.8045	18	+
40	(KA)$_8$(KKGKE)$_4$(KYKKAP)$_2$KAFKK-NH$_2$	81.3 (20.21)	5924.7456/5924.7700	18	+
*sr-***41**	(KA)$_8$(KKKAE)$_4$(KYKAKG)$_2$KLYKKG-NH$_2$	131.3 (27.8)	6015.8089//6015.8179	18	+
42	(OV)$_8$(KKGKE)$_4$(KYKGK)2KKFNGK-NH$_2$	104.5 (21.8)	5914.7612/5914.7612	18	+
43	(OV)$_8$(KKGKE)$_4$(KYKAKA)$_2$KIFKSK-NH$_2$	48.5 (10.2)	6113.9184/6113.9332	18	+
44	(OV)$_8$(KKGKE)$_4$(KYKKAP)$_2$KAFNKK-NH$_2$	49.1 (10.3)	6036.8708/6036.8901	18	+
*sr-***45**	(OV)$_8$(KKKAE)$_4$(KYKAKG)$_2$KLYKKG-NH$_2$	118.3 (24.8)	6127.9519/6127.9341	18	+
46	(KA)$_8$(KKGKE)$_4$(KYKLGK)$_2$KKFNGK-NH$_2$	95.9 (23.9)	6026.8041/6026.9039	18	+
47	(KA)$_8$(KKLKE)$_4$(KYKGKG)$_2$KQFIRA-NH$_2$	86.6 (18.2)	6181.9559/6181.9536	17	+
48	(KA)$_8$(KKAKE)$_4$(KYKGKA)$_2$KRVIKQ-NH$_2$	60.9 (15.1)	6050.8572/6050.8745	18	+
49	(OV)$_8$(KKLKE)$_4$(KYKGKG)$_2$KQFIRA-NH$_2$	93.5 (19.5)	6294.0811/6294.0984	17	+
50	(OV)$_8$(KKAKE)$_4$(KYKGKA)$_2$KRVIKQ-NH$_2$	70.3 (17.9)	6162.9824/6162.9947	18	+

[a] One-letter code amino acids are used, *K* is the branched lysine residue, NH$_2$ is carboxamide *C*-terminus [b] Isolated yields as trifluoroacetate salt after preparative RP-HPLC purification. [c] ESI-MS data. [d] Charge of a dendrimer at neutral pH. [e] Amino acid ratio without counting branching Lys. [f] Ability to induce IL-1Ra on primary monocytes after 48 h of incubation.

Biological screening for IL-1Ra indicated, that amino acid substitution did not lead to loss of the activity, even in the case of compounds with ornithine and valine at the 3th generation, suggesting that the total charge is important for triggering the response. That finding brought us to the list of compounds, where they all remain active, and a structural change do not lead to the loss of the secretion (Figure 3.6.).
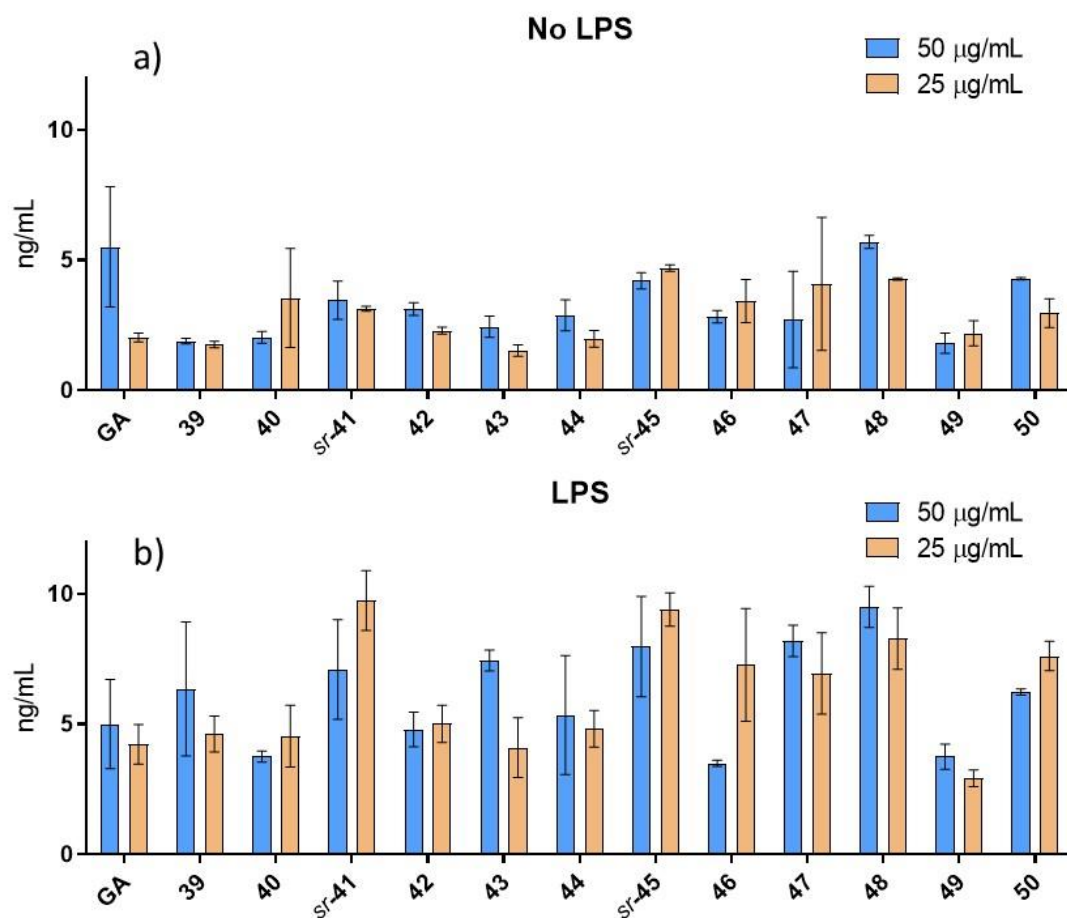
Figure 3.6. *Cytokine level of IL-1Ra in supernatants of monocytes for active dendrimers and analogues evaluated by ELISA assay on primary human monocytes of healthy donors. 5×10^4 cells/200 µL in 96 well plates, were incubated with dendrimers or GA as a control for 48 h in presence or absence of LPS (100 ng/mL), in a range of concentrations (50-25 µg/mL) (mean ± SD, n = 3 different experiments). The results are presented as the difference between each sample and the non treated sample to consider the difference between baselines for each donor.*

3.2.7. Conformation in solution by CD Spectroscopy

It was demonstrated recently that GA can form α-helical structures in solution. There were also data indicating that in presence of membrane-like environment induces α-helical structure for GA.[115]

To investigate the importance of the conformation for the activity, we performed circular dichroism measurements in phosphate PB and in the presence of dodecylphosphocholine (DPC), in order to mimic membrane-like environment.

Indeed, the spectra of GA shower a high level of α-helix, which increases in presence of DPC (Table 3.4., Figure 3.7). At the same time, the active compounds **32** and **34** and also inactive dendrimers indicated an unordered conformation, which suggests that secondary structure is not required for the

activity. The stereorandomised analogs *sr*-**32**, *sr*-**34** and *sr*-**45** had a predictable flat shape characterising the mixture of L- and D-amino acids. D-**34** had an inversed spectrum in comparison to its L analog **34**.

Table 3.4. *Circular dichroism spectra of GA and some selected dendrimers (100 μg/mL) in 8 mM phosphate PB at pH 7.4 optionally in the presence of 5 mM dodecylphosphocholine. Percentage of α-helix and β-sheet was processed by Dichroweb using the CONTIN analysis program and reference set 3.*

Compound	Helix1	Helix2	Strand1	Strand2	Turns	Unordered	Total
GA PB	0.299	0.187	0.000	0.037	0.171	0.306	1
GA DPC	0.434	0.226	0.000	0.024	0.135	0.180	0.999
17 PB	0.000	0.103	0.221	0.122	0.222	0.332	1
17 DPC	0.000	0.103	0.200	0.121	0.238	0.338	1
Ac**17** PB	0.000	0.198	0.045	0.077	0.244	0.437	1.001
Ac**17** DPC	0.000	0.123	0.151	0.106	0.247	0.372	0.999
32 PB	0.000	0.210	0.025	0.071	0.246	0.447	0.999
32 DPC	0.000	0.175	0.099	0.089	0.256	0.382	1.001
34 PB	0.000	0.111	0.156	0.110	0.216	0.406	0.999
34 DPC	0.000	0.143	0.156	0.098	0.243	0.359	0.999
sr-**32** PB	0.002	0.063	0.274	0.131	0.214	0.317	1.001
sr-**32** DPC	0.002	0.074	0.231	0.127	0.228	0.338	1
sr-**34** PB	0.000	0.051	0.278	0.139	0.208	0.323	0.999
sr-**34** DPC	0.000	0.077	0.238	0.139	0.252	0.294	1
D-**34** PB	0.053	0.047	0.278	0.137	0.197	0.288	1
D-**34** DPC	0.043	0.054	0.282	0.130	0.231	0.319	1
36 PB	0.000	0.133	0.131	0.109	0.244	0.382	0.999
36 DPC	0.000	0.118	0.166	0.115	0.255	0.346	1
38 PB	0.045	0.095	0.165	0.108	0.234	0.353	1
38 DPC	0.126	0.134	0.143	0.088	0.211	0.298	1
sr-**45** PB	0.000	0.052	0.260	0.137	0.223	0.326	0.998
sr-**45** DPC	0.000	0.071	0.265	0.132	0.224	0.308	1
47 PB	0.000	0.129	0.258	0.114	0.252	0.358	1.001
47 DPC	0.000	0.139	0.158	0.112	0.260	0.332	1.001
48 PB	0.000	0.167	0.118	0.101	0.255	0.360	1.001
48 DPC	0.000	0.137	0.156	0.108	0.255	0.344	1
49 PB	0.000	0.125	0.153	0.100	0.242	0.379	0.999
49 DPC	0.000	0.113	0.161	0.119	0.260	0.347	1
50 PB	0.000	0.115	0.172	0.114	0.241	0.358	1
50 DPC	0.000	0.148	0.130	0.108	0.272	0.343	1.001

Interestingly, the inactive GA-like 40-mer **38** similarly to GA was α-helical (Figure 3.7.), which confirms our hypothesis that the activity does not directly correlate with the secondary structure.
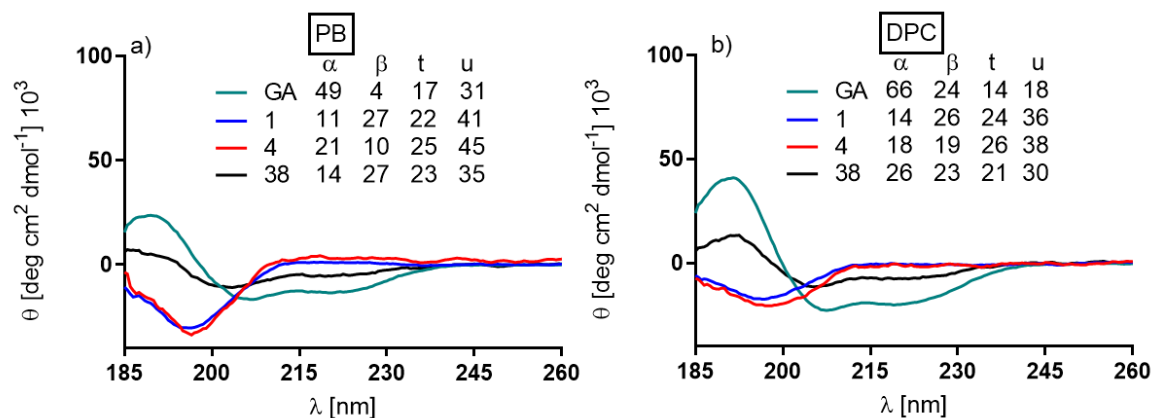
Figure 3.7. *Circular dichroism spectra of GA,* ***32*** *and* ***34*** *(100 μg/mL) in 8 mM phosphate PB at pH 7.4 (a) or in the presence of 5 mM dodecylphosphocholine. Percentage of α-helix and β-sheet was processed by Dichroweb using the CONTIN analysis program and reference set 3.*

3.3. Conclusion

We report a library of 96 peptide dendrimers with a diversity in MW, charges, amino acid ratio and structure, including linear peptides, 1st, 2nd and 3rd generation dendrimers modified or not at *N*-terminus with acetyl, chloroethyl, methylfumarate groups. We explained importance of the stereochemistry for the activity and the main features, which are relevant for the activity.

The initial screening indicated that MW plays an important role for the activity, and the dendrimers must be at least in the lowest range of MW of GA (5-6 kDa). However, MW is not enough to mimic GA, another relevant parameter is total charge of the molecule. It must be a certain positive charge for the molecule to exhibit anti-inflammatory properties. That hypothesis is confirmed by the fact that the active dendrimers **32** and **34** lost their activity when *N*-terminus were masked with acetyl groups. Addition of some extra lysine residues did not lead to significant increase of the activity; however, it did not result in the loss of the activity.

Stereochemistry plays an interesting role in the activity of the dendrimers. As it was expected similarly to D-GA, D-**32** and D-**34**, the analogs of the active dendrimers, completely lost their activity. Therefore, surprisingly stereo randomised analogs *sr*-**32** and *rs*-**34** remained active.

Substituting of some amino acids on the similar ones without changing significantly the structure does not lead to the loss of the activity. Even though it was reported that lysine is an essential for the activity of GA, substituting it on ornithine residues did tot affect the cytokine secretion. Similarly to

lysine-ornithine substitution, using valine, glycine and isoleucine instead of alanine, and phenylalanine, serine and tryptophane instead of tyrosine.

Activity of the dendrimers was accessed by using primary human monocytes of healthy, which were extracted from the whole anticoagulant-treated blood. Primary cells of different donors are sensitive towards immune modulation depending on the healthy state of the donor; hence we observed a different response in terms of amounts of secreted cytokines (1-15 ng/mL) depending on the particular donor. Therefore, this assay does not provide a reliable quantitative readout that would allow for direct comparison of the different levels of activity with different sequences, hence a comparison of the activity based on the concentration of IL-1Ra is not possible.

To better understand the action of dendrimers we conducted more detained biological evaluation of the inflammatory properties of the dendrimers.

4. Detailed evaluation of biological activity

4.1. Introduction

To better understand the action of the dendrimers and to compare their biological properties to GA, we focused on detailed biological properties of the active dendrimers. Having in our hands reliable results from the screening, which indicated the active sequences. We noticed that the response to the treatment with GA and the dendrimers differs on IL-1Ra system, we therefore decided to evaluate the more detailed dose-response. It was shown that, there is a significant donor dependency on the IL-27 secretion in response to GA treatment.[116] Response of the primary cells is not consistent and depends on many factors, including inflammations and post-inflammations occurring in the patients and individual response to the treatment. In this part we performed additional experiments in order to compare effects of GA with dendrimers on different donors. To confirm that the dendrimers are not toxic for the cells, we measured viability of the PBMC in the presence of different concentrations of the dendrimers.

IL-1Ra is an important modulator which is responsible for the reduction of inflammation, however it was reported that more cytokines are involved in the immune modulation, caused by GA. Here we decided to see if other cytokines were affected in response to treatment with our dendrimers, considering that for GA it was shown that several inflammatory cytokines were reduced. [43] To confirm the M2 phenotypical shift we checked expression of some selected surface markers in response to treatment with dendrimers.

Visualisation studies had not been done on GA due to its complicated polypeptide mixture. Taking an advantage of having an exact structure, we obtained fluorophore labelled analogs of our active and inactive dendrimers. Visualisation of the dendrimers distribution inside of the cells could provide an important information about mechanism of action and indicate how dendrimers distribute upon their action and which cells exactly do they affect. We also performed immunostaining of different white blood cells to see, which cell types interact with our dendrimers.

4.2. Results and discussion

4.2.1. Concentration dependency

Concentrations presented in the literature for GA for *in vitro* experiments usually range between 50 and 25 µg/mL. Here we asked the question if an increase or decrease would provide us more reliable response. For that, we tested our dendrimers and GA in a range of concentrations from 100 to 12.5 µg/mL. Indeed for GA the response was the most efficient at concentrations 50 and 25 µg/mL, as reported previously. [43] At the same time, for selected dendrimers **32**, **34** and sr-**34** the activity was significantly higher with 100 µg/mL in both LPS activated and neutral conditions (Figure 4.1).

Even though the response was higher with higher concentration of the dendrimer, 50 and 25 µg/mL were giving a reliable response and have the advantage to reduce the amount of material used. Concentration 12.5 µg/mL was still triggering the response, however for GA it was not enough to distinguish between untreated samples (N.T.) and considering the error bars and inconsistency between different donors we decided to focus on concentrations 50 and 25 µg/mL
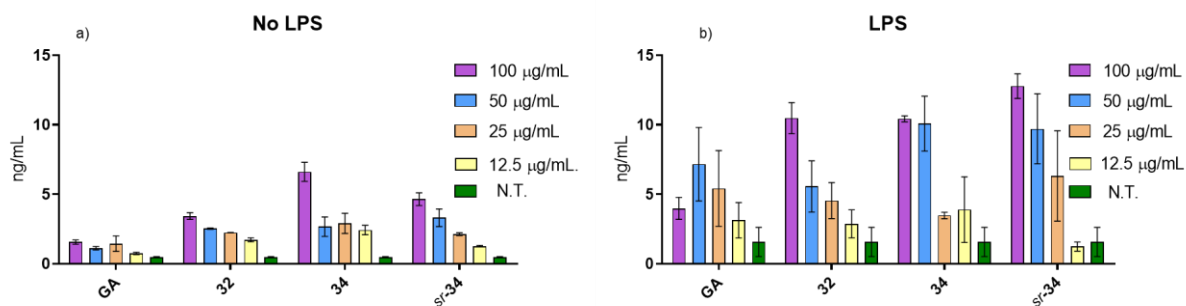
Figure 4.1. *Cytokine level of IL-1Ra in supernatants of monocytes for active dendrimers and analogues evaluated by ELISA assay on primary human monocytes of healthy donors. 5×10^4 cells/200 µL in 96 well plates, were incubated with dendrimers or GA as a control for 48 h in presence or absence of LPS (100 ng/mL), in a range of concentrations (100-12.5 µg/mL) (mean ± SD, n = 3 different experiments).*

4.2.2. Cells survival of PBMC in response to treatment with selected dendrimers

After accessing the working concentrations of the dendrimers, as a next step we accessed cytotoxicity of the dendrimers on PBMC. For that test it was not important to use monocytes since general toxicity usually would affect different cell types.

The results were accessed by Alamar Blue assay and indicated that neither GA nor dendrimers were toxic at any of the used concentrations, which is confirming our choice of the selected concentrations for the further biological investigations (Figure 4.2).
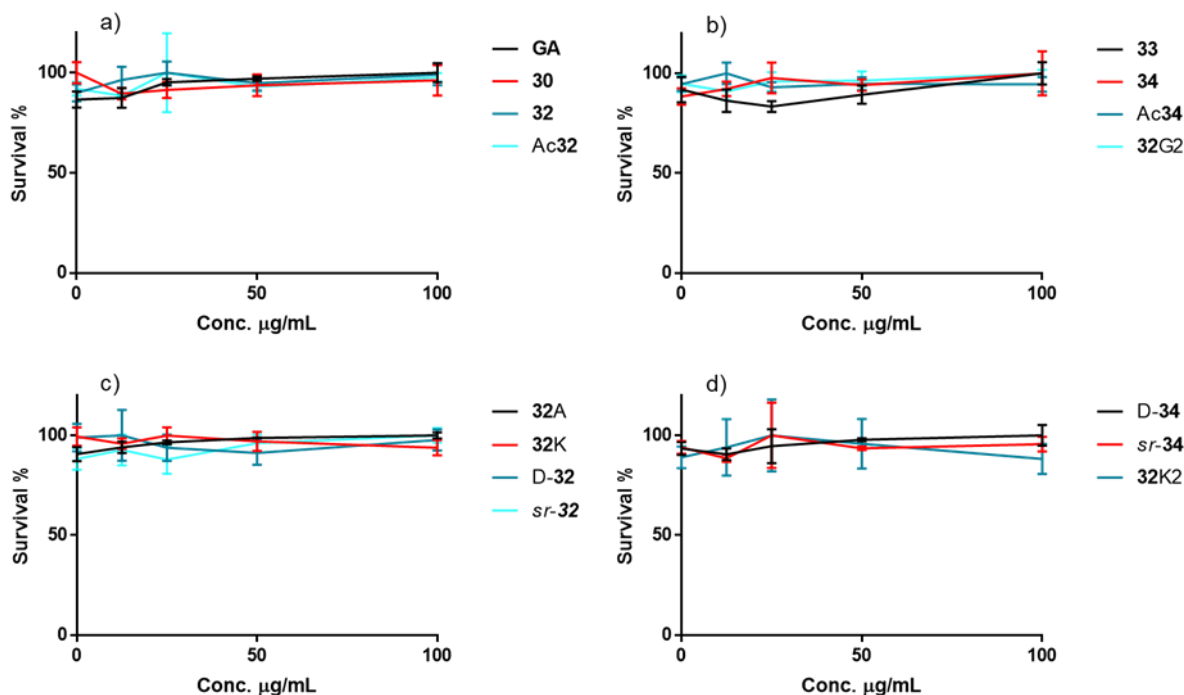
Figure 4.2. *Survival of PBMC after 24h of incubation in the presence of peptide dendrimers in a range of concentrations (100-12.5 µg/mL) 5x10^4 cells/200µL in 96 well plates, were incubated with dendrimers or GA. (Normalized rows means ± SD, n = 3 different experiments). After incubation 50 µL of 50% AlamarBlue was added in supplemented medium for additional 12 h, then fluorescence was measured according to the manufacturer protocol.*

4.2.3. Donor dependency in IL-1Ra secretion for healthy donors

While accessing the activity of the synthetized libraries we noticed, that amounts of secreted cytokines differ depending on the donor for all the conditions, including the untreated samples. Similar donor dependent responses of cytokine release to GA have been reported for IL-27.[116]

Similarly, a survey of monocytes from five different healthy donors (HD) showed different levels of secreted IL-1Ra in response to GA and the dendrimers (Figure 4.3.a-b). For instance, three donors reacted stronger to dendrimers **32** and **34** than to GA (HD1, HD4, HD5), one stronger to GA (HD2), and one donor did not react significantly to the compounds (HD3). Interestingly, HD1 and HD4 exhibit higher levels of secreted IL-1Ra even without treatment, and even higher levels in case of the treatment. At the same time, HD2 and HD5 showed lower levels of IL-1Ra with treatment and without.
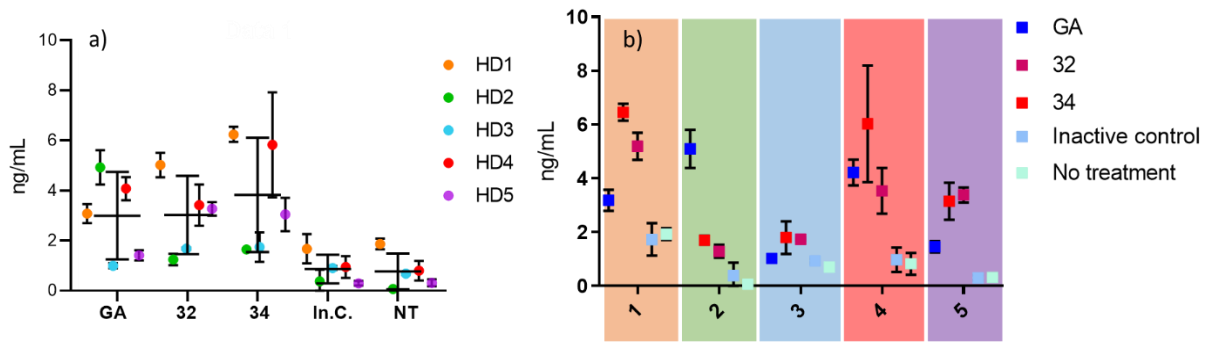
Figure 4.3. Healthy donor responses to GA, peptide dendrimers 1 and 4, In.C. – Inactive Control (inactive dendrimer from screening) and NT – No treatment in IL-1Ra secretion for 5 different donors. Each color represents a different healthy donor (HD 1-5). Supernatants were analyzed by ELISA after 48 h of incubation 5×10^4 cells/200µL in 96 well plates. Concentration of GA and peptide dendrimers was 50 µg/mL Data is presented as a mean ± SD, n = 2-3 independent experiments.

Even though different donors can respond unpredictably in terms of amounts of secreted cytokines, all of them exhibit comparatively low amounts of IL-1Ra in case of treatment with inactive control or without treatment (Figure 4.3. a).

4.3. IL-1Ra secretion on monocytes versus leukocytes

To assess if IL-1Ra was specific for monocytes or leucocytes we separated monocytes from leukocytes using Percoll gradient centrifugation which gave us two fractions: enriched monocytes and enriched leukocytes, which includes T cells, B cells and Natural Killers (NK). The induction of IL-1Ra by GA and dendrimers **32** and **34** was specific for monocytes and did not occur with lymphocytes (Figure 4.4.).

That finding indicated that monocytes are the only cells secreting IL-1Ra and can suggest that both GA and dendrimers initially react with APC, which later activate the adaptive immune system.
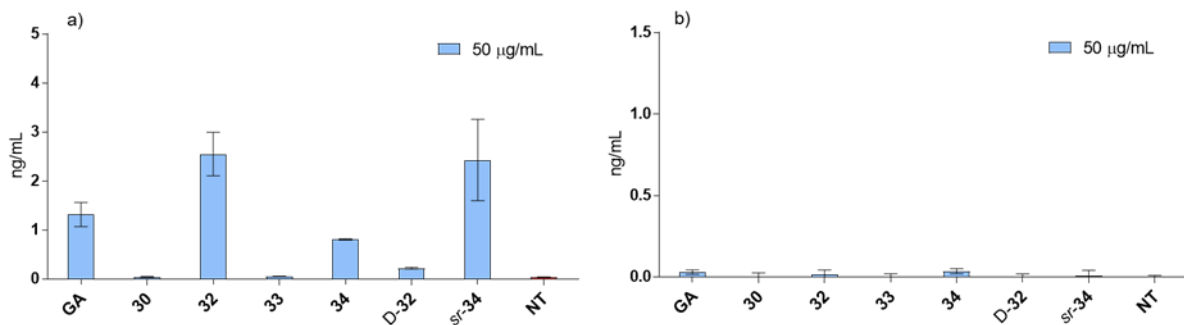
Figure 4.4. Cytokine level of IL-1Ra in supernatants of monocytes enriched fraction (a) and the rest of leukocytes (b) for active dendrimers and analogues evaluated by ELISA assay. Monocytes fraction was

separated from whole PBMC by Percoll density gradient centrifugation. Monocytes enriched fraction was separated using 5×10^4 cells/200 µL in 96 well plates were incubated with dendrimers or GA (50-25 µg/mL) as a control for 48 h (mean ± SD, n = 2 different experiments).

4.5. mRNA quantification in time

To assess more cytokines at the mRNA level we performed Real-Time quantitative Polymerase Chain Reaction (qRT-PCR) on primary monocytes in the presence and the absence of LPS. We selected active dendrimer **32**. We controlled secretion of the cytokines at different time points: 3 h, 6 h, 18 h, 24 h. mRNA synthesis is a first step of the cytokine synthesis, and for that reason the time intervals were chosen accordingly.

We choose IL-1β and TNF-α since they play a major role in MS pathogenesis, being the most well-established signals of inflammation. LSP activation stimulates an immediate strong inflammatory response and M1 phenotypical shift. At the same time, in the case of M2 anti-inflammatory shift, inhibition of the inflammation occurs which leads to IL-1 β and TNF-α suppression. LPS is known as a stimulus, which leads to a fast a strong response, however with time the initial response wanes even though the concentration of LPS remains constant.

To prove that our dendrimers are not immunogenic, we conducted a stimulation experiment. We also observed the action of our dendrimer in presence of LPS, looking for evidence of induction of inflammation. A time-profile of cytokine release showed that dendrimer **32** significantly inhibited the production of the proinflammatory cytokine IL-1β, which occurred in the first few hours in both inactivated and LPS-activated monocytes (Figure 4.5.a/b). Dendrimer **32** also inhibited the release of TNF-α triggered upon the initial activation of monocytes by LPS (Figure 4.5.c/d). Finally, dendrimer **32** induced the release of IL-1Ra both with and without LPS activation, but in the latter case the effect was detected only after 18 h incubation (Figure 4.5e/f). These cytokine modulation effects with inhibition of IL-1b and TNF-a and promotion of IL-1Ra suggested that dendrimer **32** shifted monocytes towards an anti-inflammatory M2 phenotype.
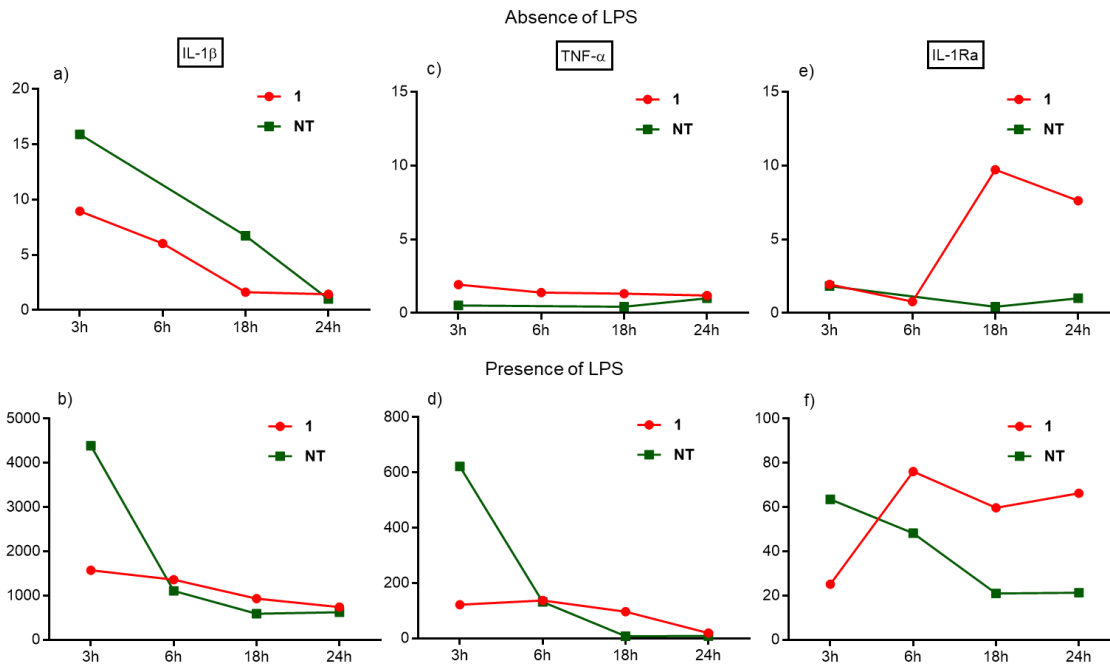
Figure 4.5. *Dendrimer **32** affected mRNA levels in both LPS-activated and resting monocytes. Monocytes 4×10^6 cells/3 mL in 6 well plates were incubated for indicated time with 50 µg/mL of **32** or without any treatment (NT) (a, c, e); or preincubated for 1 h with 100 ng/mL of LPS, and then with 50 µg/mL of **32** (b, d, f) or without any treatment (NT). Total RNA was isolated, reverse transcribed and analyzed by RT-qPCR for presence IL-1β, IL-1Ra and TNF-α.*

4.6. Confocal Microscopy with Fluorescein labelled dendrimers

In contrast to GA which is a polymeric mixture, our dendrimers are entirely well-defined and therefore can be selectively labelled.[117] Here we prepared **32**Fl, an analog of **32** bearing a fluorescein label at the dendrimer core, to directly visualize the extent of its interaction with monocytes (Table 4.1.). Dendrimer **32**Fl showed similar IL-1Ra release activity as the unlabelled dendrimer **32**. Confocal imaging in the presence or absence of LPS after 48 h of incubation showed that the **32**Fl was mostly bound to the cell surface, with only partial localization in endosomes indicated by a punctuated pattern. This localization is consistent with an interaction at the cell surface to trigger a biological response (Figure 4.6.).
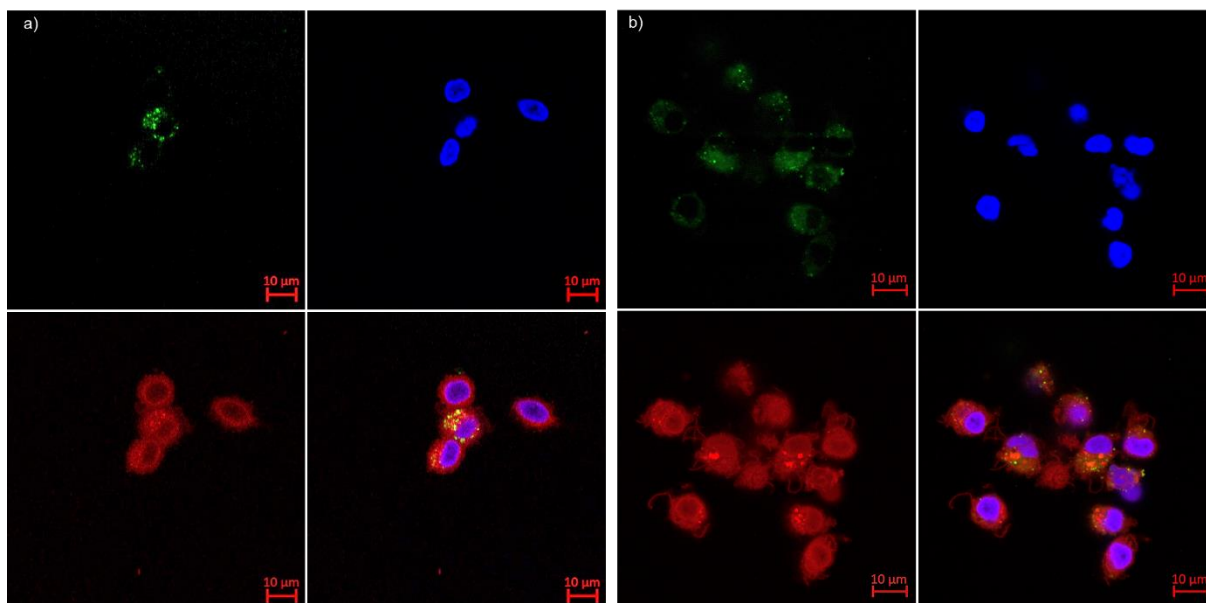
Figure 4.6. *Confocal microscopy of primary human monocytes incubated for 48 h with **32**Fl (50 µg/mL) in the absence of LPS (a) (10^5 cells/200 µL) or presence of LPS (100 ng/mL) (b). Membrane is in red (CellMask Deep Red), nucleus is in blue (Hoechst33342), compounds are in green (Fluorescein).*

Similarly to **32**Fl, we created a library consisting of selected dendrimers, which are modified with fluorophore groups, to see whether active and inactive dendrimers distribute differently within monocytes. Following the same reaction sequence, we obtained *sr*-**32** as an active analog, D-**32**, Ac**32**, and **35** as inactive derivatives. Previous findings indicated localisation of the dendrimer after 48 h of incubation, which correlates with the secretion peak. Here we asked the question, how the localisation would look like given it shorter time intervals, considering that the interaction, leading to the desired response, most likely occurs within first few hours of treatment. Confocal images were taken after 3, 6 and 18 h of treatment for each of the dendrimers. Cells were not preincubated prior the treatment to avoid morphological changes.

We observed similar effects for **32** and its inactive analog Ac**32**, after 3 h of incubation, dendrimers were mostly localised in the membrane, however after 6 h of incubation there are small amounts of fluorescein in the nucleus. After 18 of incubation dendrimer is localised in the membrane with partial distribution in endosomes. Nevertheless, it is not clear if the compound is partially digested following penetration and the metabolite of fluorescein penetrates the nucleous. Indeed, considering the whole structure of these compounds, it is unlikely for a conjugate to penetrate nucleus. Compound **35**Fl was neither active nor showed a distribution in the membrane, which suggests that a certain membrane affinity may be required for the activity (Table 4.1.).

Table 4.1. *Fluorescent labelled analogs*

ID	Sequence[a]	Yield, mg (%)[b]	MS calc./obs.[c]
32Fl	(KA)$_8$(KAK)$_4$(KEKA)$_2$$K$AKEAYC(FlTC)A-NH$_2$	6.5 (40.6)	5207.0373/5207.0391
D-**32**Fl	((ka)$_8$($k$ak)$_4$($k$eka)$_2$$k$akeayc(Fl)a-NH$_2$	6.1 (40.3)	5207.033/5207.0389
sr-**32**Fl	(KA)$_8$(KAK)$_4$(KEKA)$_2$$K$AKEAYC(Fl)A-NH$_2$	5.2 (37.8)	5207.0373/5207.0256
Ac**32**Fl	(AcKA)$_8$(KAK)$_4$(KEKA)$_2$$K$AKEAYC(Fl)A-NH$_2$	7.1 (42.5)	5545.1375/5545.1257
35Fl	(KAA)$_8$(KKAKAK)$_4$(KAAKKY)$_2$$K$EKAKC(Fl)A-OH	4.8 (38.1)	7445.5629/7446.5164

[a] One-letter code amino acids are used, *K* is the branched lysine residue, Ac is acetyl group on *N*-terminus, OH is the carboxyl *C*-terminus, NH$_2$ is carboxamide *C*-terminus, Fl is fluorescein diacetate 5-succinimide. [b] Isolated yields as trifluoroacetate salt after preparative RP-HPLC purification. [c] ESI-MS data.

Images of the racemic analog *sr*-**32** were completely different from the rest of the compounds. Cells partially lost their structure with observable fragments of the membrane present on the plates. This is suggestive of immunogenicity and a stress caused by treatment with the racemic analog. That stress can explain loss of adherent properties of monocytes and their unexpected behaviour.
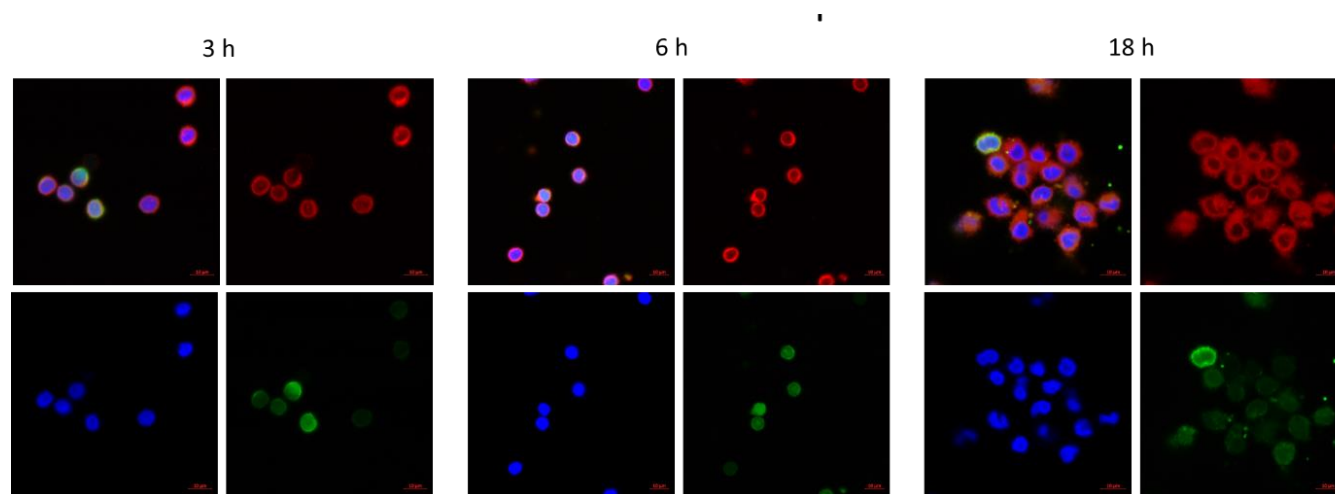
Figure 4.7. *Confocal microscopy of primary human monocytes incubated for 3 h, 6 h, 18 h with **32**Fl (50 µg/mL) (10^5 cells/200 µL) Membrane is in red (CellMask Deep Red), nucleus is in blue (Hoechst33342), compounds are in green (Fluorescein).*
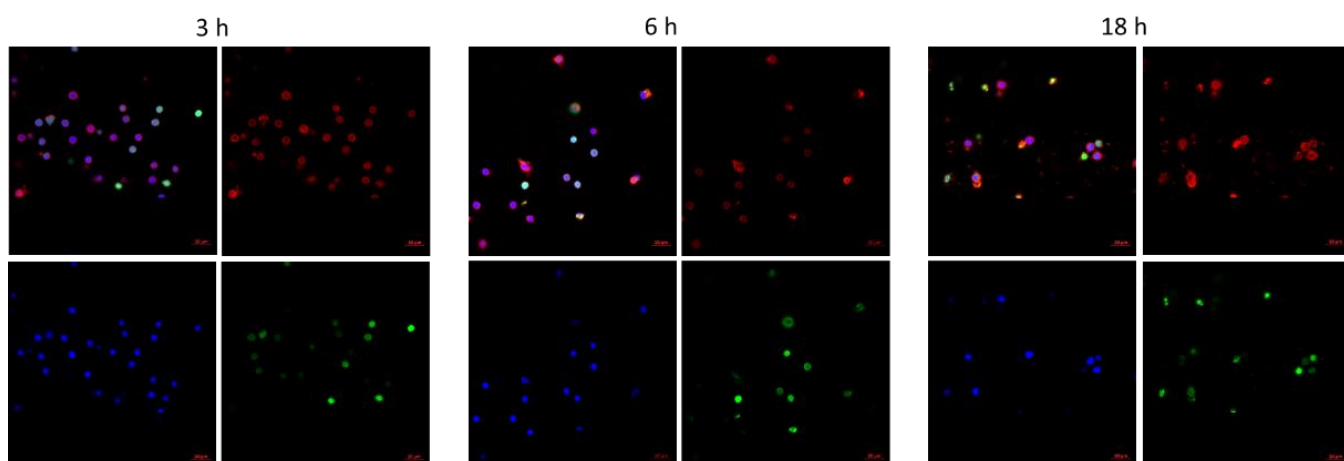
Figure 4.8. *Confocal microscopy of primary human monocytes incubated for 3 h, 6 h, 18 h with sr-32Fl (50 µg/mL) (10⁵ cells/200 µL) Membrane is in red (CellMask Deep Red), nucleus is in blue (Hoechst33342), compounds are in green (Fluorescein).*
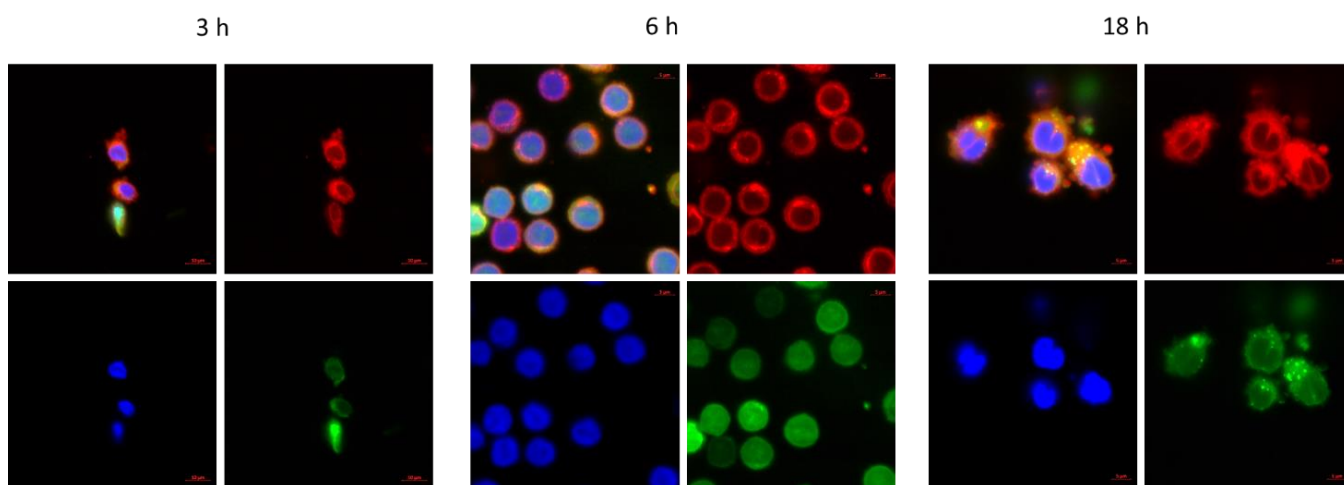
Figure 4.9. *Confocal microscopy of primary human monocytes incubated for 3 h, 6 h, 18 h with Ac32Fl (50 µg/mL) (10⁵ cells/200 µL) Membrane is in red (CellMask Deep Red), nucleus is in blue (Hoechst33342), compounds are in green (Fluorescein).*
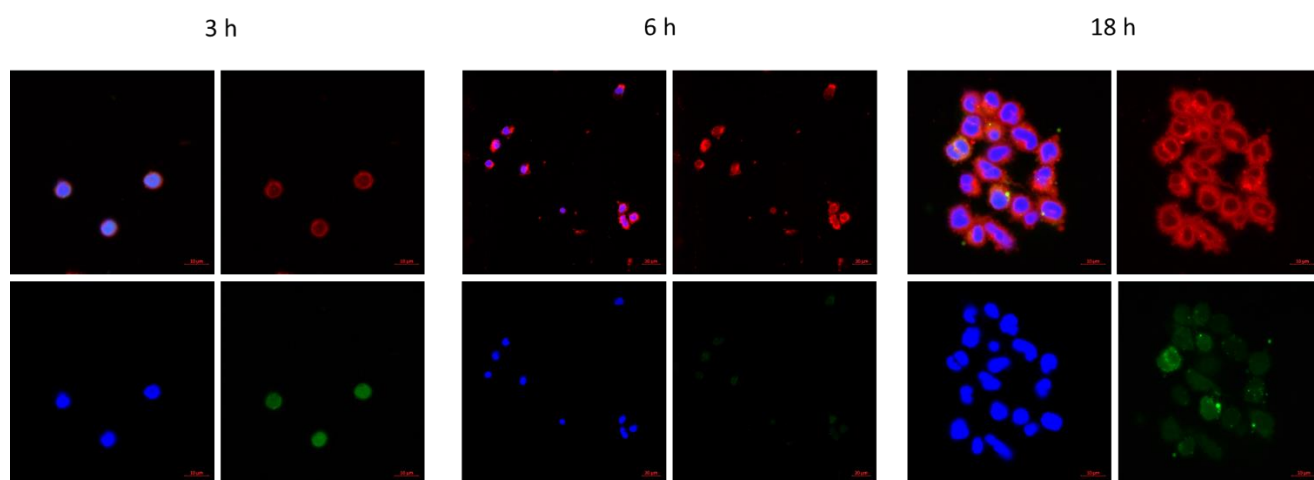
Figure 4.10. *Confocal microscopy of primary human monocytes incubated for 3 h, 6 h, 18 h with 36Fl (50 µg/mL) (10^5 cells/200 µL) Membrane is in red (CellMask Deep Red), nucleus is in blue (Hoechst33342), compounds are in green (Fluorescein).*

4.7. Immunostaining of PBMC

Literature suggests that GA affects APC cells.[17] This observation also corelates with our own experiments on leukocytes, which did not secrete IL-1Ra neither in presence of GA nor dendrimers. Here we asked the question, how does the distribution of the fluorescent labeled dendrimers look for the PBMC.

To prove that the primary interaction occurs with APC, we performed confocal imaging of PBMC stained with fluorescent labeled antibodies. Another purpose of the experiment was to see if cells increase frequency of their interactions due to the treatment and what kind of interactions is prevalent.

As we expected, fluorescent labeled dendrimers were mostly localized at APC, suggesting that the primary interaction occurs on innate immune cells, which, being polarized towards anti-inflammatory phenotype, reduce inflammation. The experiment was conducted at the CeMM Research Center for Molecular Medicine of the Austrian Academy of Sciences on the "Pharmacoscopy platfom" in Vienna. [118]

Staining of CD14 indicated, that most of the dendrimers distributed within the membrane as endosomes. At the same time, for T cells staining we choose CD3 antibody, which allows to include both T helper cells (CD4 positive) and cytotoxic T cells (CD8 positive). Dendrimers were not observed in the T cells, indicating indirect action. In presence

of T cell activator (TCR) there were no difference in the cell morphology observed, however the staining for T cells was diminished, due to competitive binding of TCR and the staining antibody.
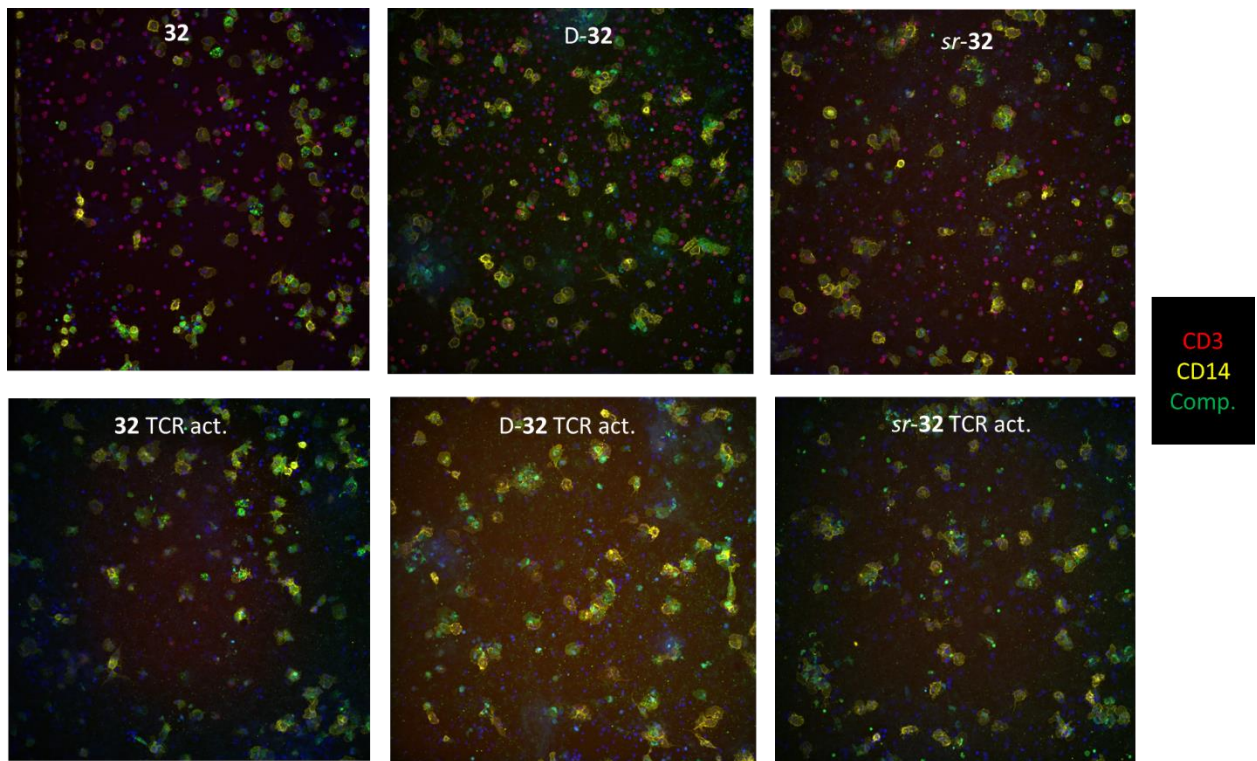
Figure 4.11. *Confocal images on PBMC stained with CD14 – monocytes (yellow) and CD3 – T cells (red). Cells were treated with fluorophore labelled compounds (green).*

4.8. Multicolor Flow Cytometry

Immunophenotyping by multicolour flow cytometry is a potent method, which allows to infer the phenotypical shift and learn about cell activation. To further probe the immunomodulatory effects of dendrimer **32** in comparison to GA, we measured the response of typical surface markers, which we measured by flow cytometry on PBMCs, labeled with fluorophore-conjugated antibodies (Figure 4.12.).
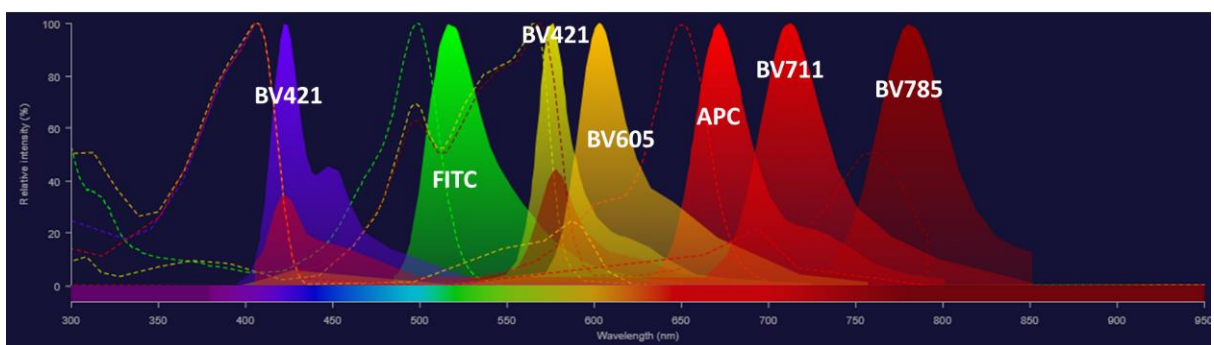
Figure 4.12. *Fluorophore multicolor panel of 7 different fluorophores. CD14 - PE, CD16 - BV605, HLA-DR - BV421, CD68 – PECy7, CCR2 – BV711, CD206 - APC.*

Under non-activated conditions, dendrimer **32** downregulated the innate immune response receptors CD14 (LPS receptor), CD16 (Fcγ receptor III), HLA-DR (Human leukocyte antigen class II) [50] and CD68 (peptide transport, antigen processing), indicative of a general immunosuppressive property (Figure 4.19.). Dendrimer **32** also downregulated the chemokine receptor CCR2, which is often used as a marker for M1 (pro-inflammatory state)[119,120] and upregulated CD206, a mannose receptor used as marker for M2 (anti-inflammatory state).[121] Similar but weaker effects occurred with analogs D-**32** and Ac**32** although they did not induce IL-1Ra release. By contrast, GA upregulated CD14, CD16 and CD68, but did not affect HLA-DR, CCR2 or CD206. Under LPS-activated conditions on the other hand the levels of all surface markers were strongly enhanced in non-treated cells but downregulated by the dendrimers and GA alike.

PBMC of healthy donors were obtained by Ficoll density gradient centrifugation. Cells were incubated for 1 h in presence or absence of LPS (100 ng/mL) in 6-well plates, 4×10^6 cells/well, then with GA, selected dendrimers (50 µg/mL) or without any treatment for 18 h. After incubation cells were detached, washed twice with staining buffer (0.5% BSA in $1 \times$ PBS) and stained according to manufacture protocols for 30 min on ice with following antibodies: CD14 - PE, CD16 - BV605, HLA-DR - BV421, CD68 – PECy7, CCR2 – BV711, CD206 – APC (Figure 4.12.). After two washes with staining buffer, samples were a acquired on LSR II SORP H274 and analyzed using FlowJo software.
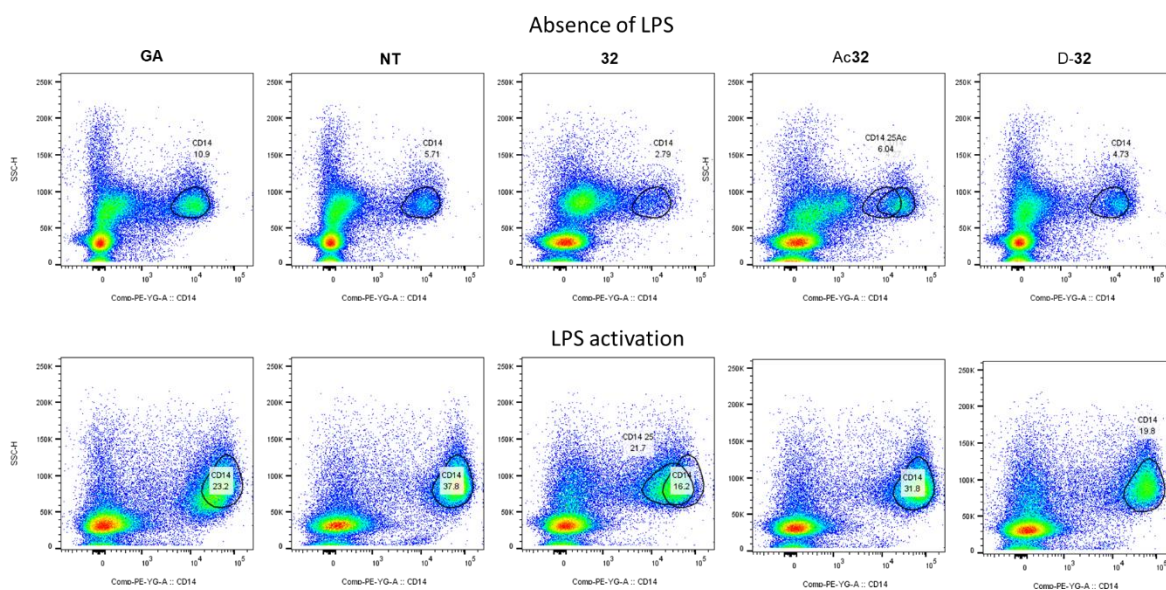
Figure 4.13. *Flow cytometry dot plot showing the difference in CD14 expression on PBMC of a healthy donor in response on the treatment (50 μg/mL) with the dendrimers and GA or without treatment (NT) in absence of LPS for 18 h.*

CD14 was diminished for active dendrimer **32** and remained constant for inactive dendrimers and untreated samples in absence of LPS. By contrast to the dendrimers, GA significantly upregulated CD14 in absence of LPS. Nevertheless, in presence of LPS we observed downregulation of CD14 for our active dendrimer **32** higher than for GA (Figure 4.13).

CD16 was significantly downregulated for both neutral and inflammatory conditions compared to untreated sample in case of treatment with GA and dendrimers (Figure 4.14). Interestingly, the inactive dendrimers Ac**32** and D-**32** retained some activity towards downregulation, but not for the IL-1Ra system.
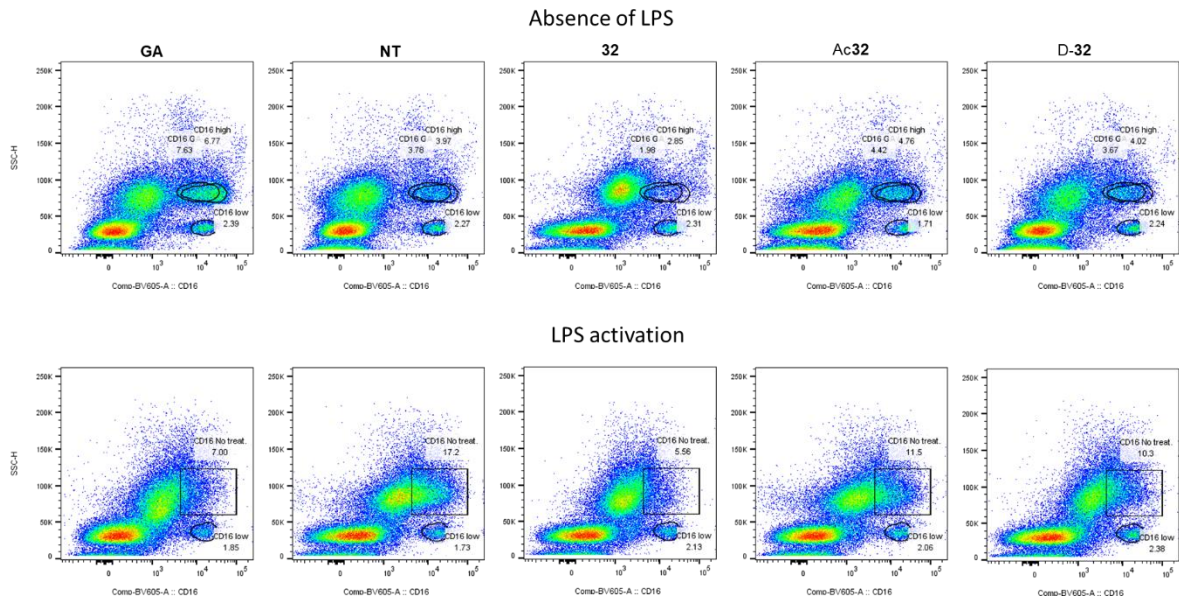
Figure 4.14. *Flow cytometry dot plot showing the difference in CD16 expression on PBMC of a healthy donor in response to the treatment (50 µg/mL) with the dendrimers and GA or without treatment (NT) in absence of LPS for 18 h.*

CD68 was upregulated for GA in neutral conditions and downregulated for active dendrimers. In case of LPS activation both active dendrimer and GA downregulated the expression. Inactive dendrimers remained similar activity to the not treated sample (Figure 4.15.).

CCR2 remained unaffected for the neutral conditions. By contrast, the action of GA and active dendrimer **32** was alike, resulting in downregulation of the CCR2 (Figure 4.16). Inactive controls were not affecting the surface marker and were similar to untreated control.

Similarly to CCR2, HLA-DR was unaffected in the absence of LPS for GA and dendrimer **32**. In the presence of LPS the expression was downregulated for GA, **32** and D-**32**, and remained untouched for the inactive dendrimer Ac**32** (Figure 4.17.).
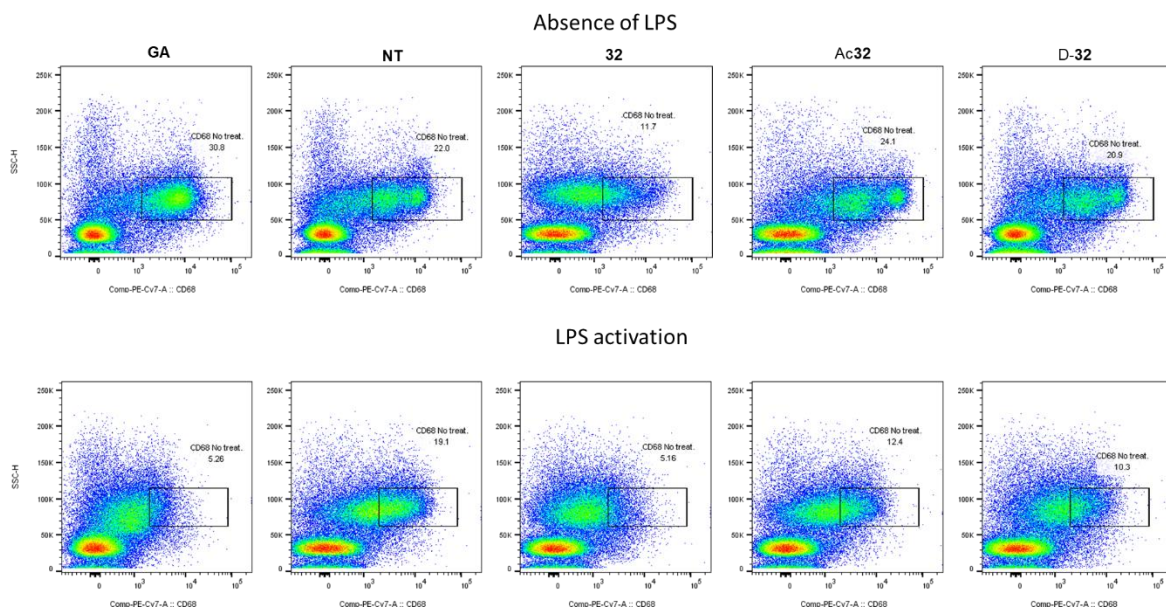
Figure 4.15. *Flow cytometry dot plot showing the difference in CD68 expression on PBMC of a healthy donor in response to the treatment (50 μg/mL) with the dendrimers and GA or without treatment (NT) in absence of LPS for 18 h.*
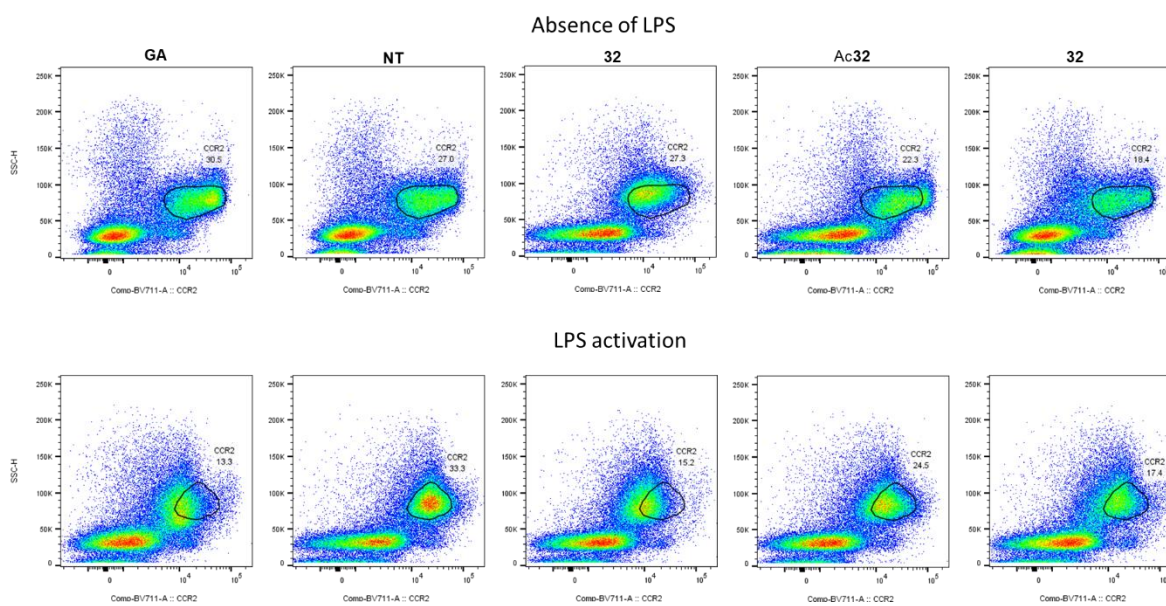
Figure 4.16. *Flow cytometry dot plot showing the difference in CCR2 expression on PBMC of a healthy donor in response to the treatment (50 μg/mL) with the dendrimers and GA or without treatment (NT) in absence of LPS for 18 h.*
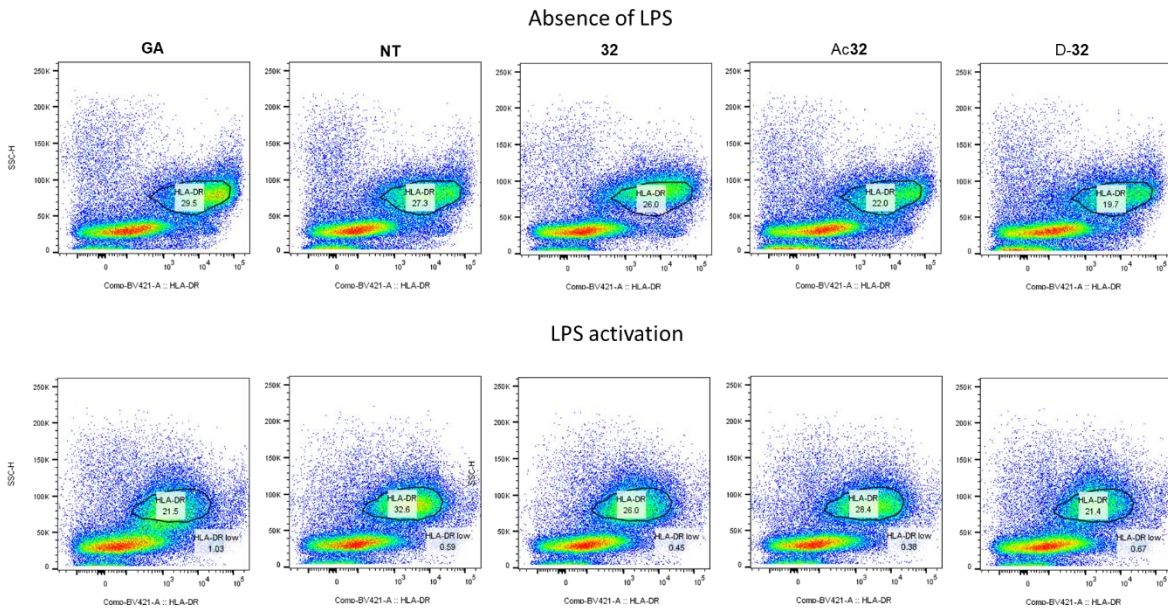
Figure 4.17. *Flow cytometry dot plot showing the difference in HLA-DR expression on PBMC of a healthy donor in response to the treatment (50 µg/mL) with the dendrimers and GA or without treatment (NT) in absence of LPS for 18 h.*

In contrast to the previously observed markers, CD206 belongs to the markers which are characteristic for M2 anti-inflammatory phenotype. Here in neutral conditions, we observe a significant upregulation for our active dendrimer **32**. D-**32**, its analog exhibit slight increase in upregulation, at the same time, GA did not affect CD206 expression or downregulate it compared to untreated control. In presence of LPS all the samples downregulated CD206 (Figure 4.18.).
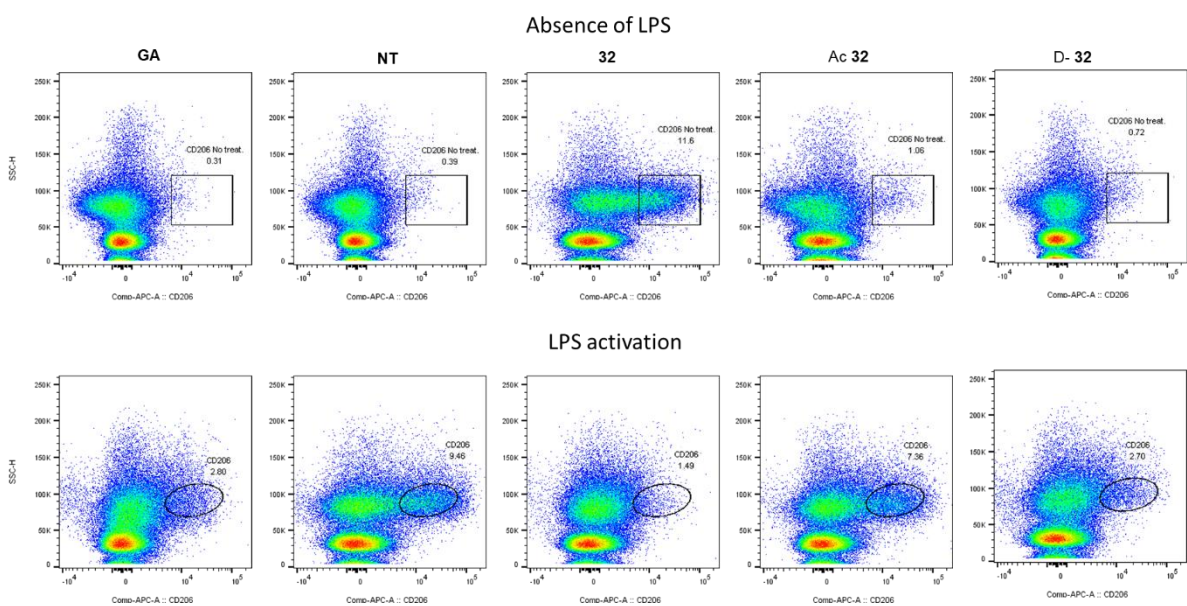
Figure 4.18. *Flow cytometry dot plot showing the difference in CD206 expression on PBMC*

of a healthy donor in response to the treatment (50 µg/mL) with the dendrimers and GA or without treatment (NT) in absence of LPS for 18 h.
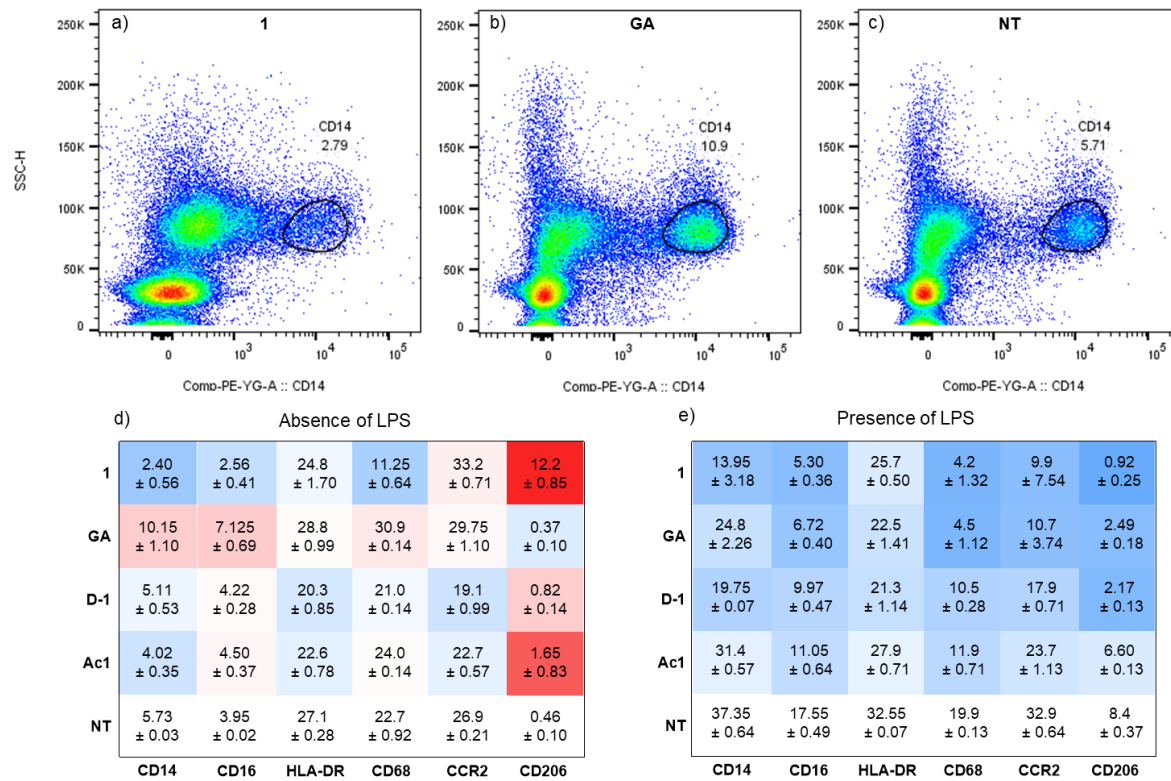
***Figure 4.19.** Flow cytometry dot plot showing the difference in CD14 expression on PBMC of a healthy donor in response on the treatment (50 µg/mL) with **32** (a), GA (b), or without treatment (c) in the absence of LPS for 18 h. Heatmap of surface markers expression in response on treatment with active dendrimer **32**, GA, inactive dendrimers D-**32** and Ac**32** in the absence (d) and presence of LPS (100 ng/mL) (e). Data is presented as a mean ± SD, n = 2 independent experiments.*

Flow cytometry experiment showed that general activity of monocytes was inhibited, hence the most of receptors were down regulated for dendrimer **32** in the absence or the presence of LPS except to CD206 which was upregulated in neutral conditions (Figure 4.19.). Downregulation suggests of reduction of the monocyte's activity, which suggests alternative activation of the monocytes in response to our dendrimers. The action of the active dendrimer **32** and GA not consistent in absence of LPS. All surface markers except CD206 were upregulated which suggests about different action. In the presence of LPS the activity of monocytes was downregulated for both GA and the dendrimers. Interestingly, while the

inactive dendrimer Ac**32** was acting equally to not treated sample. D-**32**, an analog built from D-amino acids, exhibit similar patterns in the activity to the dendrimer **32**, albeit much weaker.

4.9. Conclusion

Here we conducted detailed analysis of the biological action of the dendrimers and GA on primary human monocytes and PBMS. We confirmed that our dendrimers are not toxic in the range of concentration applied to them. At the same time, we discovered the working concentration for the dendrimers, to obtain the most reliable results.

While performing our screening and optimizing the conditions, we have noticed, that amounts of secreted IL-1Ra differed for both treated and untreated samples. We discovered that there is a strong donor dependency similarly to IL-27 and amounts of the secreted cytokines can differ from 1 ng to 10 ng. Normalization using the base levels of each donor partially mitigated this problem.

We also confirmed induction IL-1Ra on mRNA levels. Together with inhibition of TNF-α and IL-1β the results suggest about M2 phenotypical shift in response on treatment with our dendrimers.

To visualize the distribution of our dendrimers within cells, we prepared fluorescently labeled analogs of some selected active and inactive dendrimers. Confocal images revealed the higher localization on the membrane and in the endosomes. Immunostaining provided us a reliable readout about primary interaction of our dendrimers to APC. Among all the PBMCs, we observed the preferred localization of our dendrimers was in monocytes.

Finally, flow cytometry data showed general inhibition of activity for monocytes, which can be evidence of M2 shift and immunomodulatory activity of our dendrimers consistent with a possible.

5. General conclusion

Aiming to discover a well-defined compound with immunomodulatory properties similar to GA, we designed and synthesized in total 101 peptides and peptide dendrimers. Since the lower size range for GA is barely reachable by either synthesis on the solid support or in solution, here we mostly focused on dendrimer structure. By growing the compounds by concurrently extending multiple branches at higher dendrimer generation, we could easily achieve size of the target copolymers. Keeping in mind, that GA is hydrolyzed at the site of injection, we also prepared shorter sequences of linear peptides and peptide dendrimers. The design of the sequences was performed manually and by creating a virtual library *in silico*.

As an activity screen, we controlled secretion of IL-1Ra on primary monocytes, which pointed out two active sequences **32** and **34**. The SAR indicated, that the molecular weight plays an important role, since only the largest dendrimers exhibited the activity and the **32**G2 analog of the active dendrimer **32** had completely lost its activity. At the same time, the loss of activity was observed in the case of *N*-terminal modification for Ac**32**, Fum**32**, Ac**34**, Fum**34**. Activity was also lost with D-**32** and D-**34** enantiomers, however the stereorandomized analogs *sr*-**32** and *sr*-**34** remained active, which suggests that the secondary structure is not required for the activity. Remarkably, substitution of the "GLAT" amino acids by similar ones did not lead to the abolishment of the activity, opening another avenue for generating analogues.

After we discovered the SAR, we decided to investigate biological effects of our dendrimers in comparison to GA. We have shown that monocytes, but not leukocytes are the primary cells to response on the treatment. That was confirmed by ELISA assay of IL-1Ra secretion, where only the monocytes were secreting the cytokine. On the other hand, the immunostaining indicated the fluorescently labelled dendrimers diffused in the membrane of the monocytes and did not interfere with T cells. Next, we determined the action of the dendrimers on monocytes of different donors, evidencing significantly different levels of secreted cytokines in different samples. However, in all cases we observed upregulation of cytokines characteristic to M2 anti-inflammatory phenotypical shift. In addition, using qRT-PCR we showed inhibition of the proinflammatory response (such us IL-1Ra and TNF-α) in the presence of LPS and enhanced production of IL-1Ra for both inflammatory and neutral conditions. To confirm the M2 shift of the monocytes, we controlled the expression of the typical surface markers. We observed a significant downregulation of the activity (CD14, CD16, CD68, CCR2, HLA-DR receptors) in response on the treatment with our active

dendrimer **32**. At the same time, secretion of the M2 marker CD206 was enhanced in neutral conditions, suggesting M2 phenotyping.

To directly observe interactions between monocytes and our dendrimers, we prepared fluorescent labelled analogs of the active dendrimer and its inactive derivatives. We observed the increased distribution of our dendrimers on the membrane and in the endosomes, which suggests the activation occurring at the surface. The inactive dendrimer **35**Fl was not present on the surface of the treated monocytes, however the inactive dendrimers D-**32** and Ac**32** were present on the membrane but did not trigger the activity. That observation suggests that affinity to the membrane is required for the activity, nevertheless it might not be sufficient to trigger a response.

To conclude, here we present, for the first time, analogs for GA as a fully defined and well characterized peptide dendrimer. Peptide dendrimers are the convenient choice to solve the problem of synthesis of the peptide with the size of GA, especially since we have several hints that indicate that the exact secondary structure does not play a significant role in the modulation of the activity. Considering the immunomodulatory properties, well defined sequence and lack of cellular toxicity, dendrimer **32** could be a suitable starting point to develop new immunomodulatory compounds.

6 Outlook

6.1. More investigations

6.1.1. Mechanistic investigation on the cellular level

We described an immunomodulatory peptide dendrimer, which was inspired from Glatiramer acetate. Since the mechanism of action of GA remained an unsolved issue, we took advantage of the well-defined structure of our dendrimers combined with the use fluorescent labels to provide more insights at the cellular level. We discovered that the dendrimers affect CD14 cells, which results in appearance of some new populations of monocytes. To understand better the nature of those cells by using the fluorescence activated cell sorting, we could separate dendrimer-activated cells (Figure 6.1.). Detailed sequencing of these populations could help us with understanding of the pathways, which are triggered for the immunomodulation.
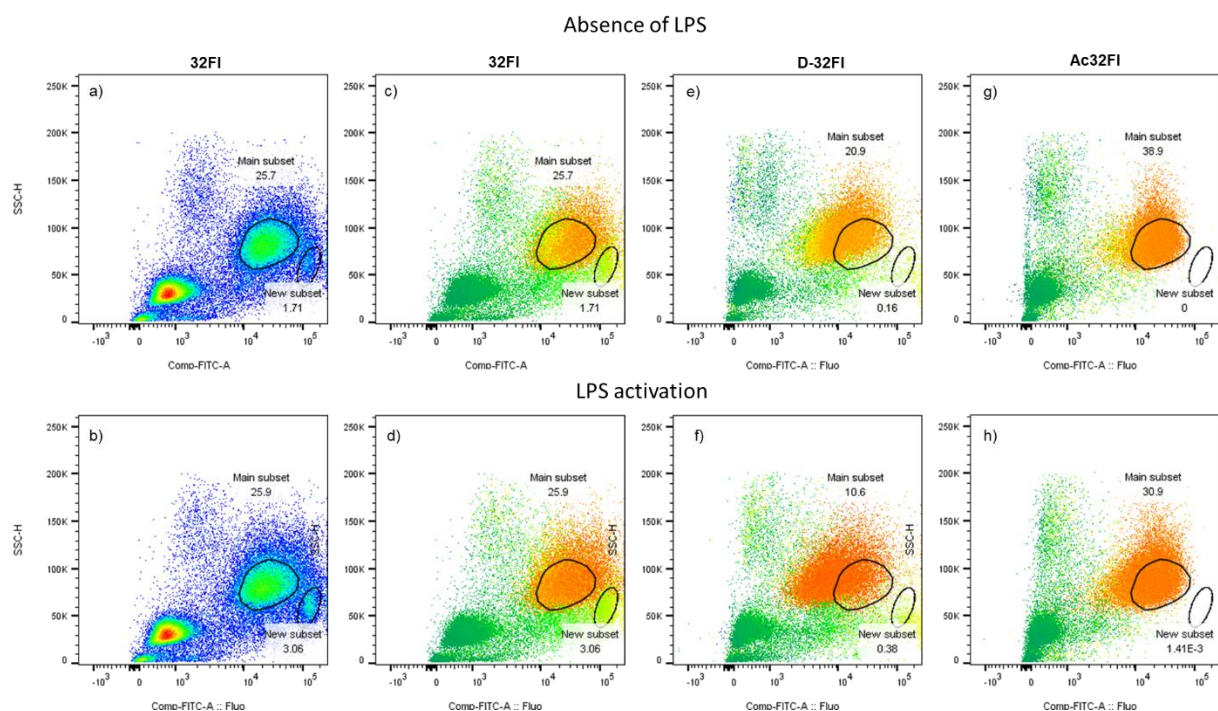
Figure 6.1. *Flow cytometry dot plot in response on treatment with fluorescein labelled dendrimers (50 µg/mL), showing the appearance of new subsets on PBMC of a healthy donor (a-d) and the absence of the subsets in response in treatment with inactive dendrimers (e-h) in the presence or the absence of LPS for 18 h. Images are present for **32Fl** in pseudocolor (a-b) and with color axis for the concentration of CD14 (c-h).*

6.1.2. Action of the dendrimers on the blood cells of MS patients

We observed effects of our dendrimers on the blood cells of healthy donors, mimicking inflammatory conditions by the LPS stimulation. However immune cells of the MS patient differ significantly from the healthy donors, exhibiting higher numbers of inflammatory activated Th1 Th17 cells together with pro-inflammatory monocytes. As a next step it is important to prove our dendrimer not only affects LPS activated monocytes, but also the autoimmune inflammation, caused by MS.

Observing the action of our active dendrimer and comparing the effect to GA would be a first step in comparison of the biological properties. Next, fluorescently labeled analogs could be challenged in terms of surface markers expression and distribution within the cells.

6.1.3. Investigation in animal model (EAE)

Experimental autoimmune encephalomyelitis (EAE) is a clinically relevant murine model of MS, hence many of pathologies, which have been observed in the CNS of mice with EAE are similar to those in the CNS of MS patients. Similarly to MS, EAE is characterized by the immune cells infiltration into the CNS and initiation of demyelination. Inflammatory-polarized macrophages, T cells, T killers, monocytes after crossing the BBB secrete pro-inflammatory cytokines increasing the inflammation and demyelination.

As we mentioned previously, the activity of GA was discovered on mice model, since GA was expected to enhance the EAE. Opposite to the expectations, GA acted by protecting from the development of the disease. Here it would be interesting to see whether our dendrimer could suppress acute EAE in mice similarly to GA. Assessing not only on the survival rates, but also the number of the new lesions in the CNS together with the monitoring of the blood cells polarization could provide a reliable readout for the anti-inflammatory properties of our dendrimers.

7. Experimental Part

7.1. Materials and reagents

All reagents, salts and buffers were used as purchased from Merc, Fluorochem Ltd, Iris Biotech Gmbh, GL Biochem. Amino acids were used as the following derivatives: Fmoc-Ala-OH, Fmoc-Glu(t-Bu)-OH, Fmoc-Cys(Trt)-OH, Fmoc-Lys(Boc)-OH, Fmoc-Lys(Fmoc)-OH, Fmoc-Tyr(t-Bu)-OH and purchased by Iris Biotech GmbH or GL Biochem. Tentagel S RAM resin was purchased from Rapp Polymere GmbH (loading: 0.24 mmol·g−1). Rink Amide AM LL was purchased from Novabiochem (loading: 0.26 mmol·g−1). Fmoc-Ala-Wang LL resin, Fmoc-Glu(t-Bu)-Wang LL resin, Fmoc-Lys(Boc)-Wang LL resin, Fmoc-Tyr(t-Bu)-Wang LL resin were purchased from Novabiochem and Merc (loading: 0.32 mmol·g−1), resins were used for manual solid phase peptide synthesis, by CEM Liberty Blue Automated Microwave Peptide Synthesizer or by semi-automated peptide synthetizer. OxymaPure (ethyl cyanoglyoxylate-2-oxime) and DIC (N,N' -diisopropyl carbodiimide) was used for peptide coupling. Peptide dendrimers synthesis was performed manually in polypropylene syringes fitted with a polyethylene frit, a Teflon stopcock and stopper or automatically by CEM Liberty Blue Automated Microwave Peptide Synthesizer or glass syringes fitted with a polyethylene frit.

Analytical RP-HPLC was performed with an Ultimate 3000 Rapid Separation LC-MS System (DAD-3000RS diode array detector) using an Acclaim RSLC 120 C18 column (2.2 µm, 120 Å, 3×50 mm, flow 1.2 mL/min) from Dionex. Data recording and processing was done with Dionex Chromeleon Management System Version 6.80 (analytical RP-HPLC). All RP-HPLC were using HPLC-grade acetonitrile and Milli-Q deionized water. The elution solutions were: A Milli-Q deionized water containing 0.05% TFA; D Milli-Q deionized water/acetonitrile (10:90, v/v) containing 0.05% TFA. Preparative RP-HPLC was performed with a Waters automatic Prep LC Controller System containing the four following modules: Waters2489 UV/Vis detector, Waters2545 pump, Waters Fraction Collector III and Waters 2707 Autosampler. A Dr. Maisch GmbH Reprospher column (C18-DE, 100×30 mm, particle size 5 µm, pore size 100 Å, flow rate 40 mL/min) was used. Compounds were detected by UV absorption at 214 nm using a Waters 2487 Tunable Absorbance Detector. Data recording and processing was performed with Waters ChromScope version 1.40 from Waters Corporation. All RP-HPLC were using HPLC-grade acetonitrile and Milli-Q deionized water. The elution solutions were: A: Milli-Q deionized water containing 0.1% TFA; D: Milli-Q deionized water/acetonitrile (10:90, v/v) containing 0.1% TFA. MS spectra were recorded on a Thermo

Scientific LTQ OrbitrapXL. MS spectra were provided by the MS analytical service of the Department of Chemistry and Biochemistry at the University of Bern (group PD Dr. Stefan Schürch).

7.2. Peptide Dendrimer Synthesis

7.2.1. Manual solid phase peptide synthesis

Manual solid phase synthesis was performed in 10 mL polypropylene syringes with porous polyethylene filters and Teflon caps. Stirring of the reaction mixture at any given step was performed by attaching the closed syringe to a rotating axis. For synthesis 300 mg of TentaGel S RAM resin (loading: 0.24 mmol·g^{-1}) or Fmoc-Wang LL preloaded resin, (loading: 0.32 mmol·g^{-1}) was swollen in DCM for 20 min. Then, the following conditions were used:

Deprotection of Fmoc group

For deprotection at each step the Fmoc protecting group was removed with 8 mL of piperidine/DMF (1:4, v/v) for 30 min. After filtration the resin was washed with DMF (3×6 mL), MeOH (3×6 mL) and DCM (3×6 mL).

Coupling of Fmoc-protected aminoacids

For coupling 5 eq. of Fmoc-protected amino acid, 5 eq. OxymaPure and DIC 5 eq. in DMF were added to the resin and the reaction was stirred for 90 min. The couplings were repeated according to the generations and performed once for the 0th generation, twice for the 1st generation, three times for the 2nd generation, four times for 3rd generation. After filtration the resin was washed with DMF (3×6 mL), MeOH (3×6 mL) and DCM (3×6 mL).

7.2.2. Automated solid phase peptide synthesis

Automated microwave synthesis was performed with Liberty Blue CEM synthesizer under SPPS conditions at 0.25 mmol scale. Was used 180 mg Rink Amide AM LL (loading: 0.26 mmol·g^{-1}) resin or Fmoc-Ala-Wang LL resin, Fmoc-Glu(*t*-Bu)-Wang LL resin, Fmoc-Lys(Boc)-Wang LL resin, Fmoc-Tyr(*t*-Bu)-Wang LL resin (loading: 0.32 mmol·g^{-1}). The resin was swollen in DMF/DCM 50:50 for 15 min at R.T.

Deprotection of Fmoc group.

For deprotection at each step the Fmoc protecting group was removed with 5 mL of piperidine/DMF (1:4, v/v) for 2 min at 75 °C. After filtration, the resin was washed 5 times with 5 mL DMF.

Coupling of Fmoc-protected amino acids.

For coupling 5 eq. of Fmoc-protected amino acid, 5 eq. of Oxyma and 5 eq. of DIC all at a concentration of 0.2 M, were used as coupling reagents in 4 mL of DMF. The reaction was stirred for 5 minutes at 75 °C. The resin was then washed with 4 mL DMF 4 times. The couplings were repeated according to the generations and performed once for the 0th generation, twice for the 1st generation, four times for the 2nd generation. For 3rd generation synthesis was performed manually.

7.2.3. Semi-automated solid phase peptide synthesis

Semi-automated synthesis was performed with an in-house built synthetzer consisting of a heating element, keeping the temperature at 50 °C, glass reaction vessels and a vacuum operated filtration system. For each synthesis 300 mg of Rink Amide AM LL (loading: 0.26 mmol·g^{-1}) resin or Fmoc-Ala-Wang LL resin, Fmoc-Glu(t-Bu)-Wang LL resin, Fmoc-Lys(Boc)-Wang LL resin, Fmoc-Tyr(t-Bu)-Wang LL resin (loading: 0.32 mmol·g^{-1}) was used. The resin was swollen in DMF/DCM 50:50 for 15 min at R.T. During all the steps the resin was mixed by passing N_2 through the syringes.

Deprotection of Fmoc group.

For deprotection at each step the Fmoc protecting group was removed with 5 mL of piperidine/DMF (1:4, v/v) for 5 min at 50 °C twice. After filtration, the resin was washed 5 times with 5 mL DMF.

Coupling of Fmoc-protected amino acids.

For coupling 5 eq. of Fmoc-protected amino acid, 5 eq. of Oxyma and 5 eq. of DIC all at a concentration of 0.2 M, were used as coupling reagents in 4 mL of DMF. The reaction was stirred for 15 minutes at 50 °C. The resin was then washed with 4 mL DMF 4 times. The couplings were repeated according to the generations and performed twice for the 0-2nd generation, four times for the 3rd generation.

7.2.4. Cleavage and Purification

The cleavage was carried out by treating the resins with 7 mL of TFA/i-Pr₃SiH/DOTT/H2O (94:2.5:2.5:1, v/v/v/v) solution for 4 h. The peptide solutions were precipitated with 40 mL of TBME, centrifuged for 10 min at 3500 rpm, evaporated and dried under high vacuum for 60 min. The crude was then dissolved in a H₂O/CH₃CN (10/1, v/v) mixture, some drops of MeOH added when needed and purified by preparative RP-HPLC. The

fractions of the crudes were then lyophilized. Yields are given as SPPS total yields. In all cases, yields are calculated for the corresponding TFA salts.

7.2.5. Coupling of peptide dendrimers in solution

Fluorophore labelled peptide dendrimers.

Peptide dendrimer (1 eq., 5-10 mg) was solubilized NH_4HCO_3 (50 mM) solution. Then, fluorescein diacetate 5-maleimide (Fl, 1.1 eq., 0.5-1 mg), 7-diethylamino-3-(4-maleimidophenyl)-4-methylcoumarin (Coum 1.1 eq, 0.5-1 mg) were solubilized in 500 μL acetonitrile and added dropwise to the stirring solution. Reaction stirred at RT for 2 h, lyophilized and purified by preparative HPLC. Yields are given for the coupling step. In all cases, yields are calculated for the corresponding TFA salts.

Dimerization of peptide dendrimers.

Peptide dendrimer (2 eq., 10-20 mg) was solubilized NH_4HCO_3 (50 mM) solution. Then, reaction stirred for 24 h, lyophilized and purified by preparative HPLC. Yield is given for the coupling step and calculated for the corresponding TFA salt.

7.3. Cell culture and Isolation of human primary monocytes

7.3.1. Materials for bioassays

Glatiramer acetate (GA) was purchased from Brunschwig AG. Ficoll-Paque PLUS solution was purchased from GE Healthcare. Hanks` Balanced Salt Solution (HBSS) was purchased from Gibco. RPMI-1640 Medium, heat-inactivated Fetal Bovine Serum (FBS), streptomycin, penicillin, PBS tablets, Lipopolysaccarides from Escherichia coli O111:B4, mRNA extraction Single Cell RNA Purification Kit, AlamarBlue, Percoll density gradient, BSA extra pure, DEPC, Poly-L-Lysine were purchased from Sigma Aldrich. dNTP Mix 10 mM each, Superscript IV Reverse Transcriptase, RNaseOU Recombinant Ribonuclease Inhibitor, Random Hexamers, PowerUp™ SYBR™ Green Master Mix, IL-1Ra ELISA kit, Hoechst 33258, Cell Mask Deep Red were purchased from Termo Fisher Scientific. Pre-Separation filters, 30 µm, Classical Monocyte Isolation Kit, CD14-FITC, Anti-Biotin-PE, autoMACS Rinsing Solution, MACS BSA Stock Solution, LC MidiMACS Separator, MACS MultiStand, LS Columns were purchased from MACS, Miltenyi Biotec. PE Mouse Anti-Human CD14, BV605 Mouse Anti-Human CD16 Clone 3G8, PE-Cy™7 Mouse Anti-Human CD68 Clone, Y1/82A, BV711 Mouse Anti-Human CCR2 (CD192) LS132.1D9, BV421 Rat Anti-Human CX3CR1 Clone, 2A9-1, APC Mouse Anti-Human CD206 Clone 19.2, BV421 Mouse Anti-Human HLA-DR, DP, DQ, Clone Tu39 were purchased from BD Bioscieces. Glycergel Mounting Medium was purchased from Agilent. 8 Chambered Coverglass System CellVis was purchased from IBL Baustoff+Labor GmbH.

7.3.2. Extraction of peripheral blood mononuclear cells (PBMC)

Anticoagulant-treated blood was obtained from Interregional Blood Transfusion SCR Ltd. Bern in blood bags 45 mL each. In accordance with the ethical committee of the Interregionale Blutspende SRK AG obtained informed consent from the healthy donors, who are thus informed that part of their blood will be used for research purposes. Blood was diluted twice with HBSS and carefully overlayed on 20 mL of the Ficoll-Paque PLUS medium (1.077 g/ml). After centrifugation (400×g, 30 min, 20 °C) buffy coat at the interface was collected, washed with 40 mL of RPMA-1640 supplemented with 10% heat-inactivated FBS, 50 g/mL streptomycin, 50 U/mL penicillin, 2 mM glutamine, (RPMI supplemented). After centrifugation (200×g, 7 min, 20 °C) sedimented cells were diluted with RPMI-1640 supplemented and overlayed for second time over 20 mL of the Ficoll-Paque PLUS medium and centrifuged at the same conditions. PBMC collected from the interface were washed 3 times with supplemented RPMI.

7.3.3. Monocytes purification using magnetic beads labelling Isolation KIT II

Monocytes were purified from whole PBMC by negative selection, all procedures were carried out according to manufacturer protocol. Briefly, the non-monocytes were labelled with a cocktail of biotin-conjugated monoclonal antibodies as a primary labelling reagent. Then as a secondary labelling reagent were used anti-biotin microbeads. The mixture was run through the MACS column (MACS, Miltenyi Biotech) in the magnetic field of a MACS Separator (MACS, Miltenyi Biotech). In this case, non-monocytes are retained in the column and the unlabelled monocytes pass through the column. The purity of the monocytes was checked by fluorescent microscopy counterstaining with CD14-FITC. In the same way, the presence of the non-monocytes can be verified by staining with fluorochrome-conjugated anti-biotin antibody (Anti-Biotin-PE, AntiBiotin-APC).

7.3.4. Monocytes enrichment using Percoll gradient centrifugation

Monocytes enriched fraction was obtained from PBMC by hyper-osmotic Percoll solution[85]. Briefly, for 100 mL of solution, 48.5 mL of Percoll, 41.5 mL of water and 10.0 mL of 1.6 M NaCl were mixed. $150\text{-}200\times10^6$ cells were overlayed over 10 min of density medium and centrifuged at 580 g for 15 min. Cells at the interface were collected and washed 2 times with RPMI supplemented.

7.4. Cell Viability assay by AlamarBlue

PBMC (5×10^4 cells/200 µL; 96-well plates) were incubated in presence of peptide dendrimers (100 µg/mL, 50 µg/mL, 25 µg/mL and 12.5 µg/mL) for 24 h in in RPMI-1640 medium supplemented with 10% heat-inactivated FBS, 50 µg/mL streptomycin, 50 U/mL penicillin, 2 mM L-glutamine, and 5 µg/mL. After the incubation 25µL of AlamarBlue was added to each well and cells were incubated for additional 12h. Then, plates were measured on a Tecan Infinite M1000 Pro plate reader at $\lambda_{ex}= 560$ nm and $\lambda_{em}= 590$ nm and value normalized to the one of untreated cells.

7.5. Cytokine production

7.5.1. Enzyme-linked immunosorbent assay (ELISA)

Monocytes (5×10^4 cells/200 µL well; 96-well plates) were preincubated for 1 h with or without compounds in RPMI-1640 medium supplemented with 10% heat-inactivated FBS, 50 µg/mL streptomycin, 50 U/mL penicillin, 2 mM L-glutamine, and 5 µg/mL polymyxin B sulfate and then cultured for 48 h in the presence or absence of LPS (100 ng/mL) (2). The

production of IL-1Ra was measured in culture supernatants by commercially available enzyme immunoassay according to manufacture protocol.

7.5.2. mRNA Quantification

Enriched monocytes after Percoll centrifugation (4×10^6 cells/3 mL well; 6-well plates) were preincubated for 1 h with or without compounds in RPMI-1640 medium supplemented with 10% heat-inactivated FBS, 50 µg/mL streptomycin, 50 U/mL penicillin, 2 mM L-glutamine, and then incubated for the indicated duration. After the incubation cells were collected, total RNA was extracted, reverse transcribed and analysed by SYBR Green Master Mix. As a housekeeping gene was used Actin 5'-CAC TGG GGG CTA CTG GAC-3', 3'-AAC ATG GTG TTG GCA GAA ACT-5', IL-1Ra 5'-TTC CTG TTC CAT TCA GAG ACG-3', 3'-CTT CTG GTT AAC ATC CCA GAT TC-5'.

7.6. Confocal Microscopy

7.6.1. Membrane and nucleus staining

8-well chambered coverglass plates were treated with poly-L-Lysine for 30 min, dried at RT for 2 h. Monocytes were plated at 2×10^5 cells/300 µL per well and incubated for the indicated duration with dendrimers in presence or absence of LPS at 37 °C in a humidified atmosphere in 5% carbon dioxide following the removal of the full growth medium. Then, cells were washed with warm PBS twice and the cell membrane was labelled with CellMask Deep Red plasma membrane stain in PBS (0.25 µL in 0.25 mL/well) and nucleus was stained with Hoechst 33258 in PBS (0.25 µL in 0.25 mL/well) for 30 min at 37 °C. After the incubation cells were washed with PBS twice and prewarmed Glycergel Mounting Medium was added. Images were taken on a Zeiss LSM 880 confocal microscope with Oil compatible lens x63/1.3.

7.6.2. Immunostaining of PBMCs

PBMC 2×10^4 cells/50 were µL per well and incubated for 24 h in 364-well plates in presence of stimuli or without and selected dendrimers at 37 °C in a humidified atmosphere in 5% carbon dioxide following the removal of the full growth medium. Then, cells were washed with warm PBS twice and stained with anti-CD3 conjugated to APC and anti-CD14 conjugated with PE according to manufacture protocols for 12 h. Images were taken in The CeMM Research Center for Molecular Medicine of the Austrian Academy of Sciences on the "Pharmacoscopy platfom".

7.7. Flow Cytometry experiments

PBMC of healthy donors were obtained by Ficoll density gradient centrifugation. Cells were incubated for 1 h in presence or absence of LPS (100 ng/mL) in 6-well plates, 4×10^6 cells/well, then with GA, selected dendrimers (50 µg/mL) or without any treatment for 18 h. After incubation cells were detached, washed twice with staining buffer (0.5% BSA in $1 \times$ PBS) and stained according to manufacture protocols for 30 min on ice with following antibodies: CD14 - PE, CD16 - BV605, HLA-DR - BV421, CD68 – PECy7, CCR2 – BV711, CD206 - APC. After two washes with staining buffer, samples were a acquired on LSR II SORP H274 and analysed using FlowJo software.

7.8. CD Spectroscopy

Circular dichroism (CD) experiments were measured on a Jasco J-715 Spectropolarimeter. All the experiments were performed using Hellma Suprasil 110-QS 0.1 cm cuvettes. For each peptide, the measurements were performed in phosphate buffer (PB, pH=7.2, 8 mM) and in the presence of 5 mM dodecylphosphocholine. The concentration of the peptides was 100.0 µg/mL and each sample was measured using one accumulation. The scan rate was 10 nm/min, pitch 0.5 nm, response 16 sec and bandwidth 1.0 nm. The nitrogen flow was kept >8.5 L/min. After each measurement, the cuvettes were washed successively with 1 M HCl, milli-Q H2O and PB buffer. The baseline was recorded under the same conditions and subtracted manually.

8. Synthesis, HPLC and MS Data for all Dendrimers

1 (AAKEYAAEKK-OH) was obtained from the CEM Liberty Blue synthetizer as foamy colourless solid after preparative RP-HPLC (30.5 mg, 34.6 µmol, 54.1%). Analytical RP-HPLC: t_R=1.17 min (100% A to 100% D in 5 min, λ= 214 nm). HRMS (ESI+): $C_{49}H_{81}N_{13}O_{16}$ calc./obs. 1107.5924/1107.5907 Da [M].

Ac1 (AcAAKEYAAEKK-OH) was obtained from the CEM Liberty Blue synthetizer as foamy colourless solid after preparative RP-HPLC (23.6 mg, 29.4 µmol, 43.9%). Analytical RP-HPLC: t_R=1.25 min (100% A to 100% D in 5 min, λ= 214 nm). HRMS (ESI+): $C_{51}H_{83}N_{13}O_{17}$ calc./obs. 1149.6030/1149.6007 Da [M].

ClAc1 (ClAcAAKEYAAEKK-OH) was obtained from the CEM Liberty Blue synthetizer as foamy colourless solid after preparative RP-HPLC (25.2 mg, 30.0 µmol, 45.8%). Analytical RP-HPLC: t_R=1.29 min (100% A to 100% D in 5 min, λ= 214 nm). HRMS (ESI+): $C_{51}H_{82}Cl_1N_{13}O_{17}$ calc./obs. 1183.5640/1183.5634 Da [M].

2 (EYAAKKEKAA-OH) was obtained from the CEM Liberty Blue synthetizer as foamy colourless solid after preparative RP-HPLC (61.6 mg, 35.0 µmol, 54.7%). Analytical RP-HPLC: t_R=1.16 min (100% A to 100% D in 5 min, λ= 214 nm). HRMS (ESI+): $C_{49}H_{81}N_{13}O_{16}$ calc./obs. 1107.5924/1107.5929 Da [M].

Ac2 (AcEYAAKKEKAA-OH) was obtained from the CEM Liberty Blue synthetizer as foamy colourless solid after preparative RP-HPLC (50.6 mg, 34.4 µmol, 51.4%). Analytical RP-HPLC: t_R=1.24 min (100% A to 100% D in 5 min, λ= 214 nm). HRMS (ESI+): $C_{51}H_{83}N_{13}O_{17}$ calc./obs. 1149.6030/1149.6019 Da [M].

ClAc2 (ClAcEYAAKKEKAA-OH) was obtained from the CEM Liberty Blue synthetizer as foamy colourless solid after preparative RP-HPLC (27.5 mg, 32.8 µmol, 50.0%). Analytical RP-HPLC: t_R=1.30 min (100% A to 100% D in 5 min, λ= 214 nm). HRMS (ESI+): $C_{51}H_{82}Cl_1N_{13}O_{17}$ calc./obs. 1183.5640/1183.5634 Da [M].

3 (YAEKEKAKAA-OH) was obtained from the CEM Liberty Blue synthetizer as foamy colourless solid after preparative RP-HPLC (41.1 mg, 36.7 µmol, 54.2%). Analytical RP-HPLC: t_R=1.16 min (100% A to 100% D in 5 min, λ= 214 nm). HRMS (ESI+): $C_{49}H_{81}N_{13}O_{16}$ calc./obs. 1107.5924/1107.5916 Da [M].

ClAc3 (ClAcYAEKEKAKAA-OH) was obtained from the CEM Liberty Blue synthetizer as foamy colourless solid after preparative RP-HPLC (41.1 mg, 36.8 µmol, 56.1%). Analytical

RP-HPLC: t_R=1.31 min (100% A to 100% D in 5 min, λ= 214 nm). HRMS (ESI+): $C_{51}H_{82}Cl_1N_{13}O_{17}$ calc./obs. 1183.5640/1183.5634 Da [M].

4 ((A)₄*K*YKACA-NH₂) was obtained from the CEM Liberty Blue synthetizer as foamy colourless solid after preparative RP-HPLC (74.0 mg, 28.8 µmol, 40.2%). Analytical RP-HPLC: t_R=1.12 min (100% A to 100% D in 5 min, λ= 214 nm). HRMS (ESI+): $C_{36}H_{61}N_{11}O_9S$ calc./obs. 823.4474/823.4375 Da [M].

5 ((AE)₂*K*AEYCA-NH₂) was obtained from the CEM Liberty Blue synthetizer as foamy colourless solid after preparative RP-HPLC (59.5 mg, 44.9 µmol, 58.9%). Analytical RP-HPLC: t_R=1.24 min (100% A to 100% D in 5 min, λ= 214 nm). HRMS (ESI+): $C_{45}H_{70}N_{12}O_{17}S$ calc./obs. 1082.4703/1082.4696 Da [M].

6 ((AEE)₂*K*AEYCA-NH₂) was obtained from the CEM Liberty Blue synthetizer as foamy colourless solid after preparative RP-HPLC (69.6 mg, 31.5 µmol, 50.0%). Analytical RP-HPLC: t_R=1.28 min (100% A to 100% D in 5 min, λ= 214 nm). HRMS (ESI+): $C_{55}H_{84}N_{14}O_{23}S$ calc./obs. 1340.5554/1340.5552 Da [M].

7 ((KA)₄(*K*AYE)₂*K*K-OH) was obtained from the CEM Liberty Blue synthetizer as foamy colourless solid after preparative RP-HPLC (77.2 mg, 11.3 µmol, 34.8%). Analytical RP-HPLC: t_R=1.02 min (100% A to 100% D in 5 min, λ= 214 nm). HRMS (ESI+): $C_{94}H_{160}N_{26}O_{25}$ calc./obs. 2053.2048/2053.2054 Da [M].

Ac7 ((AcKA)₄(*K*AYE)₂*K*K-OH) was obtained from the CEM Liberty Blue synthetizer as foamy colourless solid after preparative RP-HPLC (23.6 mg, 6.3 µmol, 17.6%). Analytical RP-HPLC: t_R=1.29 min (100% A to 100% D in 5 min, λ= 214 nm). HRMS (ESI+): $C_{102}H_{168}N_{26}O_{29}$ calc./obs. 2221.2471/2221.2492 Da [M].

ClAc7 ((ClAcKA)₄(*K*AYE)₂*K*K-OH) was obtained from the CEM Liberty Blue synthetizer as foamy colourless solid after preparative RP-HPLC (106.0 mg, 13.7 µmol, 40.2%). Analytical RP-HPLC: t_R=1.37 min (100% A to 100% D in 5 min, λ= 214 nm). HRMS (ESI+): $C_{102}H_{164}Cl_4N_{26}O_{29}$ calc./obs. 2357.0912/2358.0922 Da [M].

8 ((KA)₄(*K*EYA)₂*K*KAK-OH) was obtained from the CEM Liberty Blue synthetizer as foamy colourless solid after preparative RP-HPLC (25.8 mg, 6.0 µmol, 20.3%). Analytical RP-HPLC: t_R=1.19 min (100% A to 100% D in 5 min, λ= 214 nm). HRMS (ESI+): $C_{103}H_{177}N_{29}O_{27}$ calc./obs. 2252.3369/2252.3399 Da [M].

Ac8 ((AcKA)$_4$(*K*EYA)$_2$*K*KAK-OH) was obtained from the CEM Liberty Blue synthetizer as foamy colourless solid after preparative RP-HPLC (10.8 mg, 3.1 µmol, 9.7%). Analytical RP-HPLC: t_R=1.13 min (100% A to 100% D in 5 min, λ= 214 nm). HRMS (ESI+): C$_{111}$H$_{185}$N$_{29}$O$_{31}$ calc./obs. 2420.3791/2420.3812 Da [M].

ClAc8 ((ClAcKA)$_4$(*K*EYA)$_2$*K*KAK-OH) was obtained from the CEM Liberty Blue synthetizer as foamy colourless solid after preparative RP-HPLC (9.3 mg, 2.5 µmol, 8.0%). Analytical RP-HPLC: t_R=1.16 min (100% A to 100% D in 5 min, λ= 214 nm). HRMS (ESI+): C$_{111}$H$_{181}$Cl$_4$N$_{29}$O$_{31}$ calc./obs. 2556.2232/2556.2228 Da [M].

9 ((AK)$_4$(*K*KYE)$_2$*K*AAA-OH) was obtained from the CEM Liberty Blue synthetizer as foamy colourless solid after preparative RP-HPLC (12.2 mg, 2.8 µmol, 9.6%). Analytical RP-HPLC: t_R=1.20 min (100% A to 100% D in 5 min, λ= 214 nm). HRMS (ESI+): C$_{103}$H$_{177}$N$_{29}$O$_{27}$ calc./obs. 2252.3369/2252.3332 Da [M].

Ac9 ((AcAK)$_4$(*K*KYE)$_2$*K*AAA-OH) was obtained from the CEM Liberty Blue synthetizer as foamy colourless solid after preparative RP-HPLC (10.4 mg, 2.9 µmol, 8.9%). Analytical RP-HPLC: t_R=1.28 min (100% A to 100% D in 5 min, λ= 214 nm). HRMS (ESI+): C$_{111}$H$_{185}$N$_{29}$O$_{31}$ calc./obs. 2420.3791/2420.3770 Da [M].

10 ((AYK)$_4$(*K*E)$_2$*K*KAA-OH) was obtained after manual synthesis as foamy colourless solid after preparative RP-HPLC (34.8 mg, 8.3 µmol, 28.4%). Analytical RP-HPLC: t_R=1.23 min (100% A to 100% D in 5 min, λ= 214 nm). HRMS (ESI+): C$_{112}$H$_{178}$N$_{28}$O$_{29}$ calc./obs. 2379.3315/2379.3345 Da [M].

Ac10 ((AcAYK)$_4$(*K*E)$_2$*K*KAA-OH) was obtained after manual synthesis as foamy colourless solid after preparative RP-HPLC (50.2 mg, 9.6 µmol, 28.4%). Analytical RP-HPLC: t_R=1.36 min (100% A to 100% D in 5 min, λ= 214 nm). HRMS (ESI+): C$_{120}$H$_{186}$N$_{28}$O$_{33}$ calc./obs. 2547.3315/2547.3775 Da [M].

11 ((AKA)$_4$(*K*KEY)$_2$*K*E-OH) was obtained after manual synthesis as foamy colourless solid after preparative RP-HPLC (24.3 mg, 4.9 µmol, 17.6%). Analytical RP-HPLC: t_R=1.20 min (100% A to 100% D in 5 min, λ= 214 nm). HRMS (ESI+): C$_{111}$H$_{189}$N$_{31}$O$_{31}$ calc./obs. 2452.4166/2452.4170 Da [M].

Ac11 ((AcAKA)$_4$(*K*KEY)$_2$*K*E-OH) was obtained after manual synthesis as foamy colourless solid after preparative RP-HPLC (49.3 mg, 9.4 µmol, 31.1%). Analytical RP-HPLC: t_R=1.30

min (100% A to 100% D in 5 min, λ= 214 nm). HRMS (ESI+): $C_{119}H_{197}N_{31}O_{35}$ calc./obs. 2620.4588/2620.4615 Da [M].

ClAc**11** (**(ClAcAKA)₄(*K*KEY)₂*K*E-OH)** was obtained after manual synthesis as foamy colourless solid after preparative RP-HPLC (43.4 mg, 9.4 µmol, 32.3%). Analytical RP-HPLC: t_R=1.37 min (100% A to 100% D in 5 min, λ= 214 nm). HRMS (ESI+): $C_{119}H_{193}Cl_4N_{31}O_{35}$ calc./obs. 2756.3029/2756.3066 Da [M].

12 (**(AKA)₄(*K*EK)₂*K*YEY-OH)** was obtained from the CEM Liberty Blue synthetizer as foamy colourless solid after preparative RP-HPLC (34.2 mg, 7.4 µmol, 26.4%). Analytical RP-HPLC: t_R=1.23 min (100% A to 100% D in 5 min, λ= 214 nm). HRMS (ESI+): $C_{111}H_{189}N_{31}O_{31}$ calc./obs. 2452.4166/2452.4208 Da [M].

Ac**12** (**(AcAKA)₄(*K*EK)₂*K*YEY-OH)** was obtained from the CEM Liberty Blue synthetizer as foamy colourless solid after preparative RP-HPLC (25.0 mg, 6.4 µmol, 21.0%). Analytical RP-HPLC: t_R=1.31 min (100% A to 100% D in 5 min, λ= 214 nm). HRMS (ESI+): $C_{119}H_{197}N_{31}O_{35}$ calc./obs. 2620.4588/2620.4627 Da [M].

13 (**(KAA)₄(*K*EKA)₂*K*EKA-NH₂)** was obtained from the CEM Liberty Blue synthetizer as foamy colourless solid after preparative RP-HPLC (169.5 mg, 12.6 µmol, 49.3%). Analytical RP-HPLC: t_R=1.21 min (100% A to 100% D in 5 min, λ= 214 nm). HRMS (ESI+): $C_{120}H_{207}Cl_4N_{35}O_{32}$ calc./obs. 2650.5646/2650.5679 Da [M].

ClAc**14** (**(ClAcK)₄(*K*AYE)₂*K*AKYAEA-NH₂)** was obtained from the CEM Liberty Blue synthetizer as foamy colourless solid after preparative RP-HPLC (159.6 mg, 14.6 µmol, 46.1%). Analytical RP-HPLC: t_R=1.44 min (100% A to 100% D in 5 min, λ= 214 nm). HRMS (ESI+): $C_{113}H_{178}Cl_4N_{30}O_{30}$ calc./obs. 2575.2079/2577.1828 Da [M].

15 (**(KYA)₄(*K*EA)₂*K*KKA-OH)** was obtained after manual synthesis as foamy colourless solid after preparative RP-HPLC (87.6 mg, 10.6 µmol, 39.2%). Analytical RP-HPLC: t_R=1.24 min (100% A to 100% D in 5 min, λ= 214 nm). HRMS (ESI+): $C_{121}H_{195}N_{31}O_{301}$ calc./obs. 2578.4635/2578.4656 Da [M].

Ac**15** (**(AcKYA)₄(*K*EA)₂*K*KKA-OH)** was obtained after manual synthesis as foamy colourless solid after preparative RP-HPLC (88.0 mg, 12.5 µmol, 42.7%). Analytical RP-HPLC: t_R=1.19 min (100% A to 100% D in 5 min, λ= 214 nm). HRMS (ESI+): $C_{129}H_{203}N_{31}O_{35}$ calc./obs. 2746.5058/2746.5094 Da [M].

ClAc**15 ((ClAcKYA)$_4$(*K*EA)$_2$*K*KKA-OH)** was obtained after manual synthesis as foamy colourless solid after preparative RP-HPLC (65.3 mg, 8.5 µmol, 30.5%). Analytical RP-HPLC: t_R=1.42 min (100% A to 100% D in 5 min, λ= 214 nm). HRMS (ESI+): $C_{129}H_{199}Cl_4N_{31}O_{35}$ calc./obs. 2882.3499/2882.3549 Da [M].

Ac**16 ((AcAKA)$_4$(*K*EY)$_2$*K*YKK-NH$_2$)** was obtained from the CEM Liberty Blue synthetizer as foamy colourless solid after preparative RP-HPLC (31.7 mg, 13.4 µmol, 49.3%). Analytical RP-HPLC: t_R=1.31 min (100% A to 100% D in 5 min, λ= 214 nm). HRMS (ESI+): $C_{123}H_{200}N_{32}O_{33}$ calc./obs. 2653.4956/2653.4904 Da [M].

Fum**16 ((FumAKA)$_4$(*K*EY)$_2$*K*YKK-NH$_2$)** was obtained from the CEM Liberty Blue synthetizer as foamy colourless solid after preparative RP-HPLC (15.0 mg, 6.5 µmol, 23.6%). Analytical RP-HPLC: t_R=1.21 min (100% A to 100% D in 5 min, λ= 214 nm). HRMS (ESI+): $C_{115}H_{192}N_{32}O_{29}$ calc./obs. 2485.4533/2485.4561 Da [M].

17 ((AKE)$_4$(*K*AYA)$_2$*K*KKK-NH$_2$) was obtained from the CEM Liberty Blue synthetizer as foamy colourless solid after preparative RP-HPLC (13.5 mg, 2.9 µmol, 11.4%). Analytical RP-HPLC: t_R=1.18 min (100% A to 100% D in 5 min, λ= 214 nm). HRMS (ESI+): $C_{122}H_{209}N_{35}O_{34}$ calc./obs. 2708.5701/2708.5633 Da [M].

Ac**17 ((AcAKE)$_4$(*K*AYA)$_2$*K*KKK-NH$_2$)** was obtained from the CEM Liberty Blue synthetizer as foamy colourless solid after preparative RP-HPLC (13.8 mg, 3.4 µmol, 12.5%). Analytical RP-HPLC: t_R=1.27 min (100% A to 100% D in 5 min, λ= 214 nm). HRMS (ESI+): $C_{130}H_{217}N_{35}O_{38}$ calc./obs. 2876.6124/2876.6340 Da [M].

Fum**17 ((FumAKE)$_4$(*K*AYA)$_2$*K*KKK-NH$_2$)** was obtained from the CEM Liberty Blue synthetizer as foamy colourless solid after preparative RP-HPLC (13.5 mg, 6.5 µmol, 23.6%). Analytical RP-HPLC: t_R=1.48 min (100% A to 100% D in 5 min, λ= 214 nm). $C_{146}H_{233}N_{35}O_{46}$ calc./obs. 3212.6969/3212.7355 Da [M].

18 ((K)$_4$(*K*AYAEY)$_2$*K*AKAEYA-NH$_2$) was obtained from the CEM Liberty Blue synthetizer as foamy colourless solid after preparative RP-HPLC (108.2 mg, 11.5 µmol, 43.5%). Analytical RP-HPLC: t_R=1.31 min (100% A to 100% D in 5 min, λ= 214 nm). HRMS (ESI+): $C_{129}H_{200}N_{32}O_{34}$ calc./obs. 2741.4905/2741.4961 Da [M].

19 ((KAE)$_4$(*K*AEK)$_2$*K*YYA-OH) was obtained after manual synthesis as foamy colourless solid after preparative RP-HPLC (49.3 mg, 7.7 µmol, 30.0%). Analytical RP-HPLC: t_R=1.23

min (100% A to 100% D in 5 min, λ= 214 nm). HRMS (ESI+): $C_{123}H_{205}N_{33}O_{39}$ calc./obs. 2768.5072/2768.5122 Da [M].

Ac**19 ((AcKAE)₄(*K*AEK)₂*K*YYA-OH)** was obtained after manual synthesis as foamy colourless solid after preparative RP-HPLC (4.1 mg, 9.4 µmol, 34.1%). Analytical RP-HPLC: t_R=1.29 min (100% A to 100% D in 5 min, λ= 214 nm). HRMS (ESI+): $C_{131}H_{213}N_{33}O_{43}$ calc./obs. 2936.5495/2936.5543 Da [M].

ClAc**19 ((ClAcKAE)₄(*K*AEK)₂*K*YYA-OH)** was obtained after manual synthesis as foamy colourless solid after preparative RP-HPLC (91.6 mg, 8.9 µmol, 33.8%7). Analytical RP-HPLC: t_R=1.35 min (100% A to 100% D in 5 min, λ= 214 nm). HRMS (ESI+): $C_{131}H_{209}Cl_4N_{33}O_{43}$ calc./obs. 3072.3936/3072.3961 Da [M].

Ac**20 ((AcKAA)₄(*K*YYE)₂*K*AY-NH₂)** was obtained after manual synthesis as foamy colourless solid after preparative RP-HPLC (31.7 mg, 9.1 µmol, 29.5%). Analytical RP-HPLC: t_R=1.47 min (100% A to 100% D in 5 min, λ= 214 nm). HRMS (ESI+): $C_{132}H_{199}N_{31}O_{36}$ calc./obs. 2794.4694/2794.4734 Da [M].

ClAc**20 ((ClAcKAA)₄(*K*YYE)₂*K*AY-NH₂)** was obtained after manual synthesis as foamy colourless solid after preparative RP-HPLC (29.4 mg, 7.8 µmol, 26.3%). Analytical RP-HPLC: t_R=1.51 min (100% A to 100% D in 5 min, λ= 214 nm). HRMS (ESI+): $C_{132}H_{195}Cl_4N_{31}O_{36}$ calc./obs. 2930.3135/2930.3170 Da [M].

Ac**21 ((AcKAK)₄(*K*AEY)₂*K*AEA-OH)** was obtained from the CEM Liberty Blue synthetizer as foamy colourless solid after preparative RP-HPLC (3.0 mg, 0.7 µmol, 2.3%). Analytical RP-HPLC: t_R=1.27 min (100% A to 100% D in 5 min, λ= 214 nm). HRMS (ESI+): $C_{131}H_{221}N_{35}O_{37}$ calc./obs. 2876.6488/2876.6463 Da [M].

22 ((AKK)₄(*K*YEK)₂*K*KEA-NH₂) was obtained from the CEM Liberty Blue synthetizer as foamy colourless solid after preparative RP-HPLC (168.3 mg, 12.6 µmol, 49.3%). Analytical RP-HPLC: t_R=1.17 min (100% A to 100% D in 5 min, λ= 214 nm). HRMS (ESI+): $C_{120}H_{207}N_{35}O_{32}$ calc./obs. 2650.5646/2650.5678 Da [M].

23 ((AKE)₄(*K*KAY)₂*K*YKY-NH₂) was obtained after manual synthesis as foamy colourless solid after preparative RP-HPLC (25.4 mg, 4.8 µmol, 18.6%). Analytical RP-HPLC: t_R=1.25 min (100% A to 100% D in 5 min, λ= 214 nm). HRMS (ESI+): $C_{134}H_{217}N_{35}O_{36}$ calc./obs. 2892.6225/2892.6243 Da [M].

Ac23 ((AcAKE)₄(*K*KAY)₂*K*YKY-NH₂) was obtained after manual synthesis as foamy colourless solid after preparative RP-HPLC (35.6 mg, 7.2 µmol, 27.9%). Analytical RP-HPLC: t_R=1.32 min (100% A to 100% D in 5 min, λ= 214 nm). HRMS (ESI+): $C_{142}H_{225}N_{35}O_{40}$ calc./obs. 3060.6648/3060.6693 Da [M].

ClAc23 ((ClAcAKE)₄(*K*KAY)₂*K*YKY-NH₂) was obtained after manual synthesis as foamy colourless solid after preparative RP-HPLC (8.9 mg, 1.7 µmol, 6.7%). Analytical RP-HPLC: t_R=1.37 min (100% A to 100% D in 5 min, λ= 214 nm). HRMS (ESI+): $C_{142}H_{221}Cl_4N_{35}O_{40}$ calc./obs. 3196.5059/3196.5148 Da [M].

24 ((KYA)₄(*K*AE)₂*K*AEYKCA-NH₂) was obtained after manual synthesis as foamy colourless solid after preparative RP-HPLC (127.7 mg, 14.6 µmol, 29.5%). Analytical RP-HPLC: t_R=1.27 min (100% A to 100% D in 5 min, λ= 214 nm). HRMS (ESI+): $C_{135}H_{212}N_{36}O_{34}S$ calc./obs. 2913.5687/2915.5439 Da [M].

25 ((KAA)₄(*K*EY)₂*K*AKEYEYA-NH₂) was obtained after manual synthesis as foamy colourless solid after preparative RP-HPLC (180 mg, 10.5 µmol, 41.1%). Analytical RP-HPLC: t_R=1.25 min (100% A to 100% D in 5 min, λ= 214 nm). HRMS (ESI+): $C_{134}H_{213}N_{35}O_{38}$ calc./obs. 2920.5811/2920.5847 Da [M].

ClAc26 ((ClAcK)₄(*K*EAKAKEY)₂*K*AKEYEY-OH) was obtained from the CEM Liberty Blue synthetizer as foamy colourless solid after preparative RP-HPLC (159.9 mg, 4.9 µmol, 22.8%). Analytical RP-HPLC: t_R=1.34 min (100% A to 100% D in 5 min, λ= 214 nm). HRMS (ESI+): $C_{161}H_{253}Cl_4N_{39}O_{48}$ calc./obs. 3640.7309/3640.7259 Da [M].

27 ((AK)₄(*K*AEAKAKE)₂*K*KEYEYCA-NH₂) was obtained after manual synthesis as foamy colourless solid after preparative RP-HPLC (138 mg, 7.3 µmol, 39.1%). Analytical RP-HPLC: t_R=1.30 min (100% A to 100% D in 5 min, λ= 214 nm). HRMS (ESI+): $C_{174}H_{285}N_{47}O_{50}S$ calc./obs. 3865.0924/3865.1068 Da [M].

27Coum ((AK)₄(*K*AEAKAKE)₂*K*KEYEYC(Coumarin)A-NH₂) initial dendrimer was obtained as foamy white solid after preparative RP-HPLC, then 1eq. Of dendrimer was coupled with 1.1 eq. of 7-diethylamino-3-[4-(iodoacetamido)phenyl]-4- methylcoumarin in H_2O/ACN solution with NH_4HCO_3 50 mM buffer, pH 8. (6.1 mg, 9.6 µmol, 55.3%). Analytical RP-HPLC: t_R=1.59 min (100% A to 100% D in 5 min, λ= 214 nm). HRMS (ESI+): $C_{198}H_{307}N_{49}O_{54}S$ calc./obs. 4267.2504/4267.2627 Da [M].

Ac**28 ((AcKEAKY)$_4$(*K*KYEA)$_2$*K*EKAYKA-NH$_2$)** was obtained from the CEM Liberty Blue synthetizer as foamy colourless solid after preparative RP-HPLC (76.6 mg, 5.6 µmol, 34.3%). Analytical RP-HPLC: t_R=1.18 min (100% A to 100% D in 5 min, λ= 214 nm). HRMS (ESI+): C$_{220}$H$_{343}$N$_{53}$O$_{62}$ calc./obs. 4719.5316/4719.5442 Da [M].

ClAc**28 ((ClAcKEAKY)$_4$(*K*KYEA)$_2$*K*EKAYKA-NH$_2$)** was obtained from the CEM Liberty Blue synthetizer as foamy colourless solid after preparative RP-HPLC (56.7 mg, 4.0 µmol, 24.8%). Analytical RP-HPLC: t_R=1.21 min (100% A to 100% D in 5 min, λ= 214 nm). HRMS (ESI+): C$_{220}$H$_{339}$N$_{52}$Cl$_4$O$_{62}$ calc./obs. 4855.3757/4857.3959 Da [M].

29 ((YAKAKE)$_4$(*K*AYKAKA)$_2$*K*AYKKA-NH$_2$) was obtained after manual synthesis as foamy colourless solid after preparative RP-HPLC (169.6 mg, 3.5 µmol, 23.4%). Analytical RP-HPLC: t_R=1.23 min (100% A to 100% D in 5 min, λ= 214 nm). HRMS (ESI+): C$_{233}$H$_{378}$N$_{62}$O$_{59}$ calc./obs. 4988.8484/4988.8659 Da [M].

30 ((KAEKAYA)$_4$(*K*EKYAKA)$_2$*K*EKYKA-NH$_2$) was obtained f after manual synthesis as foamy colourless solid after preparative RP-HPLC (211.0 mg, 25.6 µmol, 25.6%). Analytical RP-HPLC: t_R=1.29 min (100% A to 100% D in 5 min, λ= 214 nm). HRMS (ESI+): C$_{251}$H$_{404}$N$_{66}$O$_{69}$ calc./obs. 5447.0133/5447.0332 Da [M].

31 ((YKAKAKY)$_4$(*K*EAKAKY)$_2$*K*AKEYEY-OH) was obtained after manual synthesis as foamy colourless solid after preparative RP-HPLC (154 mg, 1.4 µmol, 12.3%). Analytical RP-HPLC: t_R=1.14 min (100% A to 100% D in 5 min, λ= 214 nm). HRMS (ESI+): C$_{287}$H$_{443}$N$_{69}$O$_{70}$ calc./obs. 5976.3226/5976.3381 Da [M].

32 ((KA)$_8$(*K*AK)$_4$(*K*EKA)$_2$*K*AKEAYCA-NH$_2$) was obtained from the CEM Liberty Blue synthetizer as foamy colourless solid after preparative RP-HPLC (61.9 mg, 1.1 µmol, 7.7%). Analytical RP-HPLC: t_R=1.19 min (100% A to 100% D in 5 min, λ= 214 nm). HRMS (ESI+): C$_{210}$H$_{387}$N$_{67}$O$_{51}$S calc./obs. 4695.9470/4695.9625 Da [M].

Ac**32 ((AcKA)$_8$(*K*AK)$_4$(*K*EKA)$_2$*K*AKEAYCA-NH$_2$)** was obtained from the CEM Liberty Blue synthetizer as foamy colourless solid after preparative RP-HPLC (53.9 mg, 3.4 µmol, 22.8%). Analytical RP-HPLC: t_R=1.25 min (100% A to 100% D in 5 min, λ= 214 nm). HRMS (ESI+): C$_{226}$H$_{403}$N$_{67}$O$_{59}$S calc./obs. 5032.0315/5032.0448 Da [M].

Fum**32 ((FumKA)$_8$(*K*AK)$_4$(*K*EKA)$_2$*K*AKEAYCA-NH$_2$)** was obtained from the CEM Liberty Blue synthetizer as foamy colourless solid after preparative RP-HPLC (47.6 mg, 3.1 µmol,

22.9%). Analytical RP-HPLC: t_R=1.47 min (100% A to 100% D in 5 min, λ= 214 nm). $C_{258}H_{435}N_{67}O_{75}S$ calc./obs. 5704.2005/5704.2057 Da [M].

33 ((AKA)$_8$(*K*YEK)$_4$(*K*EKA)$_2$*K*AKY-OH) was obtained from the CEM Liberty Blue synthetizer as foamy colourless solid after preparative RP-HPLC (23.7 mg, 1.1 µmol, 9.4%). Analytical RP-HPLC: t_R=1.24 min (100% A to 100% D in 5 min, λ= 214 nm). HRMS (ESI+): $C_{264}H_{448}N_{74}O_{70}$ calc./obs. 5775.3771/5775.3854 Da [M].

Ac33 ((AcAKA)$_8$(*K*YEK)$_4$(*K*EKA)$_2$*K*AKY-OH) was obtained from the CEM Liberty Blue synthetizer as foamy colourless solid after preparative RP-HPLC (20.3 mg, 1.1 µmol, 8.7%). Analytical RP-HPLC: t_R=1.31 min (100% A to 100% D in 5 min, λ= 214 nm). HRMS (ESI+): $C_{280}H_{464}N_{74}O_{78}$ calc./obs. 6111.4616/6111.4644 Da [M].

ClAc33 ((ClAcAKA)$_8$(*K*YEK)$_4$(*K*EKA)$_2$*K*AKY-OH) was obtained from the CEM Liberty Blue synthetizer as foamy colourless solid after preparative RP-HPLC (20.9 mg, 1.1 µmol, 8.6%). Analytical RP-HPLC: t_R=1.37 min (100% A to 100% D in 5 min, λ= 214 nm). $C_{280}H_{464}Cl_8N_{74}O_{78}$ calc./obs. 6383.1499/6384.1461 Da [M].

34 ((KA)$_8$(*K*KAKE)$_4$(*K*YKAKA)$_2$*K*AYKKA-OH) was obtained after manual synthesis as foamy colourless solid after preparative RP-HPLC (127 mg, 1.0 µmol, 9.0%). Analytical RP-HPLC: t_R=1.20 min (100% A to 100% D in 5 min, λ= 214 nm). HRMS (ESI+): $C_{275}H_{495}N_{83}O_{66}$ calc./obs. 6016.7929/6016.7972 Da [M].

Ac34 ((AcKA)$_8$(*K*KAKE)$_4$(*K*YKAKA)$_2$*K*AYKKA-OH) was obtained from the CEM Liberty Blue synthetizer as foamy colourless solid after preparative RP-HPLC (52.8 mg, 2.4 µmol, 19.9%). Analytical RP-HPLC: t_R=1.25 min (100% A to 100% D in 5 min, λ= 214 nm). HRMS (ESI+): $C_{291}H_{511}N_{83}O_{74}$ calc./obs. 6352.8774/6352.8913 Da [M].

Fum34 ((FumKA)$_8$(*K*KAKE)$_4$(*K*YKAKA)$_2$*K*AYKKA-OH) was obtained from the CEM Liberty Blue synthetizer as foamy colourless solid after preparative RP-HPLC (51.8 mg, 1.9 µmol, 18.1%). Analytical RP-HPLC: t_R=1.42 min (100% A to 100% D in 5 min, λ= 214 nm). HRMS (ESI+): $C_{323}H_{543}N_{83}O_{90}$ calc./obs. 7025.0465/7025.0531 Da [M].

35 ((KAA)$_8$(*K*KAKAK)$_4$(*K*AAKKY)$_2$*K*EKAKCA-OH) was obtained after manual synthesis as foamy colourless solid after preparative RP-HPLC (17 mg, 0.2 µmol, 2.6%). Analytical RP-HPLC: t_R=1.21 min (100% A to 100% D in 5 min, λ= 214 nm). HRMS (ESI+): $C_{315}H_{580}N_{100}O_{71}S$ calc./obs. 6934.4362/6934.4379 Da [M].

36 ((AK)$_8$(KAKAKY)$_4$(KAKEYEY)$_2$$K$AKEYEY-NH$_2$) was obtained after manual synthesis as foamy colourless solid after preparative RP-HPLC (51.3 mg, 0.6 µmol, 5.8%). Analytical RP-HPLC: t_R=1.25 min (100% A to 100% D in 5 min, λ= 214 nm). HRMS (ESI+): $C_{323}H_{544}N_{90}O_{77}$ calc./obs. 6916.1419/6916.1596 Da [M].

37 ((X)$_{30}$-NH$_2$) was synthetised using the CEM Liberty Blue synthetizer by mixing Fmoc-L-alanine, Fmoc-L-lysine, Fmoc-L-glutamic acid, Fmoc-L-tyrosine in ratio 4.2/3.4/1.4/1 respectively. Colourless foamy solid was obtained after preparative RP-HPLC (46.3 mg). Analytical RP-HPLC: t_R=2.51- min (100% A to 100% D in 10 min, λ= 214 nm). Amino acid analysis:

ClAc37 (ClAc(X)$_{30}$-NH$_2$) was synthetised using the CEM Liberty Blue synthetizer by mixing Fmoc-L-alanine, Fmoc-L-lysine, Fmoc-L-glutamic acid, Fmoc-L-tyrosine in ratio 4.2/3.4/1.4/1 respectively. Colourless foamy solid was obtained after preparative RP-HPLC (34.0 mg). Analytical RP-HPLC: t_R=2.76- min (100% A to 100% D in 10 min, λ= 214 nm).

38 ((X)$_{40}$-NH$_2$) was synthetised using the CEM Liberty Blue synthetizer by mixing Fmoc-L-alanine, Fmoc-L-lysine, Fmoc-L-glutamic acid, Fmoc-L-tyrosine in ratio 4.2/3.4/1.4/1 respectively. Colourless foamy solid was obtained after preparative RP-HPLC (62.4 mg). Analytical RP-HPLC: t_R=2.72- min (100% A to 100% D in 10 min, λ= 214 nm).

Ac38 (Ac(X)$_{40}$-NH$_2$) was synthetised using the CEM Liberty Blue synthetizer by mixing Fmoc-L-alanine, Fmoc-L-lysine, Fmoc-L-glutamic acid, Fmoc-L-tyrosine in ratio 4.2/3.4/1.4/1 respectively. Colourless foamy solid was obtained after preparative RP-HPLC (51.3 mg). Analytical RP-HPLC: t_R=2.79- min (100% A to 100% D in 10 min, λ= 214 nm).

32G2 ((KAK)$_4$(KEKA)$_2$$K$AKEAYCA-NH$_2$)) was obtained after manual synthesis as foamy colourless solid after preparative RP-HPLC (21.9 mg, 4.66 µmol, 14.1%). Analytical RP-HPLC: t_R=1.07 min (100% A to 100% D in 5 min, λ= 214 nm). HRMS (ESI+): $C_{138}H_{251}N_{43}O_{35}S$ calc./obs. 3102.8903/3102.8874 Da [M].

32A ((AK)$_8$(KAK)$_4$(KEKA)$_2$$K$AKEAYCA-NH$_2$)) was obtained after manual synthesis as foamy colourless solid after preparative RP-HPLC (23.2 mg, 3.2 µmol, 23.2%). Analytical RP-HPLC: t_R=1.06 min (100% A to 100% D in 5 min, λ= 214 nm). HRMS (ESI+): $C_{210}H_{387}N_{67}O_{51}S$ calc./obs. 4695.9470/4695.9469 Da [M].

32K ((KK)$_8$(KAK)$_4$(KEKA)$_2$$K$AKEAYCA-NH$_2$) was obtained after manual synthesis as foamy colourless solid after preparative RP-HPLC (18.9 mg, 2.2 µmol, 18.9%). Analytical RP-

HPLC: t_R=1.07 min (100% A to 100% D in 5 min, λ= 214 nm). HRMS (ESI+): $C_{234}H_{443}N_{75}O_{51}S$ calc./obs. 5152.4098/5152.4134 Da [M].

D-**32 ((ka)$_8$(*k*ak)$_4$(*k*eka)$_2$*k*akeayca-NH$_2$)** was obtained from the CEM Liberty Blue synthetizer as foamy colourless solid after preparative RP-HPLC (56.8 mg, 2.5 µmol, 18.3%). Analytical RP-HPLC: t_R=1.33 min (100% A to 100% D in 5 min, λ= 214 nm). HRMS (ESI+): $C_{210}H_{387}N_{67}O_{51}S$ calc./obs. 4695.9470/4695.9606 Da [M].

sr-**32 ((KA)$_8$(*K*KA)$_4$(*K*KAE)$_2$*K*YEKACA-NH$_2$)** was obtained after manual synthesis as foamy colourless solid after preparative RP-HPLC (32.9 mg, 1.0 µmol, 7.6%). Analytical RP-HPLC: t_R=1.18 min (100% A to 100% D in 5 min, λ= 214 nm). HRMS (ESI+): $C_{207}H_{382}N_{66}O_{50}S$ calc./obs. 4624.9098/4624.9212 Da [M].

D-**34 ((ka)$_8$(*k*kake)$_4$(*k*ykaka)$_2$*k*aykka-NH$_2$)** was obtained from the CEM Liberty Blue synthetizer as foamy colourless solid after preparative RP-HPLC (67.1 mg, 1.8 µmol, 16.7%). Analytical RP-HPLC: t_R=1.37 min (100% A to 100% D in 5 min, λ= 214 nm). HRMS (ESI+): $C_{275}H_{496}N_{84}O_{65}$ calc./obs. 6015.8089/6015.8149 Da [M].

sr-**34 ((KA)$_8$(*K*EKAK)$_4$(*K*AYAKK)$_2$*K*KAYAK-OH)** was obtained after manual synthesis as foamy colourless solid after preparative RP-HPLC (89.6 mg, 1.7 µmol, 15.6%). Analytical RP-HPLC: t_R=1.19 min (100% A to 100% D in 5 min, λ= 214 nm). HRMS (ESI+): $C_{275}H_{495}N_{83}O_{66}S$ calc./obs. 6016.7929/6016.8081 Da [M].

32K2 **((KA)$_8$(*K*KKAK)$_4$(*K*EKA)$_2$*K*AKEAYCA-NH$_2$)** was obtained from the CEM Liberty Blue synthetizer as foamy colourless solid after preparative RP-HPLC (28.0 mg, 0.9 µmol, 8.6%). Analytical RP-HPLC: t_R=1.18 min (100% A to 100% D in 5 min, λ= 214 nm). HRMS (ESI+): $C_{258}H_{483}N_{83}O_{59}S$ calc./obs. 5720.7067/5720.7093 Da [M].

Ac**32**K2 **((AcKA)$_8$(*K*KKAK)$_4$(*K*EKA)$_2$*K*AKEAYCA-NH$_2$)** was obtained from the CEM Liberty Blue synthetizer as foamy colourless solid after preparative RP-HPLC (28.6 mg, 1.1 µmol, 9.4%). Analytical RP-HPLC: t_R=1.23 min (100% A to 100% D in 5 min, λ= 214 nm). HRMS (ESI+): $C_{274}H_{499}N_{83}O_{67}S$ calc./obs. 6056.7912/6056.7988 Da [M].

Fum**32**K2 **((FumKA)$_8$(*K*KKAK)$_4$(*K*EKA)$_2$*K*AKEAYCA-NH$_2$)** was obtained from the CEM Liberty Blue synthetizer as foamy colourless solid after preparative RP-HPLC (27.5 mg, 0.9 µmol, 8.3%). Analytical RP-HPLC: t_R=1.42 min (100% A to 100% D in 5 min, λ= 214 nm). $C_{306}H_{531}N_{83}O_{83}S$ calc./obs. 6728.9602/6728.9614.00 Da [M].

32Fl **((KA)$_8$(*K*AK)$_4$(*K*EKA)$_2$*K*AKEAYC(Fl)A-NH$_2$)** initial dendrimer was obtained as foamy white solid after preparative RP-HPLC, then 1eq. Of dendrimer was coupled with 1.1 eq. of fluorescein-diacetat-5-maleinimid in H$_2$O/ACN solution with NH$_4$HCO$_3$ 50 mM buffer, pH 8. (6.5 mg, 2.1 µmol, 40.6%). Analytical RP-HPLC: t_R=1.16 min (100% A to 100% D in 5 min, λ= 214 nm). HRMS (ESI+): C$_{238}$H$_{404}$N$_{68}$O$_{60}$S calc./obs. 5207.0373/5207.0391 Da [M].

32-32 ((KA)$_8$(*K*KA)$_4$(*K*KAE)$_2$*K*YEKACA-NH$_2$)$_2$) for dimerization the initial dendrimer was refluxed in 50 mM NH$_4$HCO$_3$ buffer for 48 h, foamy colourless solid was obtained after preparative RP-HPLC (7.9 mg, 1.0 µmol, 43.6%). Analytical RP-HPLC: t_R=1.20 min (100% A to 100% D in 5 min, λ= 214 nm). HRMS (ESI+): C$_{414}$H$_{762}$N$_{132}$O$_{100}$S$_2$ calc./obs. 9247.8040/9247.8422 Da [M].

39 (KA)$_8$(KKGKE)$_4$(KYKAKA)$_2$KIFKSK-NH$_2$ was obtained after manual synthesis as foamy colourless solid after preparative RP-HPLC (61.7 mg, 6.5 µmol, 15.4%). Analytical RP-HPLC: t_R=1.25 min (100% A to 100% D in 5 min, λ= 214 nm). HRMS (ESI+): C$_{274}$H$_{494}$N$_{84}$O$_{65}$ calc./obs. 6001.7932/6001.8045 Da [M].

40 (KA)$_8$(KKGKE)$_4$(KYKKAP)$_2$KAFKK- was obtained after manual synthesis as foamy colourless solid after preparative RP-HPLC (81.3 mg, 8.6 µmol, 20.2 %). Analytical RP-HPLC: t_R=1.22 min (100% A to 100% D in 5 min, λ= 214 nm). HRMS (ESI+): C$_{272}$H$_{478}$N$_{83}$O$_{63}$ calc./obs. 5924.7456/5924.7700 Da [M].

sr-**41 (KA)$_8$(KKKAE)$_4$(KYKAKG)$_2$KLYKKG-NH$_2$** was obtained after manual synthesis as foamy colourless solid after preparative RP-HPLC (131.3 mg, 13.9 µmol, 27.8%). Analytical RP-HPLC: t_R=1.22 min (100% A to 100% D in 5 min, λ= 214 nm). HRMS (ESI+): C$_{275}$H$_{496}$N$_{84}$O$_{65}$ calc./obs. 6015.8089//6015.8179 Da [M].

42 (OV)$_8$(KKGKE)$_4$(KYKGK)$_2$KKFNGK-NH$_2$ was obtained after manual synthesis as foamy colourless solid after preparative RP-HPLC (104.5 mg, 1.1 µmol, 21.8%). Analytical RP-HPLC: t_R=1.27 min (100% A to 100% D in 5 min, λ= 214 nm). HRMS (ESI+): C$_{271}$H$_{489}$N$_{83}$O$_{63}$ calc./obs. 5914.7612/5914.7612 Da [M].

43 (OV)$_8$(KKGKE)$_4$(KYKAKA)$_2$KIFKSK-NH$_2$ was obtained after manual synthesis as foamy colourless solid after preparative RP-HPLC (48.5 mg, 5.0 µmol, 10.2%). Analytical RP-HPLC: t_R=1.27 min (100% A to 100% D in 5 min, λ= 214 nm). HRMS (ESI+): C$_{282}$H$_{510}$N$_{84}$O$_{65}$ calc./obs. 6113.9184/6113.9332 Da [M].

44 (OV)$_8$(KKGKE)$_4$(KYKKAP)$_2$KAFNKK-NH$_2$ was obtained after manual synthesis as foamy colourless solid after preparative RP-HPLC (49.1 mg, 5.1 µmol, 10.3%). Analytical RP-HPLC: t_R=1.25 min (100% A to 100% D in 5 min, λ= 214 nm). HRMS (ESI+): C$_{280}$H$_{503}$N$_{83}$O$_{83}$ calc./obs. 6036.8708/6036.8901 Da [M].

sr-45 (OV)$_8$(KKKAE)$_4$(KYKAKG)$_2$KLYKKG-NH$_2$ was obtained after manual synthesis as foamy colourless solid after preparative RP-HPLC (118.3 mg, 12.3 µmol, 24.8%). Analytical RP-HPLC: t_R=1.30 min (100% A to 100% D in 5 min, λ= 214 nm). HRMS (ESI+): C$_{283}$H$_{512}$N$_{84}$O$_{65}$ calc./obs. 6127.9519/6127.9341 Da [M].

46 (KA)$_8$(KKGKE)$_4$(KYKLGK)$_2$KKFNGK-NH$_2$ was obtained after manual synthesis as foamy colourless solid after preparative RP-HPLC (95.9 mg, 10.0 µmol, 23.9%). Analytical RP-HPLC: t_R=1.30 min (100% A to 100% D in 5 min, λ= 214 nm). HRMS (ESI+): C$_{222}$H$_{398}$N$_{68}$O$_{53}$ calc./obs. 6026.8041/6026.9039 Da [M].

47 (KA)$_8$(KKLKE)$_4$(KYKGKG)$_2$KQFIRA-NH$_2$ was obtained after manual synthesis as foamy colourless solid after preparative RP-HPLC (86.6 mg, 9.0 µmol, 18.2%). Analytical RP-HPLC: t_R=1.30 min (100% A to 100% D in 5 min, λ= 214 nm). HRMS (ESI+): C$_{285}$H$_{514}$N$_{86}$O$_{65}$ calc./obs. 6181.9559/6181.9536 Da [M].

48 (KA)$_8$(KKAKE)$_4$(KYKGKA)$_2$KRVIKQ-NH$_2$ was obtained after manual synthesis as foamy colourless solid after preparative RP-HPLC (60.9 mg, 6.4 µmol, 15.1%). Analytical RP-HPLC: t_R=1.23 min (100% A to 100% D in 5 min, λ= 214 nm). HRMS (ESI+): C$_{274}$H$_{501}$N$_{87}$O$_{65}$ calc./obs. 6050.8572/6050.8745 Da [M].

49 (OV)$_8$(KKLKE)$_4$(KYKGKG)$_2$KQFIRA-NH$_2$ was obtained after manual synthesis as foamy colourless solid after preparative RP-HPLC (93.5 mg, 9.7 µmol, 19.5%). Analytical RP-HPLC: t_R=1.35 min (100% A to 100% D in 5 min, λ= 214 nm). HRMS (ESI+): C$_{293}$H$_{530}$N$_{86}$O$_{65}$ calc./obs. 6294.0811/6294.0984 Da [M].

50 (OV)$_8$(KKAKE)$_4$(KYKGKA)$_2$KRVIKQ-NH$_2$ was obtained after manual synthesis as foamy colourless solid after preparative RP-HPLC (70.3 mg, 7.3 µmol, 17.9%). Analytical RP-HPLC: t_R=1.27 min (100% A to 100% D in 5 min, λ= 214 nm). HRMS (ESI+): C$_{282}$H$_{517}$N$_{87}$O$_{65}$ calc./obs. 6162.9824/6162.9947 Da [M].

D-32 Fl **((ka)$_8$(*k*ak)$_4$(*k*eka)$_2$*k*akeayc(Fl)a-NH$_2$)** initial dendrimer was obtained as foamy white solid after preparative RP-HPLC, then 1eq. f dendrimer was coupled with 1.1 eq. of fluorescein-diacetat-5-maleinimid in H$_2$O/ACN solution with NH$_4$HCO$_3$ 50 mM buffer, pH 8.

(6.1 mg, 0.8 µmol, 40.3%). Analytical RP-HPLC: t_R=1.16 min (100% A to 100% D in 5 min, λ= 214 nm). HRMS (ESI+): $C_{238}H404N_{68}O_{60}S$ calc./obs. 5207.0373/5207.0391 Da [M].

*sr-***32**Fl **((KA)8(*K*AK)4(*K*EKA)2*K*AKEAYC(Fl)A-NH2)** initial dendrimer was obtained as foamy white solid after preparative RP-HPLC, then 1eq. Of dendrimer was coupled with 1.1 eq. of fluorescein-diacetat-5-maleinimid in H_2O/ACN solution with NH_4HCO_3 50 mM buffer, pH 8. (5.2 mg, 0.7 µmol, 39.8%). Analytical RP-HPLC: t_R=1.17 min (100% A to 100% D in 5 min, λ= 214 nm). HRMS (ESI+): $C_{238}H404N_{68}O_{60}S$ calc./obs. 5207.0373/5207.0391 Da [M].

Ac**32**Fl **((AcKA)8(*K*AK)4(*K*EKA)2*K*AKEAYC(Fl)A-NH2)** initial dendrimer was obtained as foamy white solid after preparative RP-HPLC, then 1eq. Of dendrimer was coupled with 1.1 eq. of fluorescein-diacetat-5-maleinimid in H_2O/ACN solution with NH_4HCO_3 50 mM buffer, pH 8. (7.1 mg, 0.9 µmol, 42.5%). Analytical RP-HPLC: t_R=1.21 min (100% A to 100% D in 5 min, λ= 214 nm). HRMS (ESI+): $C_{254}H422N_{68}O_{60}S$ calc./obs. 5545.1375/5545.1257 Da [M].

35Fl **((KAA)8(*K*KAKAK)4(*K*AAKKY)2*K*EKAKC(Fl)A-OH)** was obtained after manual synthesis as foamy colourless solid after preparative RP-HPLC (4.8 mg, 0.5 µmol, 38.1%). Analytical RP-HPLC: t_R=1.14 min (100% A to 100% D in 5 min, λ= 214 nm). HRMS (ESI+): $C_{343}H599N_{101}O_{80}S$ calc./obs. 7445.5629/7446.5164 Da [M].

9. References

[1]   B. Nourbakhsh, E. M. Mowry, *Contin. Lifelong Learn. Neurol.* **2019**, *25*, 596.
[2]   M. Filippi, A. Bar-Or, F. Piehl, P. Preziosa, A. Solari, S. Vukusic, M. A. Rocca, *Nat. Rev. Dis. Primer* **2018**, *4*, 43.
[3]   M. Bujak, N. G. Frangogiannis, *Arch. Immunol. Ther. Exp. (Warsz.)* **2009**, *57*, 165–176.
[4]   S. E. Baranzini, J. R. Oksenberg, *Trends Genet. TIG* **2017**, *33*, 960–970.
[5]   D. H. Mahad, B. D. Trapp, H. Lassmann, *Lancet Neurol.* **2015**, *14*, 183–193.
[6]   R. Dobson, G. Giovannoni, *J. Neurol.* **2013**, *260*, 1272–1285.
[7]   J. P. van Hamburg, P. S. Asmawidjaja, N. Davelaar, A. M. C. Mus, E. M. Colin, J. M. W. Hazes, R. J. E. M. Dolhain, E. Lubberts, *Arthritis Rheum.* **2011**, *63*, 73–83.
[8]   J. Tabarkiewicz, K. Pogoda, A. Karczmarczyk, P. Pozarowski, K. Giannopoulos, *Arch. Immunol. Ther. Exp. (Warsz.)* **2015**, *63*, 435–449.
[9]   N. Dargahi, M. Katsara, T. Tselios, M.-E. Androutsou, M. De Courten, J. Matsoukas, V. Apostolopoulos, *Brain Sci.* **2017**, *7*, 78.
[10]   B. Hemmer, M. Kerschensteiner, T. Korn, *Lancet Neurol.* **2015**, *14*, 406–419.
[11]   D. M. Mosser, J. P. Edwards, *Nat. Rev. Immunol.* **2008**, *8*, 958–969.
[12]   V. E. Miron, A. Boyd, J.-W. Zhao, T. J. Yuen, J. M. Ruckh, J. L. Shadrach, P. van Wijngaarden, A. J. Wagers, A. Williams, R. J. M. Franklin, C. ffrench-Constant, *Nat. Neurosci.* **2013**, *16*, 1211–1218.
[13]   M. Inglese, M. Petracca, *Schizophr. Res.* **2015**, *161*, 94–101.
[14]   M. Marta, G. Giovannoni, *CNS Neurol. Disord. Drug Targets* **2012**, *11*, 610–623.
[15]   R. Bomprezzi, *Ther. Adv. Neurol. Disord.* **2015**, *8*, 20–30.
[16]   W. Brück, R. Gold, B. T. Lund, C. Oreja-Guevara, A. Prat, C. M. Spencer, L. Steinman, M. Tintoré, T. L. Vollmer, M. S. Weber, L. P. Weiner, T. Ziemssen, S. S. Zamvil, *JAMA Neurol.* **2013**, *70*, 1315–1324.
[17]   T. Prod'homme, S. S. Zamvil, *Cold Spring Harb. Perspect. Med.* **2019**, *9*, a029249.
[18]   A. Westad, A. Venugopal, E. Snyder, *Nat. Rev. Drug Discov.* **2017**, *16*, 675–676.
[19]   L. Kappos, M. S. Freedman, C. H. Polman, G. Edan, H.-P. Hartung, D. H. Miller, X. Montalbán, F. Barkhof, E.-W. Radü, L. Bauer, S. Dahms, V. Lanius, C. Pohl, R. Sandbrink, BENEFIT Study Group, *Lancet Lond. Engl.* **2007**, *370*, 389–397.
[20]   L. Kappos, C. H. Polman, M. S. Freedman, G. Edan, H. P. Hartung, D. H. Miller, X. Montalban, F. Barkhof, L. Bauer, P. Jakobs, C. Pohl, R. Sandbrink, *Neurology* **2006**, *67*, 1242–1249.
[21]   S. Mandala, R. Hajdu, J. Bergstrom, E. Quackenbush, J. Xie, J. Milligan, R. Thornton, G.-J. Shei, D. Card, C. Keohane, M. Rosenbach, J. Hale, C. L. Lynch, K. Rupprecht, W. Parsons, H. Rosen, *Science* **2002**, *296*, 346–349.
[22]   V. Brinkmann, M. D. Davis, C. E. Heise, R. Albert, S. Cottens, R. Hof, C. Bruns, E. Prieschl, T. Baumruker, P. Hiestand, C. A. Foster, M. Zollinger, K. R. Lynch, *J. Biol. Chem.* **2002**, *277*, 21453–21457.
[23]   G. Edan, D. Miller, M. Clanet, C. Confavreux, O. Lyon-Caen, C. Lubetzki, B. Brochet, I. Berry, Y. Rolland, J. C. Froment, E. Cabanis, M. T. Iba-Zizen, J. M. Gandon, H. M. Lai, I. Moseley, O. Sabouraud, *J. Neurol. Neurosurg. Psychiatry* **1997**, *62*, 112–118.
[24]   H.-P. Hartung, R. Gonsette, N. König, H. Kwiecinski, A. Guseo, S. P. Morrissey, H. Krapf, T. Zwingers, Mitoxantrone in Multiple Sclerosis Study Group (MIMS), *Lancet Lond. Engl.* **2002**, *360*, 2018–2025.
[25]   D. Teitelbaum, A. Meshorer, T. Hirshfeld, R. Arnon, M. Sela, *Eur. J. Immunol.* **1971**, *1*, 242–248.

[26] D. Teitelbaum, C. Webb, A. Meshorer, R. Arnon, M. Sela, *Eur. J. Immunol.* **1973**, *3*, 273–279.

[27] R. Aharoni, P. G. Schlegel, D. Teitelbaum, O. Roikhel-Karpov, Y. Chen, R. Arnon, M. Sela, N. J. Chao, *Immunol. Lett.* **1997**, *58*, 79–87.

[28] J. Anderson, C. Bell, J. Bishop, I. Capila, T. Ganguly, J. Glajch, M. Iyer, G. Kaundinya, J. Lansing, J. Pradines, J. Prescott, B. A. Cohen, D. Kantor, R. Sachleben, *J. Neurol. Sci.* **2015**, *359*, 24–34.

[29] H. Varkony, V. Weinstein, E. Klinger, J. Sterling, H. Cooperman, T. Komlosh, D. Ladkani, R. Schwartz, *Expert Opin. Pharmacother.* **2009**, *10*, 657–668.

[30] M. B. Bornstein, A. I. Miller, D. Teitelbaum, R. Arnon, M. Sela, *Ann. Neurol.* **1982**, *11*, 317–319.

[31] N. J. Carter, G. M. Keating, *Drugs* **2010**, *70*, 1545–1577.

[32] M. Fridkis-Hareli, D. Teitelbaum, E. Gurevich, I. Pecht, C. Brautbar, O. J. Kwon, T. Brenner, R. Arnon, M. Sela, *Proc. Natl. Acad. Sci. U. S. A.* **1994**, *91*, 4872–4876.

[33] M. Fridkis-Hareli, J. Strominger, *Mult. Scler. J.* **1997**, *3*, 405–405.

[34] Y. Hussien, A. Sanna, M. Söderström, H. Link, Y. M. Huang, *J. Neuroimmunol.* **2001**, *121*, 102–110.

[35] S. Jung, I. Siglienti, O. Grauer, T. Magnus, G. Scarlato, K. Toyka, *J. Neuroimmunol.* **2004**, *148*, 63–73.

[36] M. S. Weber, *Brain* **2004**, *127*, 1370–1378.

[37] M. S. Weber, R. Hohlfeld, S. S. Zamvil, *Neurotherapeutics* **2007**, *4*, 647–653.

[38] N. Molnarfi, T. Prod'homme, U. Schulze-Topphoff, C. M. Spencer, M. S. Weber, J. C. Patarroyo, P. H. Lalive, S. S. Zamvil, *Neurol. - Neuroimmunol. Neuroinflammation* **2015**, *2*, e179.

[39] D. Häusler, Z. Hajiyeva, J. W. Traub, S. S. Zamvil, P. H. Lalive, W. Brück, M. S. Weber, *Neurol. - Neuroimmunol. Neuroinflammation* **2020**, *7*, e698.

[40] K. P. Johnson, *Expert Opin. Drug Metab. Toxicol.* **2010**, *6*, 643–660.

[41] Z. Song, Y. M. Khaw, L. A. Pacheco, K.-Y. Tseng, Z. Tan, K. Cai, E. Ponnusamy, J. Cheng, M. Inoue, *Biomater. Sci.* **2020**, *8*, 5271–5281.

[42] R. Carpintero, K. J. Brandt, L. Gruaz, N. Molnarfi, P. H. Lalive, D. Burger, *Proc. Natl. Acad. Sci.* **2010**, *107*, 17692–17697.

[43] D. Burger, N. Molnarfi, M. S. Weber, K. J. Brandt, M. Benkhoucha, L. Gruaz, M. Chofflon, S. S. Zamvil, P. H. Lalive, *Proc. Natl. Acad. Sci.* **2009**, *106*, 4355–4359.

[44] J. Ruppert, C. Schütt, D. Ostermeier, J. H. Peters, *Adv. Exp. Med. Biol.* **1993**, *329*, 281–286.

[45] S. B. Clarkson, P. A. Ory, *J. Exp. Med.* **1988**, *167*, 408–420.

[46] F. Lasitschka, T. Giese, M. Paparella, S. R. Kurzhals, G. Wabnitz, K. Jacob, J. Gras, K. A. Bode, A.-K. Heninger, T. Sziskzai, Y. Samstag, C. Leszinski, B. Jocher, M. Al-Saeedi, S. C. Meuer, J. Schröder-Braunstein, *Immun. Inflamm. Dis.* **2017**, *5*, 480–492.

[47] *Int. Immunopharmacol.* **2020**, *83*, 106349.

[48] K. H. Han, R. K. Tangirala, S. R. Green, O. Quehenberger, *Arterioscler. Thromb. Vasc. Biol.* **1998**, *18*, 1983–1991.

[49] O. Y. Kim, A. Monsel, M. Bertrand, P. Coriat, J.-M. Cavaillon, M. Adib-Conquy, *Crit. Care* **2010**, *14*, R61.

[50] A. E. Mengos, D. A. Gastineau, M. P. Gustafson, *Front. Immunol.* **2019**, *10*, 1147.

[51] M. Ruggieri, C. Pica, A. Lia, G. B. Zimatore, M. Modesto, E. Di Liddo, L. M. Specchio, P. Livrea, M. Trojano, C. Avolio, *J. Neuroimmunol.* **2008**, *197*, 140–146.

[52] S. Tanaka, M. Ohgidani, N. Hata, S. Inamine, N. Sagata, N. Shirouzu, N. Mukae, S. O. Suzuki, H. Hamasaki, R. Hatae, Y. Sangatsuda, Y. Fujioka, K. Takigawa, Y.

Funakoshi, T. Iwaki, M. Hosoi, K. Iihara, M. Mizoguchi, T. A. Kato, *Front. Immunol.* **2021**, *12*, 670131.

[53] S. Fukui, N. Iwamoto, A. Takatani, T. Igawa, T. Shimizu, M. Umeda, A. Nishino, Y. Horai, Y. Hirai, T. Koga, S. Kawashiri, M. Tamai, K. Ichinose, H. Nakamura, T. Origuchi, R. Masuyama, K. Kosai, K. Yanagihara, A. Kawakami, *Front. Immunol.* **2018**, *8*, 1958.

[54] A. Nawaz, A. Aminuddin, T. Kado, A. Takikawa, S. Yamamoto, K. Tsuneyama, Y. Igarashi, M. Ikutani, Y. Nishida, Y. Nagai, K. Takatsu, J. Imura, M. Sasahara, Y. Okazaki, K. Ueki, T. Okamura, K. Tokuyama, A. Ando, M. Matsumoto, H. Mori, T. Nakagawa, N. Kobayashi, K. Saeki, I. Usui, S. Fujisaka, K. Tobe, *Nat. Commun.* **2017**, *8*, 286.

[55] D. A. Chistiakov, M. C. Killingsworth, V. A. Myasoedova, A. N. Orekhov, Y. V. Bobryshev, *Lab. Invest.* **2017**, *97*, 4–13.

[56] N. Barois, B. de Saint-Vis, S. Lebecque, H. J. Geuze, M. J. Kleijmeer, *Traffic Cph. Den.* **2002**, *3*, 894–905.

[57] F. Caprioli, F. Bosè, R. L. Rossi, L. Petti, C. Viganò, C. Ciafardini, L. Raeli, G. Basilisco, S. Ferrero, M. Pagani, D. Conte, G. Altomare, G. Monteleone, S. Abrignani, E. Reali, *Inflamm. Bowel Dis.* **2013**, *19*, 729–739.

[58] Y. Sun, D. Shang, *Mediators Inflamm.* **2015**, *2015*, 167572.

[59] M. Marta Guarna, R. Coulson, E. Rubinchik, *FEMS Microbiol. Lett.* **2006**, *257*, 1–6.

[60] W. Dong, X. Mao, Y. Guan, Y. Kang, D. Shang, *Sci. Rep.* **2017**, *7*, 40228.

[61] L. O. Flowers, H. M. Johnson, M. G. Mujtaba, M. R. Ellis, S. M. I. Haider, P. S. Subramaniam, *J. Immunol. Baltim. Md 1950* **2004**, *172*, 7510–7518.

[62] W. Strober, I. Fuss, P. Mannon, *J. Clin. Invest.* **2007**, *117*, 514–521.

[63] N. Eissa, H. Hussein, L. Kermarrec, J. Grover, M.-H. E. Metz-Boutigue, C. N. Bernstein, J.-E. Ghia, *Front. Immunol.* **2017**, *8*, 1131.

[64] J. Bernard, C. Harb, E. Mortier, A. Quéméner, R. H. Meloen, C. Vermot-Desroches, J. Wijdeness, P. van Dijken, J. Grötzinger, J. W. Slootstra, A. Plet, Y. Jacques, *J. Biol. Chem.* **2004**, *279*, 24313–24322.

[65] C. Gründemann, K. Thell, K. Lengen, M. Garcia-Käufer, Y.-H. Huang, R. Huber, D. J. Craik, G. Schabbauer, C. W. Gruber, *PLoS ONE* **2013**, *8*, e68016.

[66] A. Del Gatto, M. Saviano, L. Zaccaro, *Molecules* **2021**, *26*, 5227.

[67] A.-M. Caminade, D. Yan, D. K. Smith, *Chem. Soc. Rev.* **2015**, *44*, 3870–3873.

[68] Y. Zheng, S. Li, Z. Weng, C. Gao, *Chem. Soc. Rev.* **2015**, *44*, 4091–4130.

[69] C. J. Hawker, J. M. J. Frechet, *J. Am. Chem. Soc.* **1990**, *112*, 7638–7647.

[70] E. Abbasi, S. F. Aval, A. Akbarzadeh, M. Milani, H. T. Nasrabadi, S. W. Joo, Y. Hanifehpour, K. Nejati-Koshki, R. Pashaei-Asl, *Nanoscale Res. Lett.* **2014**, *9*, 247.

[71] V. Gupta, S. Nayak, *J. Appl. Pharm. Sci.* **2015**, 117–122.

[72] D. A. Tomalia, H. Baker, J. Dewald, M. Hall, G. Kallos, S. Martin, J. Roeck, J. Ryder, P. Smith, *Polym. J.* **1985**, *17*, 117–132.

[73] R. M. Pearson, S. Sunoqrot, H.-J. Hsu, J. W. Bae, S. Hong, *Ther. Deliv.* **2012**, *3*, 941–959.

[74] P. K. Avti, A. Kakkar, *Braz. J. Pharm. Sci.* **2013**, *49*, 57–65.

[75] T. S. Barata, S. Shaunak, I. Teo, M. Zloh, S. Brocchini, *J. Mol. Model.* **2011**, *17*, 2051–2060.

[76] M. Hayder, S. Fruchon, J.-J. Fournié, M. Poupot, R. Poupot, *Sci. World J.* **2011**, *11*, 1367–1382.

[77] E. J. Park, J.-E. Kim, D. K. Kim, J.-H. Park, K. B. Lee, D. H. Na, *Bull. Korean Chem. Soc.* **2016**, *37*, 596–599.

[78] C. C. Lee, J. A. MacKay, J. M. J. Fréchet, F. C. Szoka, *Nat. Biotechnol.* **2005**, *23*, 1517–1526.

[79] U. Boas, P. M. H. Heegaard, *Chem. Soc. Rev.* **2004**, *33*, 43–63.

[80] G. M. Pavan, P. Posocco, A. Tagliabue, M. Maly, A. Malek, A. Danani, E. Ragg, C. V. Catapano, S. Pricl, *Chem. – Eur. J.* **2010**, *16*, 7781–7795.

[81] O. Rolland, L. Griffe, M. Poupot, A. Maraval, A. Ouali, Y. Coppel, J.-J. Fournié, G. Bacquet, C.-O. Turrin, A.-M. Caminade, J.-P. Majoral, R. Poupot, *Chem. - Eur. J.* **2008**, *14*, 4836–4850.

[82] M. Poupot, L. Griffe, P. Marchand, A. Maraval, O. Rolland, L. Martinet, F.-E. L'Faqihi-Olive, C.-O. Turrin, A.-M. Caminade, J.-J. Fournié, J.-P. Majoral, R. Poupot, *FASEB J. Off. Publ. Fed. Am. Soc. Exp. Biol.* **2006**, *20*, 2339–2351.

[83] Y. Degboé, S. Fruchon, M. Baron, D. Nigon, C. O. Turrin, A.-M. Caminade, R. Poupot, A. Cantagrel, J.-L. Davignon, *Arthritis Res. Ther.* **2014**, *16*, R98.

[84] S. Fruchon, M. Poupot, L. Martinet, C.-O. Turrin, J.-P. Majoral, J.-J. Fournié, A.-M. Caminade, R. Poupot, *J. Leukoc. Biol.* **2009**, *85*, 553–562.

[85] U. Repnik, M. Knezevic, M. Jeras, *J. Immunol. Methods* **2003**, *278*, 283–292.

[86] R. Aharoni, P. G. Schlegel, D. Teitelbaum, O. Roikhel-Karpov, Y. Chen, R. Arnon, M. Sela, N. J. Chao, *Immunol. Lett.* **1997**, *58*, 79–87.

[87] T. R. Webb, J. Slavish, R. E. George, A. T. Look, L. Xue, Q. Jiang, X. Cui, W. B. Rentrop, S. W. Morris, *Expert Rev. Anticancer Ther.* **2009**, *9*, 331–356.

[88] V. R. Campos-García, D. Herrera-Fernández, C. E. Espinosa-de la Garza, G. González, L. Vallejo-Castillo, S. Avila, L. Muñoz-García, E. Medina-Rivero, N. O. Pérez, I. Gracia-Mora, S. M. Pérez-Tapia, R. Salazar-Ceballos, L. Pavón, L. F. Flores-Ortiz, *Sci. Rep.* **2017**, *7*, 12125.

[89] C. Confavreux, S. Vukusic, *Clin. Neurol. Neurosurg.* **2006**, *108*, 327–332.

[90] J. H. Noseworthy, C. Lucchinetti, M. Rodriguez, B. G. Weinshenker, *N. Engl. J. Med.* **2000**, *343*, 938–952.

[91] T. Ziemssen, W. Schrempf, in *Int. Rev. Neurobiol.*, Elsevier, **2007**, pp. 537–570.

[92] J. Haas, M. Firzlaff, *Eur. J. Neurol.* **2005**, *12*, 425–431.

[93] L. D. Goldberg, **n.d.**, 13.

[94] C. C. Lee, J. A. MacKay, J. M. J. Frechet, F. C. Szoka, *Nat Biotechnol* **2005**, *23*, 1517–1526.

[95] D. Astruc, E. Boisselier, C. Ornelas, *Chem Rev* **2010**, *110*, 1857–1959.

[96] A.-M. Caminade, D. Yan, D. K. Smith, *Chem Soc Rev* **2015**, *44*, 3870–3873.

[97] S. E. Seo, C. J. Hawker, *Macromolecules* **2020**, *53*, 3257–3261.

[98] S. M. Rele, W. Cui, L. Wang, S. Hou, G. Barr-Zarse, D. Tatton, Y. Gnanou, J. D. Esko, E. L. Chaikof, *J. Am. Chem. Soc.* **2005**, *127*, 10132–10133.

[99] V. Gajbhiye, V. K. Palanirajan, R. K. Tekade, N. K. Jain, *J. Pharm. Pharmacol.* **2010**, *61*, 989–1003.

[100] J. J. García-Vallejo, M. Ambrosini, A. Overbeek, W. E. van Riel, K. Bloem, W. W. J. Unger, F. Chiodo, J. G. Bolscher, K. Nazmi, H. Kalay, Y. van Kooyk, *Mol. Immunol.* **2013**, *53*, 387–397.

[101] K. Jain, A. K. Verma, P. R. Mishra, N. K. Jain, *Antimicrob. Agents Chemother.* **2015**, *59*, 2479–2487.

[102] I. Jatczak-Pawlik, M. Gorzkiewicz, M. Studzian, D. Appelhans, B. Voit, L. Pulaski, B. Klajnert-Maculewicz, *Pharm. Res.* **2017**, *34*, 136–147.

[103] S. Fruchon, E. Bellard, N. Beton, C. Goursat, A. Oukhrib, A.-M. Caminade, M. Blanzat, C.-O. Turrin, M. Golzio, R. Poupot, *Biomolecules* **2019**, *9*, 475.

[104] R. Sapra, R. P. Verma, G. P. Maurya, S. Dhawan, J. Babu, V. Haridas, *Chem. Rev.* **2019**, *119*, 11391–11441.

[105] K. G. Chandy, R. S. Norton, *Curr. Opin. Chem. Biol.* **2017**, *38*, 97–107.

[106] S. La Manna, C. Di Natale, D. Florio, D. Marasco, *Int. J. Mol. Sci.* **2018**, *19*, 2714.

[107] K. W. Wegmann, C. R. Wagner, R. H. Whitham, D. J. Hinrichs, *J. Immunol.* **2008**, *181*, 3301–3309.

[108] S. J. Zamolo, T. Darbre, J.-L. Reymond, *Chem. Commun.* **2020**, *56*, 11981–11984.

[109] X. Cai, S. Javor, B. H. Gan, T. Köhler, J.-L. Reymond, *Chem. Commun.* **2021**, *57*, 5654–5657.

[110] J.-L. Reymond, *Chim. Int. J. Chem.* **2021**, *75*, 535–538.

[111] L. J. Scott, *CNS Drugs* **2013**, *27*, 971–988.

[112] P. Albrecht, I. Bouchachia, N. Goebels, N. Henke, H. H. Hofstetter, A. Issberner, Z. Kovacs, J. Lewerenz, D. Lisak, P. Maher, A.-K. Mausberg, K. Quasthoff, C. Zimmermann, H.-P. Hartung, A. Methner, *J. Neuroinflammation* **2012**, *9*, 638.

[113] S. K. Yadav, D. Soin, K. Ito, S. Dhib-Jalbut, *J. Mol. Med.* **2019**, *97*, 463–472.

[114] T. N. Siriwardena, B.-H. Gan, T. Köhler, C. van Delden, S. Javor, J.-L. Reymond, *ACS Cent. Sci.* **2021**, *7*, 126–134.

[115] S. H. Christiansen, X. Zhang, K. Juul-Madsen, M. L. Hvam, B. S. Vad, M. A. Behrens, I. L. Thygesen, B. Jalilian, J. S. Pedersen, K. A. Howard, D. E. Otzen, T. Vorup-Jensen, *Biochim. Biophys. Acta BBA - Biomembr.* **2017**, *1859*, 425–437.

[116] J. E. Mindur, R. M. Valenzuela, S. K. Yadav, S. Boppana, S. Dhib-Jalbut, K. Ito, *J. Neuroimmunol.* **2017**, *304*, 21–28.

[117] B.-H. Gan, T. N. Siriwardena, S. Javor, T. Darbre, J.-L. Reymond, *ACS Infect. Dis.* **2019**, *5*, 2164–2173.

[118] G. I. Vladimer, B. Snijder, N. Krall, J. W. Bigenzahn, K. V. M. Huber, C.-H. Lardeau, K. Sanjiv, A. Ringler, U. W. Berglund, M. Sabler, O. L. de la Fuente, P. Knöbl, S. Kubicek, T. Helleday, U. Jäger, G. Superti-Furga, *Nat. Chem. Biol.* **2017**, *13*, 681–690.

[119] W. Xuan, Q. Qu, B. Zheng, S. Xiong, G.-H. Fan, *J. Leukoc. Biol.* **2015**, *97*, 61–69.

[120] P. Ruytinx, P. Proost, J. Van Damme, S. Struyf, *Front. Immunol.* **2018**, *9*, 1930.

[121] Z.-J. Xu, Y. Gu, C.-Z. Wang, Y. Jin, X.-M. Wen, J.-C. Ma, L.-J. Tang, Z.-W. Mao, J. Qian, J. Lin, *OncoImmunology* **2020**, *9*, 1683347.